COMPUTATIONAL ANALYSIS OF 3D PROTEIN STRUCTURES

ZEYAR AUNG

Bachelor of Computer Science (Honours)

University of Computer Studies, Yangon, Myanmar

A THESIS SUBMITTED

FOR THE DEGREE OF DOCTOR OF PHILOSOPHY

SCHOOL OF COMPUTING

NATIONAL UNIVERSITY OF SINGAPORE

2006

Acknowledgements

I would like to express my heartfelt gratitude to my supervisor Prof Tan Kian-Lee for his guidance, enlightenment and encouragement throughout my course of research. I really appreciate his patience and understanding when my progress was slow.

Special thanks are due to the National University of Singapore (NUS), and ultimately the government and tax payers of Singapore, for generously granting me the research scholarship for four years. Without this financial support, it would have been impossible for me to carry out this research.

I am much grateful to my collaborators Dr Ng See-Kiong and Mr Tan Soon-Heng from the Institute for Infocomm Research (I^2R), and my former labmate Mr Fu Wei for their contributions towards my research. I also thank my thesis examiners for their valuable comments and suggestions which help me improve the quality of the thesis.

I owe my gratitude to all my teachers at NUS from whose courses I have acquired background knowledge for my research. I am also grateful to the researchers all over the world from whose works I have learned. I specially thank Google and NUS Digital Library, both of which I used extensively for finding the materials throughout my research.

I would like to extend my gratefulness to my parents, Dr U Thein and Madam Khin Htay Myint, and my aunt, Madam Khin Myo Myint, all of who give me everlasting love, care and support morally and materially. Last but not least, I would like to thank my wife Ms Nan Nan Tint for standing by me during these trying times.

Zeyar Aung

National University of Singapore

November 2006

CONTENTS

LIST OF TABLES

LIST OF FIGURES

Summary

Analysis of 3-dimensional (3D) protein structures plays an important role in bioinformatics. Since the functions of a protein is more closely related to its 3D structure than to its amino acid sequence, the study of proteins from structural perspective can give us more valuable information about their functions. In this thesis, we will present the methods for four different types of protein structure analyses: alignment, database search, classification and clustering.

Firstly, we address pairwise protein structure alignment, which is the most fundamental problem in protein structure analysis. We propose a new method that carries out structural alignment by means of aligning their distance profiles, followed by an iterative refinement. On a benchmark data set, our method outperforms the two widely-used methods — in terms of the alignment accuracy measured by four different criteria. Its execution time is also as fast as theirs.

Secondly, we deal with structural database searching, which is a commonly performed task for a variety of purposes. Since the protein structure databases are rapidly growing nowadays, database searching by means of exhaustive pairwise alignments becomes extremely inefficient. We propose a new index-based method for rapid structural database searching. It builds an inverted index of secondary structure element (SSE) pairs. Then, it uses this index to rank the proteins in the database with respect their similarities to the query, and retrieve the top-ranking ones. We compare our method with the other two rapid database search tools, and

observe that ours is better both in terms of speed and accuracy.

Thirdly, we focus on the problem of protein structure classification. Researchers have organized the known protein structures into hierarchical structural classes. When a new protein structure comes in, it must be classified into the most suitable among the existing classes. Given a large number of proteins and classes, a fast automated structural classification system is required. We develop a new protein structure classification method based on a nearest-neighbor scheme integrated with active learning. It adopts the filter-and-refine strategy, and utilizes a two-tier abstract representation of protein structures. In comparison with the other two structural classification schemes, it achieves a better classification accuracy still within a shorter time.

Finally, we propose a method for clustering protein–protein interfaces, which are the sub-structures most responsible for protein functions. We group the similar interfaces into their respective clusters. This can provide biologist with the better insights on the similar functional properties of the similar interfaces. We carefully choose a set of representative interfaces from PDB (Protein Data Bank); characterize them as interface matrices; and encode them as feature vectors based on the different submatrix types contained in them. Then, we cluster these feature vectors using a version of nearest-neighbor clustering algorithm. Experimental results show that we can discover a number of interface clusters that are both statistically and biologically significant.

CHAPTER 1

Introduction

Proteins are the workhorses in the cells of living organisms. They perform a wide variety of functions: storage, structural lattice, movement, transport, signaling, immunity, catalysis in metabolism, etc. Proteins are truly the physical basis of life [Kim94]. The study of proteins is an important area in molecular and cell biology.

A protein is made up of a sequence of amino acid (AA) residues which folds into a particular 3-dimensional (3D) structure by the various forces of nature. In this thesis, we will describe the computational methods for analyzing the 3D protein structures. This piece of work belongs to the area of *structural bioinformatics* (also known as *structural genomics*), which in turn falls under the wider area of *bioinformatics*.

One of the major objectives in bioinformatics is to acquire comprehensive knowledge on the functions of proteins. Such knowledge can be applied in many application such as study of fundamental biological processes, study of molecular evolution, drug design, genetic engineering, and enzyme synthesis, etc. [LI03, Yon02]. Protein functions can be studied by analysis based on either AA sequences or 3D structures of proteins. In these two approaches, sequence-based analysis sometimes gives less accurate and less sensitive results than structure-based analysis. This is

because:

- The 3D structure is more informative than the linear sequence. It is widely accepted that sequence determines structure, and structure in turns determines function. However, the exact sequence–structure and structure–function relationships are too complex and not well understood yet. Nonetheless, since function is more directly correlated to 3D structure than to AA sequence, studying protein functions from the structural point of view can provide the relatively better results [RA00].

- A protein's 3D structure is better conserved than its AA sequence during evolution [Bre01]. There are a large number of distantly related proteins whose sequences are quite different, yet whose 3D structures (and hence functions) are quite similar. In addition, there are even some proteins that share the similar shape though their sequences are totally unrelated [BCHM96, HAB+97, Ros99]. Obviously, a sequence-based analysis will fail to detect these two cases.

- Even when the sequences of two proteins are quite similar, there is no total guarantee that they will perform the similar function. There are some instances in which the two proteins have quite different 3D structures (and hence functions) despite their strong sequence similarity [KFDDG02, LG98]. Structural analysis may be required to confirm of the results obtained by sequence analysis in such a case.

However, it does not necessarily mean that sequence analysis is not effective and should be discarded at all. Structural analysis has its own limitations when compared to sequence analysis.

- The 3D structure of a protein is obviously much more complex than its sequence, and thus requires much longer time to process. For example, for two proteins with n AA residues each, the time complexity of a naive sequence comparison method is $O(n^2)$ [NW71], whilst that of a naive structure comparison method is $O(n^7)$ [Wol01].

- A protein's 3D structure is more difficult to be determined than its sequence. As a result, fewer 3D structures than sequences are available. As of November 2006, whist there are over 3.5 millions of protein sequences stored in UniProt database [BAW+05], there are merely about 40,000 protein structures deposited in PDB database [BWF+00]. Therefore, structural analysis can cover only a small percentage of proteins that sequence analysis can deal with.

Thus, although structural analysis can generally provide better quality results than sequence analysis, it is slower and limited in coverage. The purpose of structural analysis of proteins is not to substitute sequence analysis, but rather to supplement it. Both sequence and structural analysis are required to achieve the ultimate goal of comprehensive functional knowledge acquisition.

The analysis of 3D protein structures includes structural alignment, database retrieval, classification, clustering, homology modeling, and prediction [OJT03]. We will cover the first four topics in this thesis.

1.1 Motivations

In this section, we will discuss the motivations for our research in four different topics in structural bioinformatics: structural comparison, database retrieval, classification and clustering.

1.1.1 Detailed Protein Structure Alignment

Comparison of two 3D protein structures is the most fundamental and important task in structural bioinformatics [ZK03]. Given two proteins, we have to determine how "similar" they are. Different methods use different scoring functions to measure the similarity [Koe01, WFB03].

Protein structure comparison can be used for various purposes: analysis of conformational changes on ligand binding, detection of distant evolutionary relationships, inferring functional characteristics of new proteins, assigning folds to

new proteins, analysis of structural variation in protein families, identification of common structural motifs, assessment of sequence alignment methods, evaluation of structural prediction methods, etc. [Bou05, God96, LI03, OJT03].

Researchers typically solve the structural comparison problem by means of *structural alignment*, following the concept of linear sequence alignment [ZG02]. They try to find a maximal set of corresponding pairs (i.e. alignment) of AA residues that gives a good structural match when superimposed together. Thus, the terms comparison and alignment are often used interchangeably, although there are some exceptions.

Structural alignment generally implies a "global" alignment, which aligns two structures in their whole, rather than some fragments or portions of them (i.e. "local" alignment). Again, structural alignment typically means a "sequence-order dependent" alignment, i.e., the aligned residues must observe the AA sequence orders (from N to C-terminus) of two proteins, like in the case of linear sequence alignment. For example, we can only make an alignment of the residues such as: (1–1), (2–3), (3–4), etc.; but cannot make an alignment such as: (1–1), (2–3), (3–2), etc. This restriction is generally meaningful in detecting structural homologies of proteins, because insertions and deletions of AA residues are more common than their rearrangements throughout evolution [Kar03]. Thus, when the term "structural alignment" is used, it means a "sequence-order dependent global structural alignment" by default, unless stated otherwise.

Finding the optimal alignment between two structures is NP-hard [HS95]. Finding a nearly optimal alignment of two structures with n AA residues each incurs $O(n^7)$ time [Wol01]. A number of heuristic algorithms, such as [Aku95, CCI+04, Erd05, GL96, GMB96, HS93, Kle96, KN00, TO89, OSO02, SB97, SB98, YG03], have been proposed to solve the structural alignment problem in lower-order polynomial times.

Because of their heuristic nature and their use of different similarity criteria, different algorithms may not produce exactly the same results in aligning the same protein pair. Nevertheless, it has been observed that there may be more than one

alignment result which can be regarded as viable and meaningful for a given pair of proteins [FS96, God96, ZG02]. Yet, this does not necessarily mean that the alignments produced by all methods can be assumed as equally good and acceptable. There are a variety of criteria to assess the quality of alignments [KKL05, WFB03].

Out of the existing methods, DALI [HS93, HP00] and CE [SB98] are reported to be among the best schemes that can provide the most accurate results according to a number of quality criteria [NMK04, SP04]. They are also two of the most widely used methods. However, even these best methods cannot always produce the accurate results consistently [Koe01, KKL05, SP04]. It means that the desirable goal of consistent and accurate structural alignment has not been fully achieved yet. Thus, we are still in need of a detailed structural alignment algorithm that can provide accurate and viable results.

1.1.2 Rapid Protein Structure Database Retrieval

In analyzing the protein structures, it is often required to compare a particular protein against a database of other proteins in order to search and retrieve ones that are structurally similar to it. (Technically speaking, "search(ing)" means finding proteins that are similar to a query, and "retrieval" means providing them to the user. However, we use these two terms synonymously, because in our context, searching is always done for the purpose of retrieval. In addition, "search/retrieval" in this thesis always means "similarity search/retrieval" with respect to a query, rather than "exact" search/retrieval of the query itself.)

Database searching is needed for a variety of purposes [Bre01, GFH03, HS94c]. For example, we may search a new protein whose function is not known yet against a database of functionally annotated proteins, and infer its functions from those of the most similar ones. We may also search an important structural motif through a protein structure database so as to retrieve the proteins which contains this motif, etc.

Because of the advancements in the laboratory methods to determine the structures of proteins (such as MNR and X-ray crystallography), protein structure

databases such as PDB [BWF+00] are growing rapidly in size. For example, PDB stored only about 5,000 structures the years ago (in 1996). But, it is about 40,000 now (November 2006).

When the database sizes were small, in order to search a protein structure against a database, researchers could comfortably use *exhaustive searching* by doing pairwise comparison of the query structure against each and every structure in the database sequentially, using any structural alignment method. But, when the database sizes grow to the order of ten's of thousands, such an exhaustive search approach cannot provide a satisfactory response time, however fast the structural alignment method used [CKS04, CHTY05].

For example, a detailed comparison method such as CE takes about an average of 20 seconds to perform a pairwise comparison of two proteins on a standard stand-alone Pentium IV PC. So, it can be conjectured that it will take about 800,000 seconds (which means about 9 days) to search through the full PDB database with 40,000 proteins.

A number of extremely fast, yet less accurate, pairwise comparison methods, such as [AF96, CP02, DWNT99, HS95, KJ97, KL97, KH04, Mar00, OHN99, SH03, Tay02, ZW05], have been proposed for the purpose of fast sequential database scan. Unfortunately, these methods are still inadequate to handle the large databases. For example, Topscan [Mar00], which is one of the fastest database scan methods, only takes an average of 0.025 seconds to perform a pairwise comparison on the stand-alone machine mentioned above. This means it takes about 17 minutes to search a query proteins through the aforementioned database of 40,000 proteins. But, this is only for a single query. If we have to probe hundreds of queries (which is usually needed in many applications such as drug design), the time required will be very long.

Thus, there is a pressing need for us to develop a protein structure database search system capable of handling large databases in a short time. Such a database search system does not necessarily need to rely on the tradition pairwise alignment but on the indexing and hashing techniques. The main challenge here is to maintain

a good retrieval accuracy whilst speeding up the search process.

A number of index and hash table-based structural database search systems, such as [AKKS99, CGZ04, CHTY05, CKS04, GZ05, HZS05, PR04b, SCSX04, WKHK04, YCCO05], has been proposed recently. However, to our knowledge, none of these systems have been critically appraised nor popularly used yet. This research area is still relatively immature, and there are opportunities for further contributions to be made.

1.1.3 Protein Structure Classification

When the number of structurally known protein became more than a handful, biologists naturally wanted to categorize them into groups. The earliest attempts to categorize protein structures were made since 1970s [RG88]. Apart from scientific curiosity, protein structure categorization is useful for many purposes. It enables us to study the structural properties of proteins more easily by using a reductionist approach. It can give us the valuable knowledge on sequence–structure relationships which can be exploited in protein structure prediction. It can help us limit the functional search space in determining a protein's functions since some types of function are totally irrelevant to some structural groups, etc. [Bou05, Ore99].

Protein structure categorization can be subdivided into two separate yet related problems: *clustering* or building groups from scratch, and *classification* or adding a new protein into the most appropriate of the existing groups. We will discuss the latter in this section, and the former in the next section.

By definition, classification is a kind of supervised learning. A classification system is trained using a set of objects whose class labels (i.e. group designations) are known *a priori*. (Throughout this thesis, the terms "classification system" and "classifier" imply an "automatic" one [cf. manual classification] by default unless stated otherwise.) The classifier learns the relationships between the properties of the training objects and their class labels, and derive a model or a set of rules regarding these relationships. Then, when a new object is to be classified, the classifier applies the learned rules in order to determine the most appropriate group

it should belong to.

In protein structure context, a structural classification system is trained with the structural properties and the structural class labels of a given pool of proteins. (The term "structural class" here means any structural group at any level in general. It should not be confused with a particular hierarchical level named "Class" [with capital C] in SCOP and CATH systems.) The class labels of the training protein structures can be obtained from any existing structural class annotation database such as SCOP [HAB+97], CATH [OMJ+97], or FSSP [HS94a] which is considered as the standard. After the 3D structure of a protein has been determined in the laboratory, it can be fed into the classifier to predict its structural class.

Protein structure classification problem has been addressed by a number of techniques such as nearest-neighbor search (discussed below), support vector machines [HWW+04], decision trees [CCSW05], hidden Markov model [WCH05] and fingerprinting [Ore99, AT04a].

Nearest-neighbor classification is probably the most widely used structural classification method up until now. In this method, in order to classify an unknown protein structure, it is searched through a database of existing structures (training samples) whose class labels are already known. Then, k structures (k is usually a smaller number, i.e. $1 \leq k \ll n$ where n is the number of proteins in the database) which are most similar to the new structure are taken, and its class is determined by majority voting of the classes of these k structures.

Virtually every existing structural comparison and database search tool can be used for protein structure classification by using the nearest-neighbor model. Some comparison and database search methods such as [AKKS99, RG88, Tay02] are even specifically intended for structural classification. Many other methods such as [CKS04, CHTY05, KH04, SCSX04] have been explicitly proved to be capable of classification. (Here, it should be noted that although structural classification is an important application for structural comparison/database search methods, their purpose is not only limited to it [NW91, OJT03]. On the other hand, compari-

son/database search is not the only option for classification, as discussed above.)

The first advantage of the nearest-neighbor classification is its simplicity. As opposed to other classification techniques, it does not require any complex rules or models to describe the properties of classes or the distinctions among them. The second advantage is that it is generally effective. In the protein structure space, a particular protein and its structural neighbors usually, though not always, belong to the same class. Thus, finding of the nearest neighbors for an unknown protein can usually indicate the correct class for it. The third is that it is intrinsically a multi-classifier, rather than a multiple binary classifier.

But, nearest-neighbor classification has two disadvantages. The first is its inefficiency. When a structural comparison/database search method is used, it is a sort of overkill because it has to find the similarity of every protein in the database with respect to the query. However, a majority of the similarity results, except for a few top-k scorers, are totally extraneous to the final classification result. The second is that, to our knowledge, none of the present nearest-neighbor structural classification schemes really "learn" from the training protein structures and their class labels in advance — before a new instance is actually to be classified. Classification is done "on the fly", unlike other classification strategies, such as decision trees and support vector machines, that learn proactively. In other words, the knowledge of the existing classes is neither learned nor exploited yet it is readily available.

Thus, it is desirable to have a new kind of nearest-neighbor classification system that is inherently simple and effective, yet able to avoid the above two weaknesses.

1.1.4 Protein–Protein Interface Clustering

Structural clustering is another instance of protein structure categorization, whose various applications have been already discussed in the above section. The aim of clustering is to organize a given set of objects in an orderly manner in such a way that the objects that are close to each other are in the same clusters, whilst those that are far apart are in different clusters. By definition, it is unsupervised learning

in that we do not know the class or cluster labels of all the objects *a priori*; but rather we try to generate these labels [HK05].

In protein structure context, we try to organize the protein structures sharing common structural characteristics into their respective clusters. There are well-established and quite popular clustering methods such as FSSP [HS94a] for clustering protein chains, and DDD [HS98] for clustering protein domains. Therefore, we do not intend to build another protein chain or domain clustering system, but focus on a relatively less studied area of clustering protein–protein interfaces.

Any protein rarely acts alone, but rather interacts with other proteins to perform a specific function [NT04]. A pair of interacting proteins naturally forms a *protein complex*. A protein complex has a special region called *protein–protein interface* where the two protein fragments, one from each protein, actually come into contact and interact. (By default, the term "protein–protein interface", or simply "interface", means a "binary" one involving only two protein chains. Although there are interfaces involving more than two protein chains, most of the methods treat them as multiple binary interfaces.) Thus, the study of the structural properties of protein–protein interfaces, which are responsible for interactions of proteins, can give us a better overview of protein functions, as compared to studying individual protein structures separately.

Clustering of protein–protein interfaces was pioneered by [TLWN96]. More recent works include [DS05, KTWN04, MSPWN05, SPMNW04]. It should be noted that protein–protein interface clustering is not a trivial extension of ordinary protein structure comparison and clustering. Care must be given to the interacting nature of the protein fragments that constitute an interface. When a pair of interfaces is compared, two pairs of corresponding protein fragments are needed to be handled simultaneously and synchronously with regard to their respective interactions [SPMNW04].

Although existing works are significant and can provide valuable information, they all lack the feature that inspects the quality of the interface clusters by means of a statistical validation. They instead inspect the clusters by visually means, and

conduct some biological analysis on a few sample clusters in order to indicate the usefulness of their methods.

It is suggested in [HKK05] that for any clustering method handling any type of biological data (not only for protein–protein interfaces) to be useful for practical purposes, a statistical validation should be carried out on the resultant set of clusters. Thus, we opt to develop a protein–protein interface clustering scheme in which the quality of the interface clusters are guaranteed by a statistical validation, in addition to the visual and biological verifications.

1.2 Contributions

In this section, we will discuss the contributions that we have made to the research in structural bioinformatics on the four topics of structural comparison, database retrieval, classification and clustering — in response to the motivations discussed in the above section.

1.2.1 Detailed Protein Structure Alignment

Based on the motivation descried in Section 1.1.1, we propose a new structural alignment algorithm named **MatAlign** (Matrix Alignment) [AT06]. Our design objective is to develop a system that can provide a high alignment accuracy (in terms of the fitness and the length of alignment) whist keeping the running time reasonably fast enough for practical purposes. We intend to build an ideal tool for the detailed comparative structural analysis involving a limited number of proteins.

We solve the structural alignment problem by means of matrix alignment. We represent 3D protein structures as 2-dimensional (2D) *distance matrices* (see Section 2.4), and align these matrices instead of the original 3D structures.

The basic MatAlign algorithm works in two steps. Firstly, we compare every row from the distance matrix of one protein against every row from the other protein's distance matrix using dynamic programming, and store the row–row matching scores. Dynamic programming is applied again on these row–row matching

scores to find the initial aligned residue pairs, one from each protein. Secondly, we refine this initial alignment iteratively. Then, we rotate and translate the second protein to superimpose its aligned residues onto those of the first protein. We remove the farthest residue pair from the alignment, and do superimposition again. This process is repeated until the alignment score cannot be further improved. We also implement some speed and accuracy enhancements on the basic algorithm.

We compare our method against the standard DALI [HS93] and CE [SB98] methods. On a thoroughly designed benchmark set of 68 protein structure pairs, MatAlign archives more accurate alignment results, according to 4 different quality criteria, than both DALI and CE in a majority of cases. MatAlign's alignments are usually tighter, albeit shorter, than those of DALI and CE. It means that MatAlign's alternative alignments can effectively detect the highly conserved common structural cores in pairs of related proteins.

The theoretical worst-case time complexity of the algorithm for two proteins with m and n residues respectively is $O(m^2n^2)$. However, in practice, MatAlign is reasonably fast. It is about 3 times faster than DALI, and has about the same speed as CE.

The MatAlign software is available for download from the web site: `http://xena1.ddns.comp.nus.edu.sg/~genesis/MatAlign/`.

1.2.2 Rapid Protein Structure Database Retrieval

In response to the motivation descried in Section 1.1.2, we propose rapid protein structure database search schemes based on *inverted indexing*. We first proposed **ProtDex** (Protein Indexing) [AFT03], and later it was superseded by the more powerful **ProtDex2** (Protein Indexing version 2) method [AT04b]. These are among the pioneering works in index-based structural database searching. We will focus on ProtDex2 in this thesis.

ProtDex2 can efficiently handle large protein structure databases, and provide reasonably accurate results in a very short time. In this method, we represent 3D proteins as 2D distance matrices, and partition these matrices into a set of *contact*

patterns each representing an interaction between a pair of *secondary structure elements* (see Section 2.2). We associate each contact patterns with 8 attribute values describing its various elemental, geometrical, and spatial properties. Then, we pool all the contact patterns from all protein structures in the database, and hash them into a 8 dimensional *hash table*. An *inverted index* is constructed in such a way that each hash table cell holds a pointer to a list of proteins which contain the types of contact patterns belonging to this cell.

When a query protein structure is to be searched, it is also represented as a contact pattern set. Then, all the proteins in the database are ranked simultaneously and incrementally by their similarities with respect to the query protein. This ranking is done with the help of the inverted index of contact patterns constructed beforehand. A certain number of top-ranking protein structures (i.e. those most similar to the query protein) are retrieved and returned as the answer. No pairwise comparison needs to be performed in this database search process at all.

The ideas of inverted indexing and protein ranking are adopted from the area of *information retrieval (IR)* [BYRN99, BOSD+97]. ProtDex2 is particularly efficient in searching large databases. Its query time only increases sub-linearly when the database size grows, because of the inverted indexing strategy.

The degree of accuracy provided by ProtDex2 is adequate for the practical purposes, as can be observed in our experiments. In comparison with the aforementioned Topscan [Mar00] fast database scan method, ProtDex2 is not only much faster (from 4 to 113 times depending on database size), but also slightly more accurate. ProtDex2 is also both speedier and more effective than its predecessor ProtDex method [AFT03]. In comparison with exhaustive searching using DALI and CE detailed alignment methods, ProtDex2 is very much faster, whilst not much sacrificing the accuracy. It takes only a few seconds for a database retrieval task that costs several hours for DALI and CE.

The ProtDex2 software is available for download from the web site: `http://xena1.ddns.comp.nus.edu.sg/~genesis/ProtDex2/`.

1.2.3 Protein Structure Classification

In order to fulfill the motivation descried in Section 1.1.3, we propose a new structural classification algorithm named **ProtClass** (Protein Classification) [AT05]. ProtClass is basically a nearest-neighbor classification system with some augmentations.

We use a two-level scheme to represent a protein structure. In the first level, we represent a protein structure in a very concise format called *protein abstract* which describes 6 global structural features of the protein. In the second level, we represent a protein structure as a set of 10-attribute contact patterns, which is very to the one mentioned above in Section 1.2.2. We encode each contact pattern as a 4-bit integer by discretizing and concatenating its 10 attribute values.

In the learning phase, given a database of protein structures with their class labels (i.e. training protein structures), we study the distributions of the 6 protein abstract attribute values in each distinct class, and determines the allowable threshold parameters of each attribute for each class. We also determine relative membership value (weight) of each training protein structure with respect to the other members in its class and its nearest class, in terms of its protein abstract distance and contact pattern set distance to them. If a protein is around the center of its class, it is given a high membership weight; if it is an outlier, a negative membership weight is given.

In the classification phase, we use a filter-and-refine approach. In the filtering step, we compare the protein abstract of the query protein against those of the database proteins, and filter out the improbable ones using the threshold parameters obtained from the learning phase. In the refinement step, we match the query's discretized contact pattern set (i.e. a set of 4-bit integers) with those of the database proteins using a fast linear-time algorithm. The final ranking for a database protein is determined using all its protein abstract score, contact pattern set score and membership value. Then we can take the k-top ranking proteins, and determine the class of the query by majority voting of the classes of those k proteins. Alternatively, we can supply all the distinct classes of these k proteins

as the possible answers.

In ProtClass, we have made two important contributions on top of conventional nearest-neighbor classification. Firstly, we design our data structures and similarity scoring function to be just enough to highlight a few nearest structures that will be relevant in determining the class for the query (rather than trying to cover all or a majority of structures, as would be required in a normal database search system). This strategy greatly improves the system's speed whist not much sacrificing the classification accuracy. Secondly, we incorporate some "learning" elements into the scheme. We learn and reapply the characteristics of the existing classes and their members such as the class-dependent threshold parameters and the membership weights. This learning system offers better accuracy than the basic algorithm without any learning.

We compare our proposed ProtClass method against two other purpose-built protein structure classification schemes, namely SGM [RF03] and CPMine [AT04a] using a subset of SCOP database [HAB+97] as a benchmark. ProtClass is found to be much faster than SGM, and still slightly more accurate than it. ProtClass is as fast as CPMine, whilst offering much greater accuracy. We also compare ProtClass against two conventional nearest-neighbor classification schemes based on the DALI and CE detailed structure alignment methods respectively. ProtClass is very much faster than these methods, whilst the accuracy is only marginally compromised.

The ProtClass software is available from: `http://xena1.ddns.comp.nus.edu.sg/~genesis/ProtClass/`.

1.2.4 Protein–Protein Interface Clustering

With a view to develop a protein–protein interface clustering system in accordance with the motivation discussed in Section 1.1.4, we propose **PICluster** (Protein–Protein Interface Clusterer) [ATNT06].

We use a new concept of *spatial ordering* to arrange the residues in the fragments of an interface. In order to capture the interacting nature of two spatially ordered protein fragments in the interface, we represent it as an *interface matrix*

capturing the geometrical configuration of the interacting residues.

Naturally, when we try to cluster the interfaces, we need an algorithm to compare them (i.e. their interface matrices in this case) in order to calculate their similarities all-against-all. Unfortunately, we cannot directly use the existing matrix comparison algorithms such as DALI and MatAlign, because they are not only slow, but also are not designed to handle asymmetrical matrices like the interface matrices. Thus, we propose an algorithm to compare the interfaces by representing them as multi-dimensional feature vectors, and calculate the similarity between two vectors by a simple mathematical function.

First, we select a set of non-redundant protein–protein interfaces to be clustered based on the sequence similarities of their constituent protein fragments. We subdivide each interface matrix into 6×6 overlapping submatrices, pool all possible submatrices from all interfaces, and select a few representative "types" of them. Then, we formulate a feature vector for each interface by counting the types of submatrices it contains. Finally, we can calculate all-against-all similarities of all interfaces by the cosine similarity measures [BOSD+97] between the pairs of vectors.

Then, we build the interface clusters using a modified nearest-neighbor clustering algorithm [Dun03]. We validate the quality of the clusters by silhouette analysis [KR90], and confirm that the quality is acceptable. We also conduct a visual inspection of the clusters and find that the members in the same cluster are visually similar in general. In addition, we also carry out a biological analysis of the clusters regarding the structural diversity of the parent protein complexes. We also observe that we can rediscover some well-known biological motifs in our clusters. Furthermore, we compare our method with the sequence-only clustering approach, and find out that ours is much better in terms of the statistical significance of the resultant clusters.

The PICluster software is available from: `http://xena1.ddns.comp.nus.edu.sg/~genesis/PICluster/`.

1.2.5 Publications

The work in this thesis have been published or submitted for publications. The work in Chapter 4 is presented in [AT06]. The work in Chapter 5 appears in [AT04b], The work in Chapter 6 is published in [AT05]. The work in Chapter 7 is presented in [ATNT06].

1.3 Thesis Layout

The remaining of the thesis is organized as follows. In **Chapter 2**, we cover the miscellaneous background information regarding 3D protein structures. In **Chapter 3**, we outline some of the previous and contemporary works that are related to the methods discussed in this thesis. We propose four novel methods for analyzing protein structures in the subsequent chapters. **Chapter 4** describes the detailed protein structure alignment tool named "MatAlign". **Chapter 5** deals with the rapid protein structure database retrieval method called "ProtDex2". **Chapter 6** is about the quick and effective protein structure classification scheme named "ProtClass". **Chapter 7** gives a detailed account on the protein–protein interface clustering system called "PICluster". Finally in **Chapter 8**, we discuss the future works and concludes the thesis.

CHAPTER 2

Preliminaries

We will discuss general information regarding 3D protein structures in this chapter. We will cover four topics, namely protein formation, protein structure hierarchy, protein structure information resources, and distance matrix representation.

2.1 Protein Formation

Amino acids (AAs) are the basic building blocks of life. There are 20 different AA types as given in Table 2.1. Each AA consists of:

1. central carbon atom (called C_α atom)
2. hydrogen atom (H)
3. amino group (H_3N^+)
4. carboxyl group (COO^-)
5. side chain (R) group

There are 20 different R groups each corresponding to one AA type. Figure 2.1 shows the formation of an AA called Alanine as an example.

Table 2.1: 20 amino acid (AA) types.

Name	3-letter Symbol	1-letter Symbol	Name	3-letter Symbol	1-letter Symbol
Alanine	ALA	A	Leucine	LEU	L
Arginine	ARG	R	Lysine	LYS	K
Asparagine	ASN	N	Methionine	MET	M
Aspartic acid	ASP	D	Phenylalanine	PHE	F
Cysteine	CYS	C	Proline	PRO	P
Glutamic acid	GLU	E	Serine	SER	S
Glutamine	GLN	Q	Threonine	THR	T
Glycine	GLY	G	Tryptophan	TRP	W
Histidine	HIS	H	Tyrosine	TYR	Y
Isoleucine	ILE	I	Valine	VAL	V

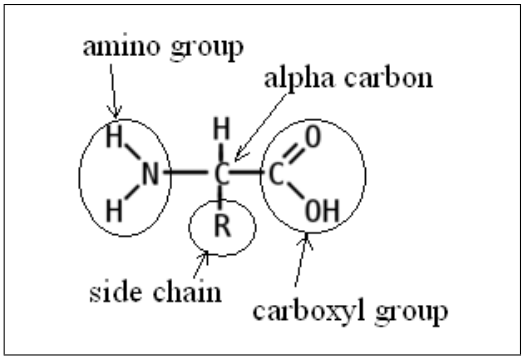

Figure 2.1: Formation of an amino acid (adapted from Wikipedia [Wik06] public domain image resource).

AAs are linked together by *peptide* bonds, each between a pair of adjacent AAs. As an example, Figure 2.2 demonstrates the formation of peptide bonds in 3 consecutive AAs.

A group of linked AAs form a *polypeptide chain* (or sometimes simply a *peptide chain*). In a polypeptide chain, each AA, except the very first and the last ones, has to give up two hydrogen atoms from its amino group to form a peptide bond

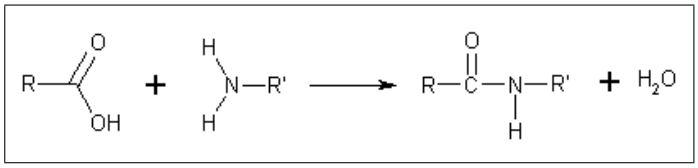

Figure 2.2: Chaining of amino acids by peptide bonds (reproduced from Wikipedia [Wik06] public domain image resource).

at one end, and one oxygen atom from its carboxyl group to form another peptide bond at the other end. Thus, the remaining structure of an AA in a polypeptide chain is called a *residue*. (However, sometimes an "AA residue" is just referred to as an "AA" [without residue] for simplicity.) The very first AA has a free amino group, and is called the *N-terminus* of the polypeptide chain, the last AA has a free carboxyl group, and is called the *C-terminus*. Figure 2.3 shows an example of polypeptide chain. One or more polypeptide chains make up a *protein*. (Technically speaking, one polypeptide chain corresponds to one protein chain. A group of two or more interacting polypeptide chains [protein chains] form a protein complex. However, for simplicity, both "protein chain" and "protein complex" are referred to just as "protein" when no distinction is required.)

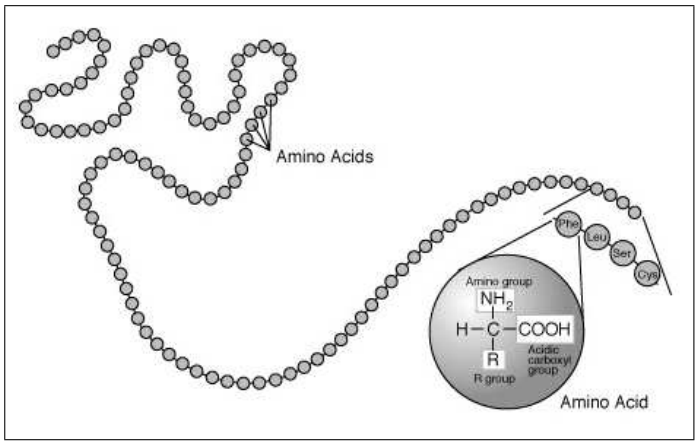

Figure 2.3: A polypeptide chain (adapted from Wikipedia [Wik06] public domain image resource).

2.2 Protein Structure Hierarchy

The central dogma in molecular biology is that DNA transcribes RNA, and RNA is translated into a protein. Immediately after translation, the protein folds into its most stable three-dimensional (3D) form that requires the minimum energy. This folding takes only a few milliseconds. Folding of a protein is driven by the various forces of nature such as hydrophobicity, hydrogen bonding, Van der Waals interactions, ion pairing, disulfide bonds, etc. formed by its constituent AA residues [BT99].

It has been discovered that the AA residue composition (or AA sequence) of a protein "uniquely" determines its 3D structure [EA62]. (An "AA sequence" of a protein refers to the linear composition of its constituent AA residues. It is merely a logical form of representation for a protein. In nature, a protein cannot physically exist as a linear sequence [unfolded state] for a long time.) However, the exact nature of sequence–structure relationship, i.e. which properties of AA residues actually cause which kinds of 3D shapes, is very complicated and not fully understood yet. In other words, given an AA sequence, we still cannot accurately predict what definite 3D structure the protein will have [Ros03].

2.2.1 Primary, Secondary, Tertiary, and Quaternary Structures

The AA sequence of protein is called its *primary structure*. The folded 3D structure of a protein is called its *tertiary structure*. Within the tertiary structure of a protein, there are some recurring sub-structures with particular shapes called the *secondary structures*, which are principally formed by the hydrogen bonds between the residues. *Alpha helix* and *beta sheet/strand* (also known as *pleated sheet/strand*) are the two common types of *secondary structure elements* (SSEs). The other portions in the tertiary structure which are not parts of any SSE are called *loop* (or *turn*) regions. Loops usually have random shapes. The annotation of SSEs, i.e. which portions in a particular protein should be defined as the SSEs,

is somewhat subjective. Nevertheless, the two major SSE annotation methods, namely DSSP [KS83] and STRIDE [FA95], agree in their SSE definitions in 95% of the cases [MLM+05].

Often, a tertiary structure only means the 3D form of a single protein (polypeptide) chain. The 3D structure of an entire protein complex formed by a collection of tertiary structures is referred to as a *quaternary structure*. However, there are also some standalone tertiary structures that do not further make up any quaternary structure. (The general term "protein structure" may refer to either tertiary structure or quaternary structure depending on the context.)

The relationships among the primary, secondary, tertiary and quaternary structures of a protein are depicted in Figure 2.4.

For illustration, let us look at a sample protein named "Class pi Glutathione S-transferase protein from Mouse" whose PDB ID is `1glq`. It is a protein complex composed of two proteins chains namely *Chain A* (denoted as `1glqA`) and *Chain B* (denoted as `1glqB`). Let us first look at the chain `1glqA`. Figure 2.5 shows the primary structure (AA sequence) of `1glqA`. Figure 2.6 depicts the tertiary (3D) structure of `1glqA` in the space-fill model, which approximately represents the actual shape of protein in its natural existence.

Figure 2.7 illustrates `1glqA` in the cartoon model, which emphasizes its constituent SSEs. Alpha helices are depicted as spirals, the beta sheets as arrows, and the loops as small tubes. Figure 2.8 shows the quaternary structure of the whole protein complex of `1glq` made up of two chains `1glqA` and `1glqB`.

2.2.2 Super Secondary Structure and Domain

There are two intermediate levels of structures between the secondary and tertiary structures of proteins, namely *super secondary structure* and *domain*. A super secondary structure is a collection SSEs with a particular pattern that can be found in a number of proteins. Some examples of super secondary structures are helix-loop-helix, beta ribbon, beta-alpha-beta, zinc finger, EF hand, Greek key, etc. [BT99]. A super secondary structure is sometimes called a *structural motif*.

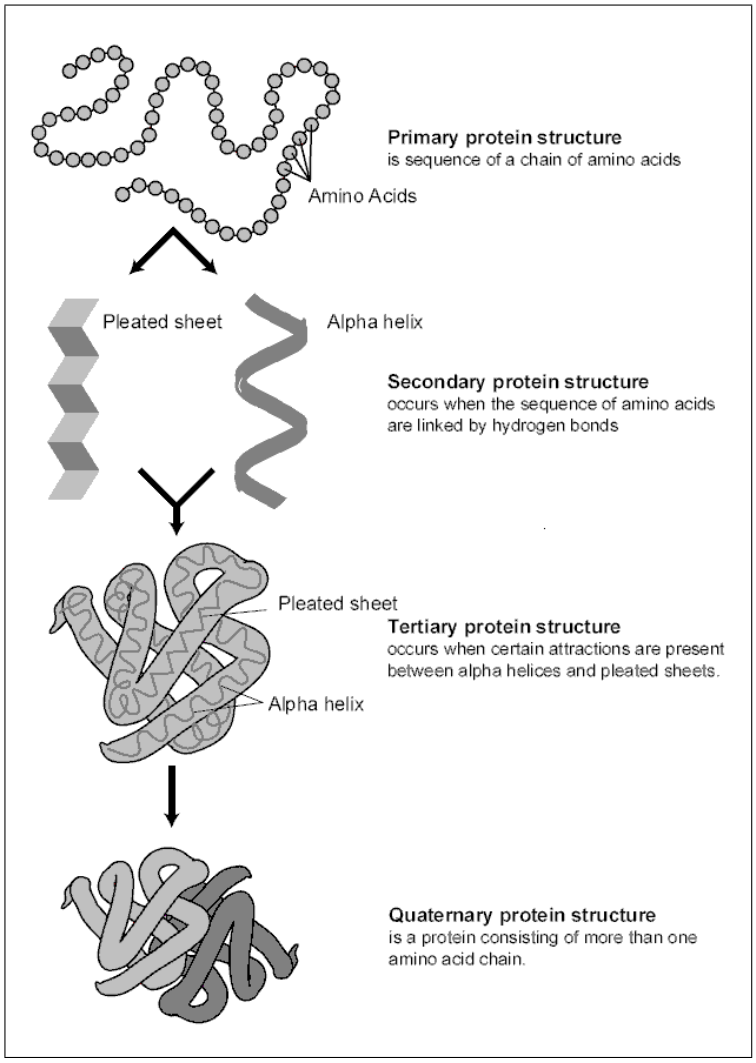

Figure 2.4: Protein primary, secondary, tertiary and quaternary structures (reproduced from Wikipedia [Wik06] public domain image resource).

(However, the term "structural motif" is more general, and can also be used in other contexts such as [BKB02, JECT02].)

A domain is a semi-autonomous region that is only weakly interconnected to the other regions within a protein structure. Some tertiary structures comprises two or more domains, whereas some are each made up of only a single domain. There are even some cases in which a domain exists across two or more tertiary structures in a quaternary structure. Most of the protein structure class annotation schemes, such as [HAB+97, HS98, OMJ+97], mainly focus on the domains rather than the whole tertiary or quaternary structures.

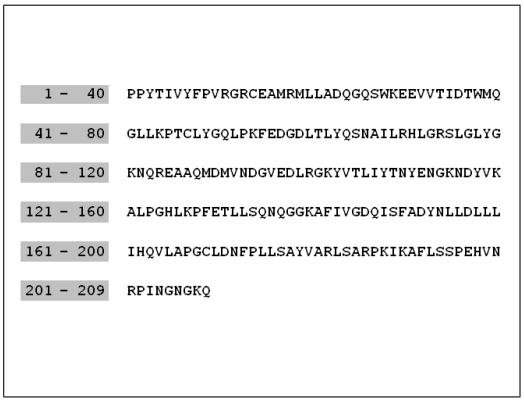

Figure 2.5: Primary structure (AA sequence) of protein `1glqA` with 209 residues.

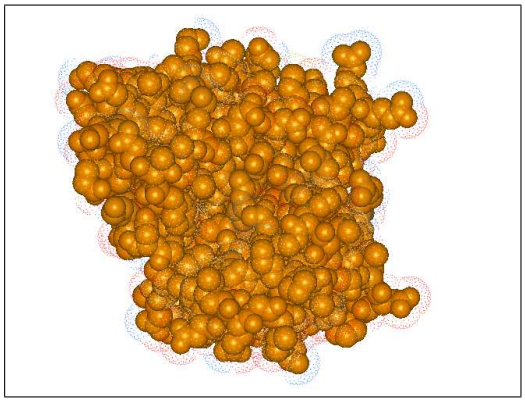

Figure 2.6: Tertiary structure (3D structure) of protein `1glqA` in space-fill model (generated with Molsoft ICM-Browser [ABC+97]).

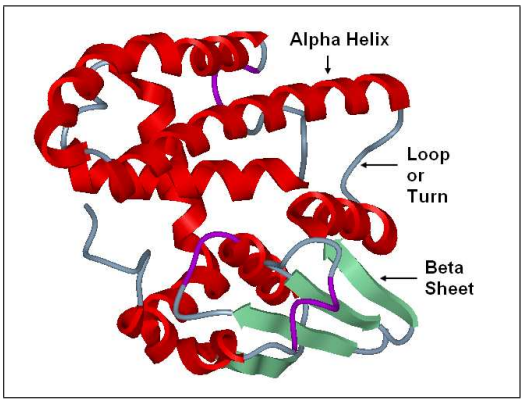

Figure 2.7: Secondary structure elements (SSEs) in protein `1glqA` (generated with Molsoft ICM-Browser [ABC+97]).

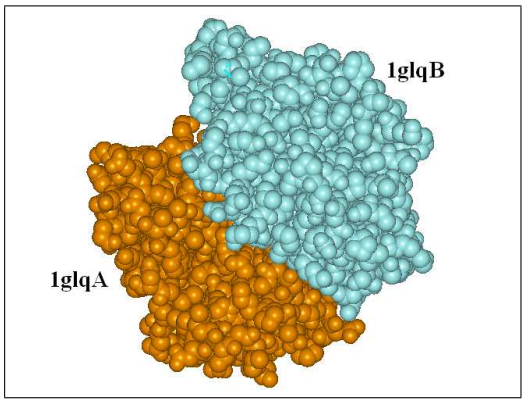

Figure 2.8: Quaternary structure of protein complex `1glq` with two chains `1glqA` and `1glqB` (generated with Molsoft ICM-Browser [ABC+97]).

Unlike the SSE annotation, the annotations of super secondary structure and domain are much more subjective. Super secondary structures are usually defined based on their corresponding biological functions. To our knowledge, there is no comprehensive system for either manual or automatic annotations of super secondary structures yet. SCOP [HAB+97] and CATH [OMJ+97] provide manual and semi-manual identifications of the protein domains, along with their struc-

tural class annotations. PPU [HS94b] and PDP [AS03] are available for automatic domain annotations. However, the domain definitions given by all these methods are different from each other's in a number of cases [VBAS04].

Figure 2.9 exhibits the existences of two super secondary structures, namely helix-loop-helix and zinc finger-like motifs, in `1glqA`. Figure 2.10 shows two structural domains in `1glqA` according to SCOP definitions. Residue numbers 1–78 is annotated as *domain* 2 (denoted as `d1glqa2` in SCOP), and residue numbers 79–209 as *domain* 1 (denoted as `d1glqa1`).

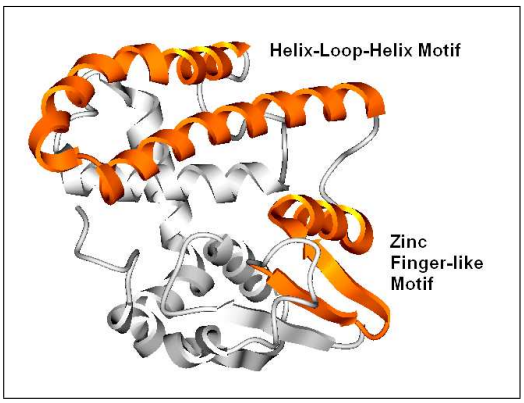

Figure 2.9: Super secondary structures (motifs) in protein `1glqA` (generated with Molsoft ICM-Browser [ABC+97]).

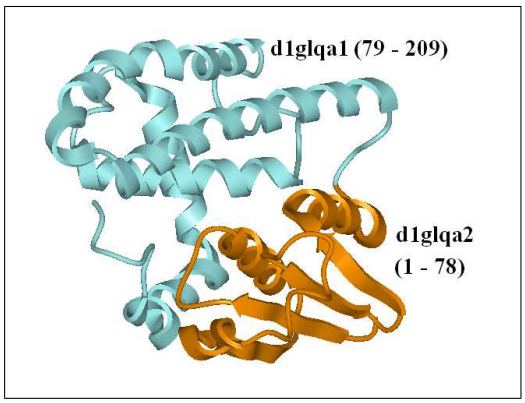

Figure 2.10: Two domains in protein `1glqA` (generated with Molsoft ICM-Browser [ABC+97]).

2.3 Protein Structure Information Resources

2.3.1 3D Structure and AA Sequence

PDB (Protein Data Bank) [BWF+00] is the largest repository and the primary source of information for 3D protein structures. It stores the structural information and annotations of several bio-molecules: mainly proteins, along with some nucleic acids and carbohydrates. Each protein in PDB is identified by a unique ID of the format `naaa`, where `n` is an integer and `a` is an alphanumeric character (e.g. `1glq`). PDB stores both multi-chain proteins (protein complexes) and single-chain

(standalone) proteins. A chain in a complex is denoted with its chain ID suffixed to its main PDB ID (e.g. `1glqA`). A single-chain protein is denoted just the same as its PDB ID or with an underscore suffixed to it (e.g. `1mbd` or `1mbd_`).

As of November 2006, PDB stores about 40,000 protein structures. The size of PDB database has been growing rapidly during the recent years because of the advancements in the laboratory methods, such as nuclear magnetic resonance (NMR) and X-ray crystallography, to determine the 3D structures of proteins. Figure 2.11 shows the growth of PDB database over the years. (The data is obtained from PDB website `http://www.rcsb.org/pdb/`.)

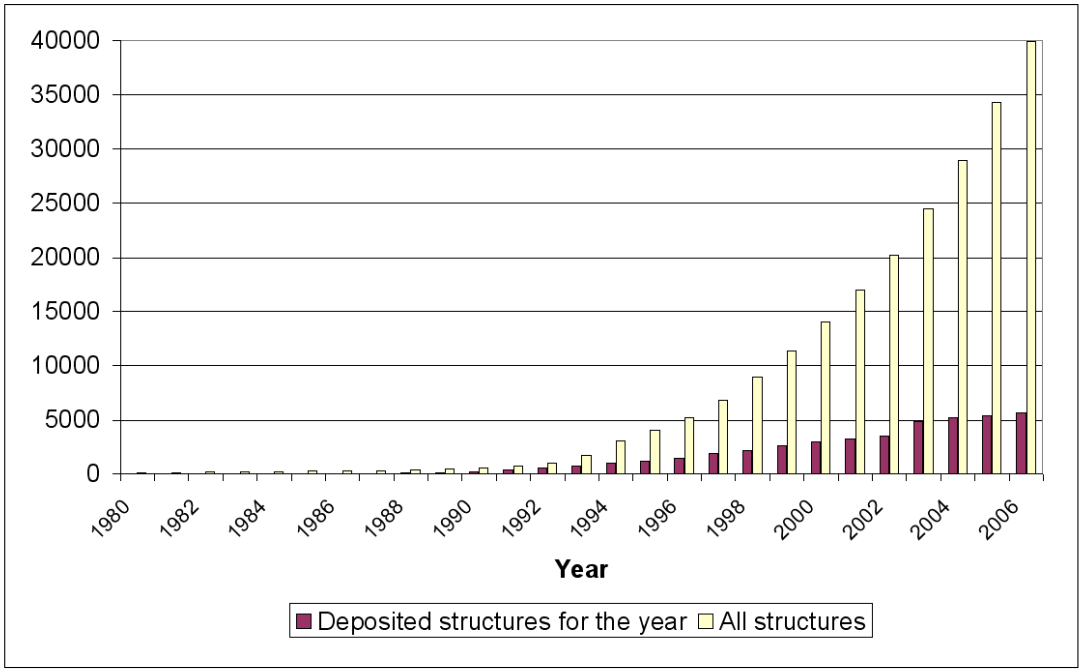

Figure 2.11: Growth of PDB database over the years.

For each protein, PDB provides the 3D (x, y, z) coordinates of the constituent atoms of its AA residues in a particular reference frame, alongside with other information about the protein such as its AA sequence, related publications, cross-references to other data sources, crystallization parameters, bio-chemical properties, ligands, and SSE annotations, etc. PDB stores all these 3D coordinates and other information for each protein as a formatted text file. Figure 2.12 is an excerpt from the `ATOM` section of the PDB file of protein `1glq`. It shows the 3D (x, y, z) coordinates of the chain `1glqA` in the box. The AA sequence of the protein

is also readily available, as shown in the highlight column. (The AA sequence can alternatively be obtained from the `SEQRES` section of the PDB file.)

```
ATOM      1  N   PRO A   1      71.393  -3.633  -4.205  1.00 19.20          1GLQ 217
ATOM      2  CA  PRO A   1      70.301  -4.557  -3.979  1.00 18.50          1GLQ 218
ATOM      3  C   PRO A   1      70.930  -5.713  -3.201  1.00 20.58          1GLQ 219
ATOM      4  O   PRO A   1      72.163  -5.661  -3.016  1.00 20.71          1GLQ 220
ATOM      5  CB  PRO A   1      69.792  -4.952  -5.349  1.00 19.36          1GLQ 221
ATOM      6  CG  PRO A   1      70.615  -4.136  -6.332  1.00 20.18          1GLQ 222
ATOM      7  CD  PRO A   1      71.068  -2.995  -5.461  1.00 20.18          1GLQ 223
ATOM      8  N   PRO A   2      70.234  -6.726  -2.687  1.00 18.71   1      1GLQ 224
ATOM      9  CA  PRO A   2      68.766  -6.840  -2.682  1.00 18.85   1      1GLQ 225
ATOM     10  C   PRO A   2      68.027  -5.809  -1.804  1.00 16.93   1      1GLQ 226
ATOM     11  O   PRO A   2      68.667  -5.226  -0.920  1.00 16.21   1      1GLQ 227
ATOM     12  CB  PRO A   2      68.566  -8.264  -2.261  1.00 19.84   1      1GLQ 228
ATOM     13  CG  PRO A   2      69.752  -8.610  -1.376  1.00 18.95   1      1GLQ 229
ATOM     14  CD  PRO A   2      70.866  -7.878  -2.065  1.00 18.55   1      1GLQ 230
ATOM     15  N   TYR A   3      66.749  -5.495  -2.053  1.00 16.14          1GLQ 231
ATOM     16  CA  TYR A   3      65.992  -4.510  -1.306  1.00 14.37          1GLQ 232
ATOM     17  C   TYR A   3      64.950  -5.217  -0.476  1.00 14.61          1GLQ 233
ATOM     18  O   TYR A   3      64.331  -6.180  -0.957  1.00 15.09          1GLQ 234
ATOM     19  CB  TYR A   3      65.260  -3.565  -2.212  1.00 12.45          1GLQ 235
ATOM     20  CG  TYR A   3      66.127  -2.805  -3.171  1.00 13.79          1GLQ 236
ATOM     21  CD1 TYR A   3      67.026  -1.850  -2.692  1.00 15.13          1GLQ 237
ATOM     22  CD2 TYR A   3      65.981  -3.020  -4.545  1.00 15.18          1GLQ 238
ATOM     23  CE1 TYR A   3      67.781  -1.088  -3.595  1.00 15.96          1GLQ 239
ATOM     24  CE2 TYR A   3      66.737  -2.264  -5.450  1.00 15.90          1GLQ 240
ATOM     25  CZ  TYR A   3      67.632  -1.299  -4.964  1.00 15.48          1GLQ 241
ATOM     26  OH  TYR A   3      68.397  -0.532  -5.822  1.00 16.62          1GLQ 242
.                .                    .                .
.                .                    .                .
.                .                    .                .
ATOM   1632  N   GLY A 207      41.823   3.072   9.115  1.00 32.56          1GLQ1848
ATOM   1633  CA  GLY A 207      40.638   3.049   8.271  1.00 33.72          1GLQ1849
ATOM   1634  C   GLY A 207      40.210   4.396   7.695  1.00 32.87          1GLQ1850
ATOM   1635  O   GLY A 207      39.355   4.423   6.811  1.00 37.71          1GLQ1851
ATOM   1636  N   LYS A 208      40.720   5.543   8.132  1.00 28.02          1GLQ1852
ATOM   1637  CA  LYS A 208      40.376   6.797   7.494  1.00 26.50          1GLQ1853
ATOM   1638  C   LYS A 208      41.216   7.048   6.243  1.00 27.14          1GLQ1854
ATOM   1639  O   LYS A 208      42.320   6.518   6.110  1.00 26.03          1GLQ1855
ATOM   1640  CB  LYS A 208      40.534   7.869   8.536  1.00 25.77          1GLQ1856
ATOM   1641  CG  LYS A 208      39.477   7.531   9.557  1.00 29.09          1GLQ1857
ATOM   1642  CD  LYS A 208      39.695   8.285  10.809  1.00 34.79          1GLQ1858
ATOM   1643  CE  LYS A 208      38.681   7.750  11.791  1.00 39.90          1GLQ1859
ATOM   1644  NZ  LYS A 208      38.819   8.452  13.057  1.00 45.12          1GLQ1860
ATOM   1645  N   GLN A 209      40.618   7.714   5.266  1.00 27.17          1GLQ1861
ATOM   1646  CA  GLN A 209      41.196   8.073   3.984  1.00 26.91          1GLQ1862
ATOM   1647  C   GLN A 209      40.282   9.140   3.361  1.00 26.77          1GLQ1863
ATOM   1648  O   GLN A 209      39.222   9.433   3.932  1.00 26.62          1GLQ1864
ATOM   1649  CB  GLN A 209      41.299   6.855   3.028  1.00 27.07          1GLQ1865
ATOM   1650  CG  GLN A 209      40.069   6.024   2.653  1.00 26.60          1GLQ1866
ATOM   1651  CD  GLN A 209      40.453   4.773   1.884  0.00 27.28          1GLQ1867
ATOM   1652  OE1 GLN A 209      39.880   4.410   0.864  0.00 27.41          1GLQ1868
ATOM   1653  NE2 GLN A 209      41.463   4.034   2.319  0.00 27.42          1GLQ1869
ATOM   1654  OXT GLN A 209      40.620   9.693   2.310  1.00 23.93          1GLQ1870
TER    1655      GLN A 209                                                  1GLQ1871
```

Figure 2.12: 3D Coordinates of `1glqA` in PDB format. (The measurements are in Angstroms (Å).)

In an AA residue, its C_α atom is usually regarded as the center and representative atom of the residue, because it is centrally connected to all amino, carboxyl and side chain groups of the residue (see Figure 2.1). (Thus, when the term "residue" is used in geometrical context, it usually means its "C_α atom" unless explicitly

stated otherwise. For example, a distance between two residues actually means the distance between their C_α atoms.) It should be noted that the C_α atom is not necessarily the geometric center or the center of mass of a residue.

A *backbone* of a protein structure is an imaginary line in 3D space connecting all its C_α atoms from its N-terminus to C-terminus sequentially. The entire 3D shape of a protein can be roughly approximated by its backbone. Many structural comparison, classification and clustering applications usually take only the C_α backbone of a protein into account, and ignore all other atoms for simplicity [HS93].

The C_α atoms are shown highlighted in Figure 2.12. The backbone of protein `1glqA` is illustrated in Figure 2.13.

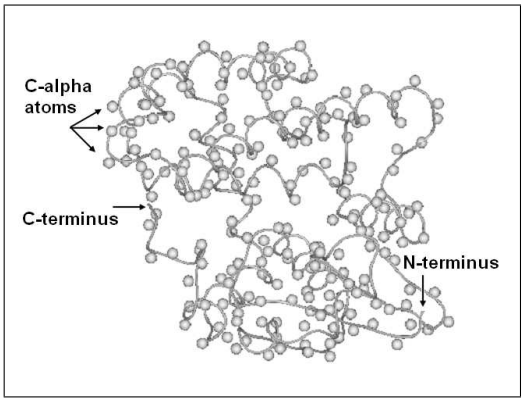

Figure 2.13: C_α backbone of `1glqA` (generated with ICM-Browser [ABC+97]).

2.3.2 Secondary Structure Annotation

PDB does not always provide the SSE annotations for all of its proteins. Even when provided, some annotations are incomplete [MLM+05]. As mentioned in Section 2.2, researchers typically use DSSP [KS83] or STRIDE [FA95] as SSE annotation tools. We use the latter in our research presented in this thesis. Figure 2.14 demonstrates the SSE annotation for protein `1glqA` by STRIDE. The alpha helix are denoted as `H`, and the beta sheet (strand) as `E`. The 3–10 helix, denoted as `G`, is a special type of helix, and can generally be treated as the normal alpha helix [SB97].

```
REM  ------------------- Secondary structure summary ------------------  ~~~~
REM                                                                     ~~~~
CHN  c:\thesis\1glqA.pdb A                                              ~~~~
REM                                                                     ~~~~
REM                .         .         .         .         .          ~~~~
SEQ  1    PPYTIVYFPVRGRCEAMRMLLADQGQSWKEEVVTIDTWMQGLLKPTCLYG   50      ~~~~
STR         EEEEE      HHHHHHHHHHH    EEEE  HHHHHH   GGG             ~~~~
REM                                                                     ~~~~
REM                .         .         .         .         .          ~~~~
SEQ  51   QLPKFEDGDLTLYQSNAILRHLGRSLGLYGKNQREAAQMDMVNDGVEDLR  100     ~~~~
STR          EEEE  EEEE HHHHHHHHHHHHH      HHHHHHHHHHHHHHHHHH         ~~~~
REM                                                                     ~~~~
REM                .         .         .         .         .          ~~~~
SEQ  101  GKYVTLIYTNYENGKNDYVKALPGHLKPFETLLSQNQGGKAFIVGDQISF  150     ~~~~
STR       HHHHHHHHHHHHHHHHHHHHHHHHHHHHHHHHHHH GGG          H         ~~~~
REM                                                                     ~~~~
REM                .         .         .         .         .          ~~~~
SEQ  151  ADYNLLDLLLIHQVLAPGCLDNFPLLSAYVARLSARPKIKAFLSSPEHVN  200     ~~~~
STR       HHHHHHHHHHHHHHH        HHHHHHHHHHHH HHHHHHHH HHHHH          ~~~~
REM                                                                     ~~~~
REM                                                                     ~~~~
SEQ  201  RPINGNGKQ                                          209       ~~~~
STR                                                                     ~~~~
REM                                                                     ~~~~
REM                                                                     ~~~~
REM                                                                     ~~~~
LOC  AlphaHelix   CYS    14 A      GLN     24 A                        ~~~~
LOC  AlphaHelix   ILE    35 A      GLN     40 A                        ~~~~
LOC  AlphaHelix   SER    65 A      LEU     76 A                        ~~~~
LOC  AlphaHelix   GLN    83 A      GLN    135 A                        ~~~~
LOC  AlphaHelix   PHE   150 A      LEU    165 A                        ~~~~
LOC  AlphaHelix   PRO   174 A      ALA    185 A                        ~~~~
LOC  AlphaHelix   PRO   187 A      SER    194 A                        ~~~~
LOC  AlphaHelix   PRO   196 A      ASN    200 A                        ~~~~
LOC  310Helix     LYS    44 A      THR     46 A                        ~~~~
LOC  310Helix     GLN   137 A      GLY    139 A                        ~~~~
LOC  Strand       TYR     3 A      TYR      7 A                        ~~~~
LOC  Strand       LYS    29 A      VAL     32 A                        ~~~~
LOC  Strand       LYS    54 A      ASP     57 A                        ~~~~
LOC  Strand       LEU    60 A      TYR     63 A                        ~~~~
```

Figure 2.14: STRIDE secondary structure annotation for `1glqA`.

2.3.3 Domain Definition and Structural Class Annotation

SCOP [HAB+97] and CATH [OMJ+97] are the two standard domain identification and structural class annotation schemes. (Although the term "structural classification" is widely used for SCOP and CATH, we avoid it here, in order to distinguish them from the automatic classification [supervised learning] systems, which are also contained in this thesis.) We use SCOP in our research. It is a manually constructed system, in which human experts identify the domains in PDB's protein structures, and assign the hierarchical class labels — Class, Fold, Superfamily and Family — to these domains. SCOP is usually regarded as a gold standard for structural class annotation by biologists [Lic01].

Figure 2.15 shows an excerpt from SCOP database highlighting the entries for the two domains `d1glqa1` and `d1glqa2` of protein chain `1glqA`. The structural class

designation of `d1glqa1` is `a.45.1.1` in short format or `(46456, 47615, 47616, 47617)` in long format. Similarly, the structural class designation of `d1glqa2` is `c.47.1.5` or `(51349, 52832, 52833, 52862)`.

ASTRAL [BKL00] database provides the actual 3D coordinates of the SCOP domains as PDB-format files, one for each domain.

```
# dir.cla.scop.txt
# SCOP release 1.65 (December 2003)  [File format version 1.00]
# http://scop.mrc-lmb.cam.ac.uk/scop/
# Copyright (c) 1994-2003 the scop authors; see http://scop.mrc-lmb.cam.ac.uk/scop/lic/copy.html
d1dlwa_   1dlw    A:        a.1.1.1    14982 cl=46456,cf=46457,sf=46458,fa=46459,dm=46460,sp=46461,px=14982
d1dlya_   1dly    A:        a.1.1.1    14983 cl=46456,cf=46457,sf=46458,fa=46459,dm=46460,sp=46462,px=14983
.                           .                                                                        .
.                           .                    Class  Fold  Superfamily  Family                  .
.                           .                                                                        .
d2gsra1   2gsr    A:77-207  a.45.1.1   17586 cl=46456,cf=47615,sf=47616,fa=47617,dm=81347,sp=47620,px=17586
d2gsrb1   2gsr    B:77-207  a.45.1.1   17587 cl=46456,cf=47615,sf=47616,fa=47617,dm=81347,sp=47620,px=17587
d1glqa1   1glq    A:79-209  a.45.1.1   17588 cl=46456,cf=47615,sf=47616,fa=47617,dm=81347,sp=47621,px=17588
d1glqb1   1glq    B:79-209  a.45.1.1   17589 cl=46456,cf=47615,sf=47616,fa=47617,dm=81347,sp=47621,px=17589
d1glpa1   1glp    A:79-209  a.45.1.1   17590 cl=46456,cf=47615,sf=47616,fa=47617,dm=81347,sp=47621,px=17590
.                                                                                                   .
.                    Class  Fold  Superfamily  Family                                              .
.                                                                                                   .
d2gsra2   2gsr    A:1-76    c.47.1.5   32880 cl=51349,cf=52832,sf=52833,fa=52862,dm=81358,sp=52865,px=32880
d2gsrb2   2gsr    B:1-76    c.47.1.5   32881 cl=51349,cf=52832,sf=52833,fa=52862,dm=81358,sp=52865,px=32881
d1glqa2   1glq    A:1-78    c.47.1.5   32882 cl=51349,cf=52832,sf=52833,fa=52862,dm=81358,sp=52866,px=32882
d1glqb2   1glq    B:1-78    c.47.1.5   32883 cl=51349,cf=52832,sf=52833,fa=52862,dm=81358,sp=52866,px=32883
d1glpa2   1glp    A:1-78    c.47.1.5   32884 cl=51349,cf=52832,sf=52833,fa=52862,dm=81358,sp=52866,px=32884
.                           .                                                                        .
.                           .                                                                        .
.                           .                                                                        .
```

Figure 2.15: SCOP entries for two domains of `1glqA`.

2.4 Distance Matrix Representation

A 3D protein structure can be represented as a 2D distance matrix. The distance matrix $\mathcal{DM}_A$ of protein A with $|A|$ residues is an $|A| \times |A|$ matrix. The cell $\mathcal{DM}_A[i, j]$ of the distance matrix stores the inter-atomic distance d_{ij} between the two C_α atoms i and j ($1 \leq i, j \leq |A|$) of the protein as shown in Figure 2.16. The inter-atomic distance d_{ij} is the Euclidean distance in 3D space, defined as:

$$d_{ij} = \sqrt{(x_i - x_j)^2 + (y_i - y_j)^2 + (z_i - z_j)^2} \tag{2.1}$$

where (x_i, y_i, z_i) and (x_j, y_j, z_j) are the coordinates of C_α atoms i and j respectively. The main diagonal of a distance matrix consists of the cells with zero distance values, i.e. $d_{ij} = 0$ if $i = j$. In addition, the matrix is symmetrical along its main diagonal, i.e. $d_{ij} = d_{ji}$.

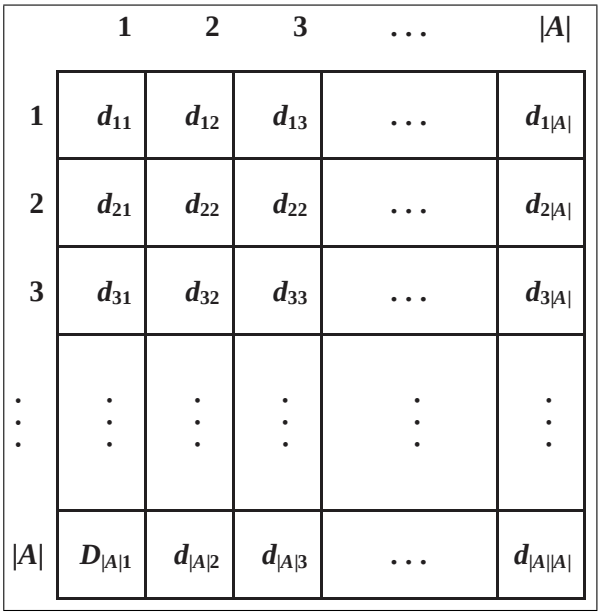

Figure 2.16: 2D distance matrix representation for 3D protein structure.

Distance matrix representation has been used in protein structure studies since 1970s, and is still being popularly used [HP00, HS93]. Representing a protein structure as a distance matrix is useful because it is rotation and translation invariant, yet it still can capture all the structural information about a protein as much as the original 3D representation can. It has been proved that we can reconstruct the original 3D form of a protein from its distance matrix [CH88].

The distance matrix of protein `1glqA` is shown in Figure 2.17. The shaded cells illustrate the diagonal of the matrix, and the arrows indicates the matrix's symmetrical property. Figure 2.18 shows the color-coded distance matrix of `1glqA`, in which we can easily visualize the distributions the C_α–C_α distance values in the matrix. The shorter distances are represented by the brighter colors, and the longer distances by the darker colors.

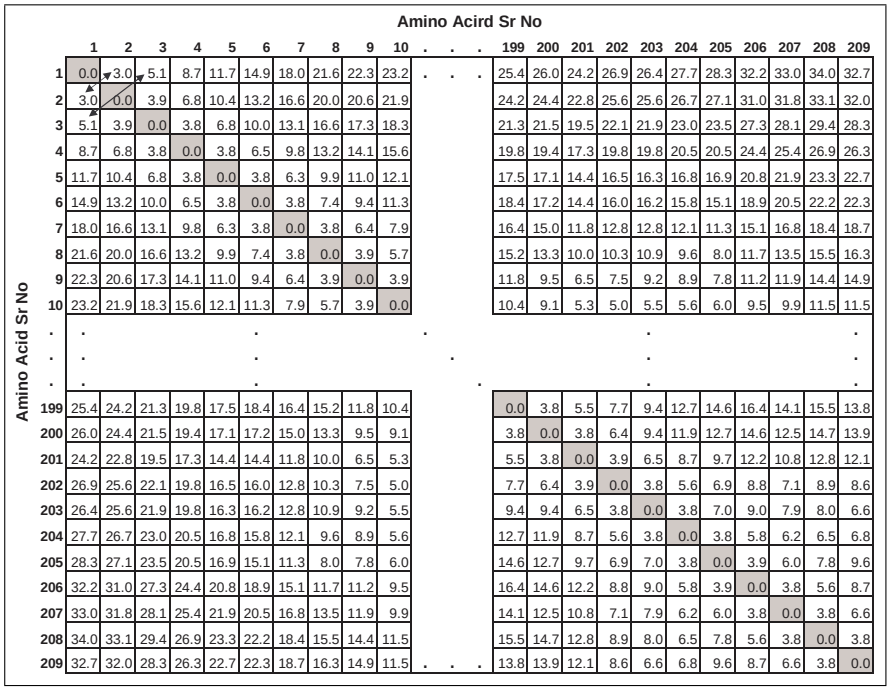

Amino Acid Sr No	1	2	3	4	5	6	7	8	9	10	.	.	.	199	200	201	202	203	204	205	206	207	208	209
1	0.0	3.0	5.1	8.7	11.7	14.9	18.0	21.6	22.3	23.2				25.4	26.0	24.2	26.9	26.4	27.7	28.3	32.2	33.0	34.0	32.7
2	3.0	0.0	3.9	6.8	10.4	13.2	16.6	20.0	20.6	21.9				24.2	24.4	22.8	25.6	25.6	26.7	27.1	31.0	31.8	33.1	32.0
3	5.1	3.9	0.0	3.8	6.8	10.0	13.1	16.6	17.3	18.3				21.3	21.5	19.5	22.1	21.9	23.0	23.5	27.3	28.1	29.4	28.3
4	8.7	6.8	3.8	0.0	3.8	6.5	9.8	13.2	14.1	15.6				19.8	19.4	17.3	19.8	19.8	20.5	20.5	24.4	25.4	26.9	26.3
5	11.7	10.4	6.8	3.8	0.0	3.8	6.3	9.9	11.0	12.1				17.5	17.1	14.4	16.5	16.3	16.8	16.9	20.8	21.9	23.3	22.7
6	14.9	13.2	10.0	6.5	3.8	0.0	3.8	7.4	9.4	11.3				18.4	17.2	14.4	16.0	16.2	15.8	15.1	18.9	20.5	22.2	22.3
7	18.0	16.6	13.1	9.8	6.3	3.8	0.0	3.8	6.4	7.9				16.4	15.0	11.8	12.8	12.8	12.1	11.3	15.1	16.8	18.4	18.7
8	21.6	20.0	16.6	13.2	9.9	7.4	3.8	0.0	3.9	5.7				15.2	13.3	10.0	10.3	10.9	9.6	8.0	11.7	13.5	15.5	16.3
9	22.3	20.6	17.3	14.1	11.0	9.4	6.4	3.9	0.0	3.9				11.8	9.5	6.5	7.5	9.2	8.9	7.8	11.2	11.9	14.4	14.9
10	23.2	21.9	18.3	15.6	12.1	11.3	7.9	5.7	3.9	0.0				10.4	9.1	5.3	5.0	5.5	5.6	6.0	9.5	9.9	11.5	11.5
.	.					.					.							.						.
.	.					.						.						.						.
.	.					.							.					.						.
199	25.4	24.2	21.3	19.8	17.5	18.4	16.4	15.2	11.8	10.4				0.0	3.8	5.5	7.7	9.4	12.7	14.6	16.4	14.1	15.5	13.8
200	26.0	24.4	21.5	19.4	17.1	17.2	15.0	13.3	9.5	9.1				3.8	0.0	3.8	6.4	9.4	11.9	12.7	14.6	12.5	14.7	13.9
201	24.2	22.8	19.5	17.3	14.4	14.4	11.8	10.0	6.5	5.3				5.5	3.8	0.0	3.9	6.5	8.7	9.7	12.2	10.8	12.8	12.1
202	26.9	25.6	22.1	19.8	16.5	16.0	12.8	10.3	7.5	5.0				7.7	6.4	3.9	0.0	3.8	5.6	6.9	8.8	7.1	8.9	8.6
203	26.4	25.6	21.9	19.8	16.3	16.2	12.8	10.9	9.2	5.5				9.4	9.4	6.5	3.8	0.0	3.8	7.0	9.0	7.9	8.0	6.6
204	27.7	26.7	23.0	20.5	16.8	15.8	12.1	9.6	8.9	5.6				12.7	11.9	8.7	5.6	3.8	0.0	3.8	5.8	6.2	6.5	6.8
205	28.3	27.1	23.5	20.5	16.9	15.1	11.3	8.0	7.8	6.0				14.6	12.7	9.7	6.9	7.0	3.8	0.0	3.9	6.0	7.8	9.6
206	32.2	31.0	27.3	24.4	20.8	18.9	15.1	11.7	11.2	9.5				16.4	14.6	12.2	8.8	9.0	5.8	3.9	0.0	3.8	5.6	8.7
207	33.0	31.8	28.1	25.4	21.9	20.5	16.8	13.5	11.9	9.9				14.1	12.5	10.8	7.1	7.9	6.2	6.0	3.8	0.0	3.8	6.6
208	34.0	33.1	29.4	26.9	23.3	22.2	18.4	15.5	14.4	11.5				15.5	14.7	12.8	8.9	8.0	6.5	7.8	5.6	3.8	0.0	3.8
209	32.7	32.0	28.3	26.3	22.7	22.3	18.7	16.3	14.9	11.5	.	.	.	13.8	13.9	12.1	8.6	6.6	6.8	9.6	8.7	6.6	3.8	0.0

Figure 2.17: Distance matrix of `1glqA`.

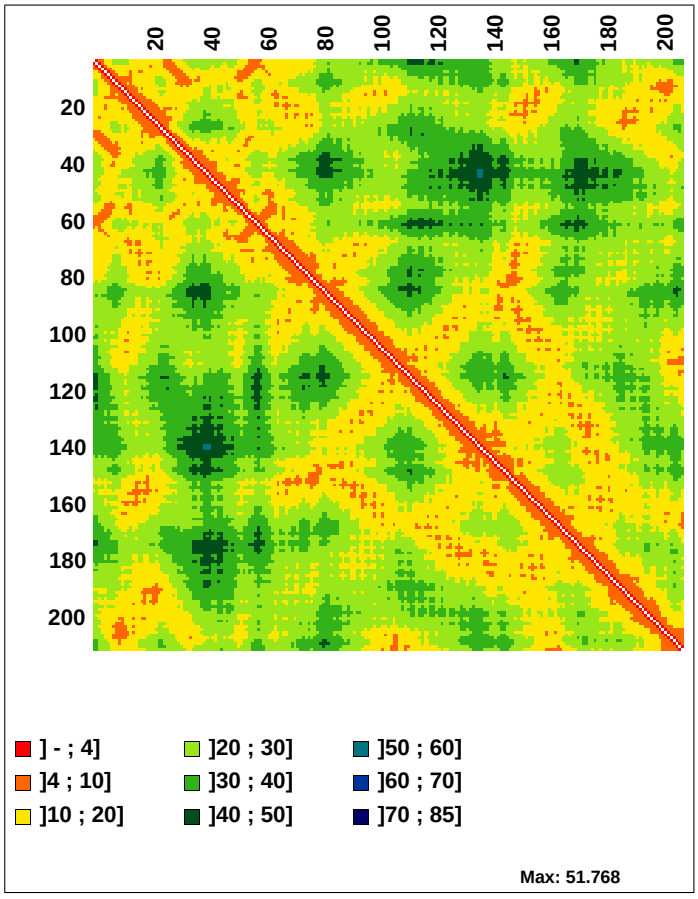

Figure 2.18: Color-coded distance matrix of `1glqA` (generated with MatrixPlot [GSLB99]).

CHAPTER 3

Related Works

In this chapter, we will outline the previous and the contemporary research works — in the four areas of structural bioinformatics, namely structural comparison, database retrieval, classification, and clustering — that are closely related to our work presented in this thesis.

We categorize the methods into groups corresponding to the above four areas (and their sub-areas where applicable). Our categorization is general and does not mean to be specific and exclusive. No clear categorical distinctions can be made for some methods, and we only categorize them into groups which we consider to be most appropriate. For example, we categorize FATCAT [YG03] as a detailed structural comparison method; yet it can be also be considered as a fast database scan method. Similarly, Geometric Hashing [NW91] can be regarded either as a fast database scan method or as an index-based method depending on the mode of implementation.

3.1 Methods for Detailed Structural Alignment

Comparison of 3D protein structures is a fundamental task in structural bioinformatics. Structural comparison problem has been addressed since the 1970's [PD75,

RA76]. Conventionally, structural comparison is done by means of structural alignment. (However, there are also some non-alignment structural comparison methods.)

Given two proteins structures A and B with $|A|$ and $|B|$ residues respectively, the problem of structural alignment is to find the two sets of aligned residues $A_{al} \in A$ and $B_{al} \in B$ which will give the optimum similarity score according to the structural similarity criteria used. $|A_{al}| = |B_{al}| = N$ can be regarded as the length of the alignment. The corresponding residues from A_{al} and B_{al} are considered aligned (equivalenced) to each other, i.e., $A_{al}[i]$ is aligned to $B_{al}[i]$ $(1 \leq i \leq N)$.

The structural similarity of the two sets of aligned residues is determined by a fitness criteria, typically the root-mean-square deviation (RMSD) measure. Given two residue sets, each with N one-to-one corresponding residues, the best superimposition (rotation and translation) that yields the minimum RMSD between them can be easily calculated in $O(N)$ time [AHB87].

The general goodness or accuracy of an alignment can be evaluated by a number of quality criteria, each of which is primarily based on the fitness (RMSD) and the length (number of pairs), and sometimes the number of gaps of the alignment [KKL05, WFB03]. The alignment accuracies of proteins can also be checked by the degree of correlation of the alignment scores and the biological relatedness (as defined by some standard systems such as SCOP) of the structures.

As mentioned in Section 1.1.1, structural alignment problem is NP-hard, and thus, a number of heuristics methods have been proposed. In this section, we will cover the "detailed" structural alignment methods, which emphasize on the alignment quality (accuracy) typically at the expense of speed (in contrast to the ones that emphasize more on rapidness than on accuracy, as will be covered in the next section).

Consequently, the methods discussed in this section are "fine-grained" methods, in which the structure alignment is done straight at the residue level; or the alignment is first done at the fragment or SSE (secondary structure element) level, and then refined at the residue level (unlike the "coarse-grained" methods in the

next section).

There are a number of survey papers and books, such as [EJT00, Koe01, KKL05, LI03, NMK04, OJT03, SP04], that review and/or evaluate various structural comparison techniques — both detailed methods described in this section and coarse methods covered in the next section.

Now, we will briefly describe some methods that we believe to have made important contributions to the field of detailed structural comparison. Chronologically (based on the date of the first publication on each method), these are:

SSAP

SSAP (Sequential Structure Alignment Program) [TO89] is one of the first well received methods in structural alignment. It is later partly used in the construction of CATH [OMJ+97] semi-manual structural class annotation system. SSAP first defines the local coordinate frame and the view (vector environments) of each residue in both protein structures. Then, for each residue pair (one from each protein), their local coordinate frames are superimposed, and a dynamic programming is applied to align the views of the residues. Then, another high-level dynamic programming is applied on the accumulated scores of previous low-level alignments in order to the find the final alignment of the structures. SSAP is known to be a very accurate, but rather slow alignment method [KKL05].

COMPARER

COMPARER [SB90] is another early proposed structural alignment method. It is reported to be powerful [OJT03]. It uses both properties of residues (such as its SSE type, torsion angles, accessibility, side-chain orientation, local conformations) and relationships among residues (such as residue–residue distance, residue–structure center distance, disulfide bond, hydrogen bond). Then, based on the various properties of residues, inter-protein dissimilarity matrices (for all-against-all comparison of the residues from the two proteins) are computed. These matrices are analyzed by dynamic programming procedures in order to find the initial alignment. Then,

the initial alignment is refined by the simulated annealing technique based on the relationships of residues.

DALI

DALI (Distance Matrix Alignment) [HS93] is one of the most widely used structural comparison method. It is also reported to be one of the most accurate alignment methods [NMK04, SP04]. DALI represents 3D protein structures as 2D distance matrices (see Section 2.4), and subdivides the distance matrix of each protein into 6×6 overlapping submatrices. Then, it compiles a list of matching submatrix pairs (each pair being made up of one submatrix from each protein) based on the elastic submatrix–submatrix similarity scoring. After that, it tries to assemble these individual matching submatrix pairs (each representing to two pairs of corresponding 6-residue fragments) into larger sets of corresponding residues that give the maximum similarity score. This is done by using Monte-Carlo optimization or branch-and-bound search. DALI can optionally use SSE information in finding the initial submatrix pairs. DALI has been used for developing FSSP [HS94a] and DDD [HS98] structural class annotation systems.

DaliLite [HP00] is a standalone version of DALI. We use DaliLite in comparative performance evaluations of our proposed methods in this thesis.

VAST

VAST (Vector Alignment Search Tool) [GMB96] is also among the most popular structural alignment methods, and is reported to be relatively fast. It represents SSEs as line segments (vectors) in 3D space, and uses a graph theory-based alignment of them. All pairs of SSEs (vectors) that have the same type are represented as nodes of a graph, and the nodes (SSE pairs) that share the similar distance and angle properties are connected by edges. Then, maximal clique detection algorithm is applied to find the common isomorphic subgraph, and hence the initial alignment of SSEs between the two structures. Then, Gibbs sampling applied to extend the initial alignment into the residue-level detailed alignment. It also takes

the statistical significance of an alignment into account in calculating the best superimposition.

STRUCTAL

STRUCTAL [GL96, LG98] is another noteworthy detailed structural alignment scheme. It starts with an arbitrary alignment of the residues in the two proteins. It superimposes the two aligned residue sets to achieve the minimum RMSD. Then, STRUCTAL calculates the all-against-all similarity scores of the two proteins' residues (based on the inter-protein residue distances in the current superimposed position), and stores them in a structural alignment matrix. Then, dynamic programming is applied to this matrix in order to yield the next alignment. The superimposition—score calculation—alignment cycle is repeated until the overall score converges. The whole process can be repeated with a number of initial alignments, and the one that leads to the optimum score can be selected.

LSQMAN

LSQMAN [Kle96] is a fairly popular structural alignment tool. The basic algorithm subdivides each protein structures into an number of fixed-size overlapping sliding windows (fragments with consecutive residues) with a predefined step size. Then, the sliding window pairs from the two proteins are superimposed one-by-one. This process can be done exhaustively for all possible window pairs, or can be stopped after a satisfactory pair (with an RMSD below a certain threshold) has been found. The best pair is then taken for extending and improving the alignment. This is achieved by an iterative superimposition operator improvement based on the consecutive stretches of closely-fitted residues. A number of other enhancements (e.g., dynamic programming-based improvement) can be made on top of the basic algorithm.

LOCK

LOCK [SB97] is also a hierarchical scheme like VAST. It also represents SSEs as vectors, and aligns them using dynamic programming to get the initial alignment and superimposition. The dynamic programming's scoring matrix is calculated based on a combination of orientation dependent and orientation independent scoring functions. Then, the atomic superimposition is done using a greedy search by repeatedly removing the aligned (superimposed) residue pairs that are farther than a cutoff distance — until the RMSD converges. Finally, the core superimposition is performed in the same manner on the mutually found nearest neighbor pairs.

CE

CE (Combinatorial Extension) [SB98] is another popular structural alignment scheme. It first selects an initial aligned fragment pair (AFP), which is a locally matched pair of 8-residue fragments (one from each protein), to initialize an alignment path. Then, it combinatorially extends the alignment path by incrementally adding "good AFPs" (defined by a distance constraint) with subject to the condition that simultaneous gaps are not allowed in the alignment path. This process is repeated until the length of each protein is traversed, or until no good AFPs remain. CE measures the statistical significance of the alignment by comparing it to the alignment of a random pairs of structures, and computing the Z-score. An additional optimization can be performed in order to remove excess gaps using dynamic programming.

We also use CE in comparative performance studies of our proposed methods in this thesis.

Other Methods

Some other detailed structural alignment algorithms with notable characteristics include: **StrAlign** [Aku95] (residue triplet–triplet probing followed by bipartite matching); **MINAREA** [FC96] (triangulation of residues to minimize the stretched surface area between the backbones); **MATRAS** [KN00] (Markov transi-

tion with log-odds scoring function); **Kenobi** [SW00] (genetic algorithm with a variety of operators); **MAMMOTH** [OSO02] (effective alignment for low-resolution protein structures based on unit-vector RMSD); **FATCAT** [YG03] (flexible alignment with hinge detection); **Caprara *et al.*, 2004** [CCI+04] (fast heuristics solving of contact map overlap problem by integer programming); and **Erdmann, 2005** [Erd05] (knot theory and robot motion planning).

3.2 Methods for Structural Database Retrieval

As discussed in Section 1.1.2, researchers traditionally carry out protein structure database searching by exhaustive pairwise comparison of the query against each and every structure in the database — either by using slow and detailed alignment methods (Section 3.2.1) or by fast and coarse methods (Section 3.2.2). New structural database search and retrieval methods based on indexing and hashing techniques have recently emerged (Section 3.2.3).

3.2.1 Detailed Alignment-based Methods

Conventional pairwise comparison methods such as DALI, CE, and VAST, which are described in Chapter 3.1, are currently being widely used for searching large structural databases (typically the PDB database). Although these detailed alignment methods are inherently slow, database searching with them is made possible by using each or some of the following speed enhancement approaches:

1. Using a very powerful server such as a multi-processor super computer.

2. Using a smaller representative database (typically a non-redundant database filtered by a particular sequence identity cutoff) instead of the full PDB database. The user can infer the structural similarity of his/her query to the remaining structures in the full database in terms of their sequence similarities (either pre-calculated or determined on the fly) to the query's structural neighbors in the representative database. This is illustrated in Figure 3.1.

3. Using all-against-all structural similarity results pre-computed from the existing proteins in the database. If a database protein is found to be structurally very similar to a query, the structural similarities of the query and the protein's pre-computed structural neighbors in the database can be inferred. This is illustrated in Figure 3.2.

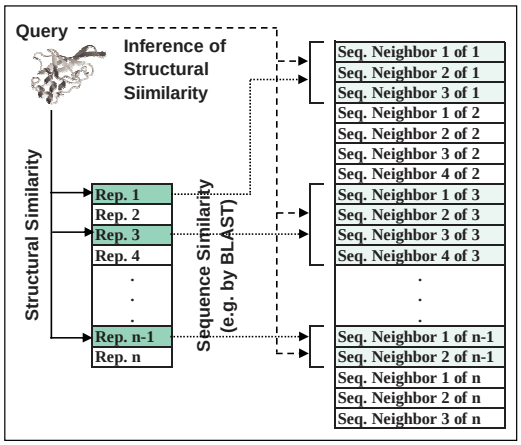

Figure 3.1: Inference of structural similarity from sequence similarity.

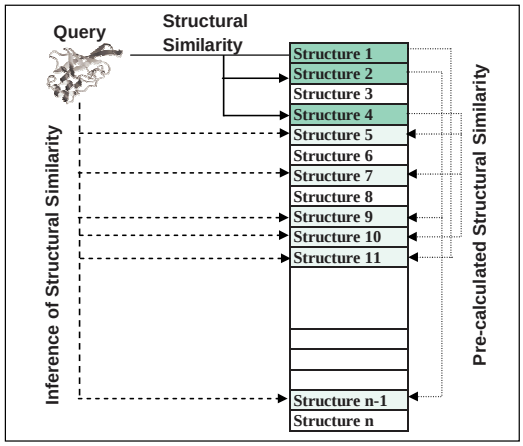

Figure 3.2: Inference of structural similarity from pre-calculated structural similarity.

All of the above approaches have their own disadvantages. The first approach requires a large financial investment, and yet it still can face scalability problems as the sizes the structural databases are growing rapidly. The second approach is not fool-proof, because a sequence similarity does not always means a structural similarity — as already discussed in Chapter 1. The third approach's pre-computation is very time consuming. In addition, since most of the structural similarity measures do not observe triangular inequality, a similarity inference to a neighbor's neighbor can be problematic [RF03].

3.2.2 Fast Database Scan Methods

Fast database scan methods are in fact the coarse pairwise structure comparison/alignment methods that carry out database searching in exhaustive manner.

They are characteristically different from the fine-grained methods described in Section 3.1 in that they give priority to speed than to detailed accuracy. They are designed with the practical purpose of fast searching for large databases in mind, thus focus more on ease and simplicity of processing. An analogy can be drawn from the area of alignment. Smith-Waterman algorithm [SW81] can be regarded as a detailed alignment tool, and BLAST [AGM+90], as a fast database scan tool. (However, there is no definite boundary between the detailed and the fast methods. For example, SSM [KH04] is both fast and detailed, each to some extent [KKL05].)

A majority of these fast comparison methods use SSEs or their interactions as the basic units, without using detailed AA residue information. (Although a few methods, such as [AF96, KJ97, KH04], involve refinement at the residue level, their refinement may not be as thorough as those of the detailed methods such as [GMB96, SB97].) Some methods such as [AF96, NW91] are sequence-order independent (i.e. they consider a protein structure as a constellation of disconnected residues in 3D space), while others are not. For faster database searching, some methods may also use the speed enhancement approaches mentioned in the above sub-section.

Now, we will briefly discuss some fast pairwise methods that we believe to have made important contributions to fast database search. These are chronologically listed below.

Geometric Hashing

Geometric hashing [NW91, BFNW93] is class of algorithms based on a general purpose computer vision technique [WR97]. Given two proteins, it chooses a set of reference frames (each often being a non-linear residue triplet) for the first protein structure. It rotates and translates the protein structure in accordance with each frame at a time, and places the residues into a 3D grid (hash table). (A common 3D grid is used for all frames.) Similarly, for each of the second protein's reference frames, the residues are hashed into the same 3D grid. The coincidences of the first and the second proteins' residues in the grid cells are counted as votes. All

pairs of reference frames from the two proteins that obtain enough votes are taken for further analysis, e.g., for superimposition and calculating RMSD, etc. (For superimposition, the structurally corresponding pairs of residues can readily be known for their coincidences in the cell grids.)

Although Geometric hashing is primarily a pairwise comparison method, it can be easily extended as an index-based method. We can preprocess the reference frames in all database proteins, and store each frame's corresponding residues in the common hash table. Then, a query's reference frames can be compared simultaneously to all database proteins [EJT00].

3D-lookup [HS95] is a geometric hashing scheme based on SSEs. It defines a reference frame with a pair of SSE vectors. It is used as a fast pre-filter for the DALI [HS93] detailed alignment method.

SAFR2

SARF2 (Spatial Arrangement of Backbone Fragments) [AF96] is a quite popular fast database scan method. It is somewhat similar to VAST. It finds four different kinds of distances and an angle between each pair of SSE vectors. Then, it searches for the compatible SSE pairs from two proteins (using distance and angle constraints). After that, SARF2 incrementally searches for large ensemble of mutually compatible pairs of SSEs, with a constraint that the pairs in the ensemble are not made up of very distantly located SSEs. This incremental searching is repeated many times with different initial seeds of SSE pairs. After finding the initial alignment (optimum ensemble of SSE pairs), iterative refinement is done at the residue level. Unlike VAST, SARF2 does not use the expensive maximal clique detection to produce the initial alignment of SSEs, and thus is faster.

DEJAVU

DEJAVU [KJ97] is another fairly popular fast comparison method. It describes each SSE by type, number of residues, and coordinates of the fast and last residues. For two SSEs to be similar, they must have the same type. The user can define

additional similarity constraints (distance, directional, topological, etc.), and the weights for the scoring scheme. Then, DEJAVU conducts an exhaustive, depth-first tree search with backtracking to find the set of matching SSEs. Then, refinement at the residue level is carried out by finding the consecutive stretches of closely packed residue, and finding the new superimposition using them. This is iteratively done until the similarity score converges. DEJAVU is used is a pre-filter for LSQMAN [Kle96].

Topscan

Topscan [Mar00] uses symbolic linear representation of SSE vectors using the properties such as SSE type and length, accessibility, proximity, element length, loop length, etc, and applies dynamic programming to align two linear symbolic strings. For each pairwise comparison, Topscan requires to rotate one structure in 24 different directions, and the one that gives the best alignment result is taken. Topscan was designed to be used as a fast pre-filter for SSAP [TO89] in CATH [OMJ+97] structural class assignment. It is among the fastest pairwise database scan methods [NMK04].

We use Topscan for comparative performance studies of our proposed database search method in this thesis.

PRIDE

PRIDE (Probability Identity) [CP02] represents each protein structure as a histogram of residue–residue distances (i.e. histogram on its distance matrix). It defines a residue position difference n, and calculate all the distances between residue i and $i + n$ to construct a distance histogram. The probability of identity of two histograms (representing two protein structures) is assessed by contingency-table analysis based on χ^2 test. 28 histogram pairs (with $n = 3$ to 30) are constructed, and the probability of identity of two protein structures is calculated by comparing each of the 28 histogram pairs, and averaging the resulting probability values. PRIDE is an example of non-alignment based structural comparison method. The

method is reported to be very fast.

SSM

SSM (Secondary Structure Matching) [KH04] represents a protein as a complete graph of SSE vectors. Each node is an SSE vector, and each edge between two nodes represents four different types of angles and the length between two SSE vectors. The similarity between two SSE graphs (representing two protein structures) is carried out by a rapid common subgraph isomorphism algorithm. This algorithm is reported to be much faster than the similar algorithms used in [GMB96, GARW93, HPS$^+$03, KL97]. Then, the initial alignment is iteratively refined and expanded into the final one (at the residue level) by a combination of four techniques. The significance of the alignment is evaluated with statistical means, viz, P value and Z score. SSM is reported to be quite fast and pretty accurate [KKL05], and is quite popularly nowadays.

Other Methods

Some other fast structural comparison methods with notable characteristics include: **PROTEP** [GARW93] (first graph-based clique detection for SSE alignment); **Koch and Lengauer, 1997** [KL97] (edge product graph based on SSEs and van der Waals volumes); **TOPS** [DWNT99] (simple cartoon representation of SSE topology and backtracking search); **Ohkawa *et al.*, 1999** [OHN99] (various SSE–SSE interaction matrices and sequential similarity detection algorithm); **FLASH** [SH03] (probabilistic SSE matching and greedy alignment); **Taylor, 2002** [Tay02] (bipartite graph matching for paring by optimal SSEs); **GRATH** [HPS$^+$03] (another SSE graph-based clique detection used for CATH); **Bostick *et al.*, 2004** [BSV04] (topological representation of protein using two metrics: based on Delaunay tessellation and residue distance in sequence space); and **FAST** [ZW05] (residue pairing with heuristics elimination of bad pairs).

3.2.3 Index-based methods

An index-based database search method is characteristically different from a fast pairwise database scan method in that:

1. The system always performs pre-computing and construction of an index and/or a hash table before database searching is actually carried out. When actual query evaluation (database searching) is done, only the index/hash table is used, and the original protein structures are not needed to be looked up.

2. The index-based search itself abandons the idea of sequential pairwise comparison. (However, we may optionally use the *filter-and-refine* strategy, in which the possible candidates are first filtered in by the index-based search, and later refined by a detailed pairwise alignment, as illustrated in Figure 3.3.)

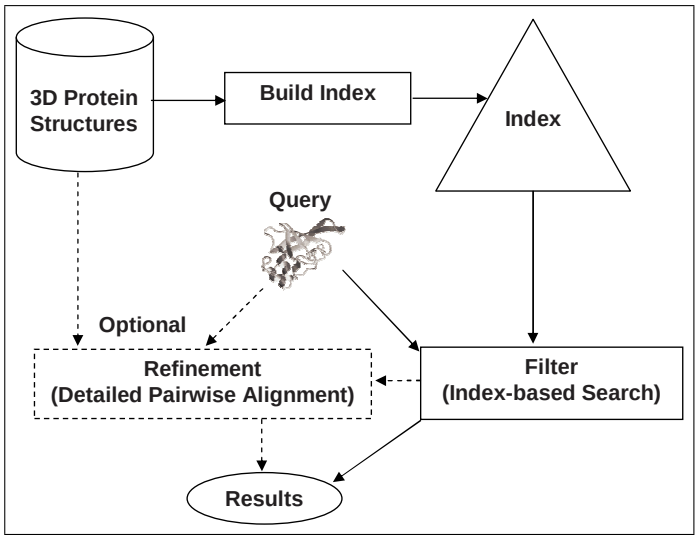

Figure 3.3: Filter-and-refine strategy for database searching.

Index-based methods can be categorized into:

1. *Component Indexing*: The system extracts relevant components from protein structures, manipulates them (discretizing, sorting, etc.), and stores them together with their parent proteins' IDs in the index/hash table. SSEs and

relationships among them are usually used are the components of a protein. Query evaluation is carried out simultaneously and incrementally for all database proteins.

2. *Whole Protein Indexing*: The system extracts important features from a protein structure as a whole, and represents the protein as a single point in a multi-dimensional space. All the points for database protein structures are stored in a multi-dimensional index (typically a tree-structured index). Query evaluation is carried out using this index.

The ProtDex2 [AT04b] method proposed in this thesis is a component indexing method. Now, we will summarily describe the other index-based database search methods chronologically. It should be noted that the area of index-based structural database searching is relatively immature and none of the method is known to be popularly used up until now.

Shape Histogram-based Method

Ankerst *et al.*, 1999 [AKKS99] is a pioneering work in index-based protein structure database searching. It is a whole protein indexing method. It uses the similar ideas from image and multimedia database indexing and searching. It partitions the shape of each protein structure (defined by the uniformly distributed surface points taken from the molecular surface) into shells and bins, and constructs a shape histogram from them. The method encodes each shape histogram (which represents a protein structure) as a point in a multi-dimensional metric space (with up to 256 dimensions). It uses the quadratic form function to measure the distance between the two multi-dimensional points. It reduces the number of dimensions of the original space using a feature selection method that supports the quadratic form function. For query evaluation, it uses a filter-and-refine strategy. In the filtering step, it uses a pre-constructed multi-dimensional index (based on the X-tree method) to filter out the impossible answers by using the quadratic form-based minimum bounding boxes. Then, the method refines the remaining answers by the actual (relatively expensive) quadratic form function.

ProtDex

ProtDex (Protein Indexing) [AFT03] is a component indexing method proposed by us. It was a predecessor of the ProtDex2 method [AT04b] presented in this thesis. ProtDex extracts a feature vector from each fixed-size overlapping sliding windows of a distance matrix, capturing the information such as sum of C_α–C_α distances, SSE–SSE contact type, contact size, contact position, etc. of each sliding window. It then constructs an inverted-index on all these feature vectors in the database. When a query evaluated, it is also represented as a set of feature vectors, which are searched through the index one-by-one. The matching feature vectors' parent proteins are ranked simultaneously and incrementally using a scoring scheme adapted from the IR (information retrieval) systems.

ProtDex is found to be less effective than the ProtDex2 system reported in this thesis.

PSI

PSI (Protein Structure Indexing) [CKS04] is another recently proposed component indexing approach using filter-and-refine strategy. It takes the various properties of a SSE triplet as a feature vector in a six-dimensional space, describing three distances and three angles among the SSE triplet. Then, PSI constructs an R*-tree on all such feature vectors extracted from the database. When evaluating a query, the index is searched to quickly find the database protein's triplets that are compatible with those of the query. For each database protein with enough matching triplets, a triplet pair graph (TPG) — with each pair being made up of one triplet from the query and one from the database protein — is constructed. Then, a depth first search algorithm is used on the TPG to find the largest weighted connected component (LWCC). Then, a bipartite graph matching is used on the LWCC to find the initial alignment of the SSEs. The significance of each database protein's initial alignment is evaluated by a p-value statistical model. Then, the detailed refinement using the VAST method [GMB96] is carried out on the database proteins whose initial alignments are significant.

K-clique Hashing

K-clique hashing [WKHK04] exploits both the accuracy advantage of maximum clique detection-based techniques and the speed advantage of geometric hashing methods. Protein structure comparison using graph representation (usually SSE graphs) customarily applies a time-consuming maximum clique detection to find the common isomorphic subgraphs [GMB96, GARW93, HPS+03, KL97]. The K-clique Hashing method subdivides all graphs for database proteins into k-cliques (complete sub-graphs of a fixed size k); maps them as a point into a Euclidean space; and indexes them using an R*-tree (which can be regarded as a hash table with variable-sized cells based on the points' distribution). When a query is evaluated, the index is used to find the matching k-cliques of the database proteins to those of the query. The matching k-cliques pairs for each database protein are assembled into a larger clique using a method called hits list voting in order to build a product graph, which is used for the final maximum clique detection.

ProteinDBS

ProteinDBS (Protein Database Search) [SCSX04] is an image processing-based method for whole protein indexing. It represents a protein structure as a 2D distance matrix, and maps it into a high-dimensional point which features a number of distance histograms (based on diagonal partitioning of distance matrices) and a number of texture attributes (energy, entropy, homogeneity, contract, correlation, etc.). Then, the method stores the points (representing the database protein structures) in a EBS (Entropy Balanced Statistical) k-d tree. The EBS k-d tree is trained with a selected set of points (a subset of the entire database) with the known SCOP [HAB+97] class labels. It learns from these labeled points and performs a partial clustering and dimensionality reduction for the remaining points in the database. This results in 23-dimensional points indexed in the EBS k-d tree. In evaluating a query, a binary search is performed on the tree and finally the leaf pages that contain the IDs of relevant proteins are returned as the answer. Since ProteinDBS involves training of the EBS k-d tree with some labeled samples, it

can also be regarded as a learning-based structural classification method (as will be discussed in Section 3.3).

PSIST

PSIST (Protein Structure Indexing using Suffix Trees) [GZ05] is a recent component indexing method that maps a protein structure into a structure-feature sequence (SF-sequence) representing the spatial properties of each of the adjacent residue–residue pairs. Each SF is a feature vector with 6 attributes (3 translation and 3 rotational relationships of each residue pair). The attributes of a feature vector is normalized (discretized) to generate a SE sequence with discrete values. Then, the SF-sequences for all proteins in the database are used to construct a generalized suffix tree (GST) — in the same way as constructing DNA or AA sequences into a suffix tree. In query evaluation, the most similar SF-sequences to that of the query SF-sequence are retrieved using a typical suffix-tree searching algorithm, and are refined using Smith-Waterman sequence alignment algorithm [SW81].

SCALE

SCALE (Structure-Continuous Alignment of Secondary Structure Elements) [CHTY05] is another recently proposed filter-and-refine approach. It constructs a hierarchical index of SSE triplets with three levels: (1) nodes with SSE triplet type ($\alpha\alpha\alpha$, $\alpha\alpha\beta$, etc.), (2) nodes with two SSE–SSE torsion angle ranges, and (3) nodes with two SSE–SSE distance ranges. Each third-level node points to a leave page containing the protein IDs in which the corresponding triplets occur. When evaluating a query, the index is used to find the IDs of the proteins containing an enough number of matching SSE triplets with respect to those in the query. These candidate proteins are refined with a dynamic programming-based SSE alignment algorithm, using the torsion angle and the distance properties of each SSE pair, and a scoring function based on maximally common subsequence (MCS).

Other Methods

Other index-based structural database retrieval methods include: **PROuST** [CGZ04] (geometric hashing of SSE triplets for filtering, and dynamic programming for alignment); **Park and Ryu, 2004** [PR04a, PR04b] (Filtering using histograms of SSE types, charged residues and hydrophobicity; refinement using topology string of SSEs — something like Topscan's [Mar00]); **Yeh *et al.*, 2005** [YCCO05] (whole protein indexing with multi-projection view descriptors); and **Bowties** [HZS05] (indexing residue quartets using commercial RDBMS).

3.3 Methods for Protein Structure Classification

As discussed in Section 1.1.3, classification is supervised machine learning, in which we predict the class label of a new protein using the knowledge learned from the previous instances of proteins and their class labels.

There have already been a number of dedicated classification methods that try to predict the structural class labels of proteins using their AA sequences (such as [CSM04, DD01, GRSE99, IYS04] and many more). But, to our knowledge, there only exists a few purpose-built methods that predict the structure class labels of proteins based on their 3D structures themselves. As discussed in Section 1.1.3, many researchers use ordinary structure comparison and database search systems (which are already descried in the above two sections) for classification purpose in the nearest-neighbor framework.

In this section, we will cover the purpose-built structure classification methods. Each method described here involves a learning component of some kind, as opposed to the ordinary static nearest-neighbor systems. Most of these methods have been proposed recently.

CORA

CORA [Ore99] is a structural classification method using templates or fingerprints. For each CATH structural class, it preforms an incremental multiple structural

alignment of the member proteins by using SSAP [TO89] pairwise alignment tool. The consensus 3D template representing all structures in this class is encoded by the properties of each position of the multiple alignment. Such properties include the average and standard deviation values of each aligned residue set's accessibility, torsion angles, and conservation of the vector environment. It also generates a consensus distance matrix for the aligned residues. When a new protein structure instance is to be classified, CORA also uses SSAP to align the protein's residue vector environments to each class template's consensus structural environments (average vectors). The distance matrix of the aligned residues is also compared against the consensus distance matrix of the class. The class label of the best scoring class (in terms of both template alignment and distance matrix matching) is assigned to the new protein.

SGM

SGM (Scaled Gauss Matrix) [RF03] uses Gauss integrals (topological invariants based on knot theory) to represent a 3D protein structure as a point in 30-dimensional pseudo-metric (nearly metric) space. It uses a simple Euclidean distance function to measure the distance between two points in this 30-dimensional space. It uses CATH designations as the proteins' class labels. When a new (query) protein is to be classified, its 2 nearest neighbors (with distinct class labels) are searched. If the distance of the query to its first nearest neighbor is much (i.e. 1.75 times) shorter than the distance to its second nearest neighbor, the system confidently assigns the first neighbor's class label to the query. Otherwise, both neighbors' classes are reported as the possible answers, or the query itself is suggested to be of a new class. (Although, SGM is another nearest-neighbor classification scheme, we put it in this section, because it is dedicated for classification purpose, and it involves learning of the parameter 1.75 from the existing CATH system.)

We compare SGM against our proposed structure classification system for comparative performance analysis.

Coherent Subgraph-based Method

Huan *et al.*, 2004 [HWW+04] is another recently proposed dedicated protein structure classifier based on coherent subgraph analysis. It presents a 3D protein structure as a labeled undirected graph where each residue is represented as a node (with its AA type label). The residues are connected with either peptide edges or proximity edges. It represents all database (training) proteins as labeled graphs in canonical form; extracts all possible subgraphs from these graphs; and select the k-coherent subgraphs (each has k nodes and a "mutual information" above a threshold) among these subgraphs. Then, the system encodes each protein structure as a feature vector representing the number of distinct k-coherent subgraphs the protein contains. It then trains a support vector machine (SVM) classifier with the feature vectors of database proteins (with SCOP class labels), and the SVM is later used for classifying new protein structures.

CPMine

CPMine (Contact Pattern Mining) [AT04a] is a fingerprint-based structural classifiable system previously proposed by us. It presents 3D protein structures as CPsets (sets of feature vectors for inter-SSE contact patterns). Each feature vector represents the elemental and spatial relationships of a pair of SSEs. We encodes each CPset as a set of integer values by means of discretization. Then, it mines the sub-CPsets (integer subsets) that occur frequently in each distinct SCOP structural class using Eclat frequent pattern mining algorithm. A collection of frequent sub-CPsets that corresponds to a class is regarded as its fingerprint. When a new protein structure instance is to be classified, each fingerprint's sub-CPset are probed into the new protein's CPset, and the label of the class that has most hits is assigned to the new protein.

CPMine is found to be not as effective as the ProtClass method proposed in this thesis.

HMM-based Method

Wang *et al.*, 2005 [WCH05] is a structural classifier based on hidden Markov model (HMM). It extracts a number of pentamer (5-residue) fragments from a selected set of training (database) proteins. It represents each fragment as a feature vector of 6 non-adjacent residue distances; clusters them using an expectation maximization (EM) algorithm; and refines the clusters to achieve high within-cluster homogeneity. Then, it assigns a unique local structural alphabet (LSA) to each cluster's centroid. A 3D protein structure is represented as a 1D string using LSAs. The method performs multiple alignment of the structures in each selected SCOP structural class using FLASH [SH03] fast alignment algorithm. The resultant multiple alignment is represented in the form of a multiple LSA sequence alignment. All the distinct SCOP classes are represented in this way and fed into the HMM machine learner for training. When a query is evaluated, it is also represented as a LSA string and classified with the trained HMM model.

Decision Tree-based Method

Camoglu *et al.*, 2005 [CCSW05] is an ensemble classifier for protein structures. It uses 3 structural comparison methods (DALI, CE, and VAST) and 2 sequence comparison methods (PSI-BLAST and HMM) as a committee of component classifiers (in nearest-neighbor framework), and uses their consensus decision. The authors conducted a comparative performance analysis of the component classifiers on a training SCOP data set. Then, they manually constructed a decision tree based on the parameters acquired from the analysis. Each node of the decision tree is assigned an individual component classifier method with its predefined lower and upper bound parameters. When a new protein is to be classified, its nearest neighbor is searched by the method assigned at the tree's root node. If the similarity score of the nearest neighbor is less than the lower bound, the new protein is reported as a new class. If the score is higher than the upper bound, the nearest neighbor's class label is confidently assigned to the new protein. Otherwise, the new protein is passed down to a lower level node (i.e. another method) in the tree

for further investigation, and so on. This ensemble classifier approach is reported to be better than using each classifier method individually.

3.4 Methods for Protein–Protein Interface Clustering

Clustering of protein–protein interfaces falls in the wide area of studies of protein–protein interactions (PPI) [NT04, vMKS+02]. Researchers study the PPI problem from the sequence perspective (such as [SM01, TSN04]); from the structural perspective (such as [DS05, KTWN04, LCCJ99, MSPWN05]); or both from the sequence and structural perspectives (such as [AGK05, LLTN04, PLT01]).

In this thesis, we study the PPI from the structural perspective. In particular, we study the 3D structural properties of the protein–protein interfaces where proteins physically come into contact and interact. Structural studies of protein–protein interfaces can be subdivided into two separate yet related categories: characterization of interfaces, such as [CJ02, FPVC02, HMWN00, LCCJ99, MEWN03], and quantitative comparison or alignment of interfaces (which often leads to clustering of them), such as [DS05, KTWN04, MW03, MSPWN05, SPMNW04, TLWN96]. We will focus on the latter in this thesis. Now, we will briefly describe the existing interface comparison and clustering methods.

Backbone-based Interface Clustering

Tsai *et al.*, 1996 [TLWN96] is a pioneering work in protein–protein interface clustering. It defines an interface as a set of backbone C_α atoms of interacting residues and their neighboring residues. (An interaction between 2 residues is defined if there exists any two atoms, one from each residue, whose distance is less than the sum of their corresponding van der Waals radii plus 5Å.) It uses a geometric hashing-based algorithm for sequence-order independent pairwise comparison of two interfaces. In order to reduce the effect of random matches, it uses the connectivity score (which also takes matching of the immediate linked-neighbors of the

interface residues in account) in measuring the similarity between two interfaces. The method uses a heuristic and iterative clustering algorithm (a variation of hierarchical clustering) with gradual relaxation of similarity score in each iteration. Thus, the clustering procedure only needs to perform a sparse comparison of interface pairs instead of an all-against-all comparison. From 1,629 interfaces, 351 clusters were generated.

This cluster data set was later used in deriving the structural motifs of interfaces [TXN97]; study of the conservation of polar residues in interfaces [HMWN00]; and study of the conservation of interface and non-interface residues [MEWN03].

Recently, the clustering is extended with a larger number of interfaces from the latest version of PDB (as of 2004) [KTWN04]. From 21,686 interfaces, 3,799 clusters are produced, which are later filtered into 103 significant clusters (with at least 5 members each) having a total of 949 non-redundant interfaces.

I2I-SiteEngine

I2I-SiteEngine (Interface-to-Interface Site Engine) [MSPWN05, SPMNW04] uses the same definition for an interface as in above method. It regards an interface as a set of interacting triangles (I-triangles), which is a triplet of functional groups (pseudocenters) in one chain that is recognized to form 3 interactions with the other chain. It determines the structural (as well as physico-chemical) similarity of a pair of protein interfaces by an alignment method based on geometric hashing of I-triangles. Being based on I-triangles, the method, in effect, performs simultaneous alignments on the two pairs of chains. The method starts with 23,912 interfaces, which are filtered into 4,602 by filtering out the biologically insignificant ones using PQS (Protein Quaternary Structure) sever, and the structurally redundant ones using MASS multiple structural alignment. It performs all-against-all comparison of these 4,602 interfaces and stores the similarity scores. Then, the method performs an average linkage hierarchical clustering of the interfaces based on these similarity scores. This results in 2,582 clusters. A BLAST-based filtering is applied on these clusters resulting in 59 significant clusters with a total of 604

interfaces.

PIBASE

PIBASE (Protein Interface Data Base) [DS05] focuses on domain–domain interfaces (rather than chain–chain interfaces as in the above two methods). Either SCOP or CATH domain definitions can be used. An interface is defined as having at least one pair of residues (one from each domain) with an interatomic distance less than 6.05Å and a minimum of buried solvent accessible surface area of 300Å^2. The method uses a hierarchical representation of interfaces: (1) a complex as a domain connectivity graph (using crude linear representation), (2) domains as solvent accessible area, SSE assignment, and class annotation (by SCOP or CATH), and (3) interfaces as types of residue–residue contact (14 geometric, physico-chemical and topological properties encoded as a 210-bit vector), buried solvent accessible area and the number of residues in the interface. A similarity score based on Hamann distance function is used to compare the interface information at various (complex, domain, and interface) levels. A hierarchical clustering procedure is applied on $158,915$ SCOP domain–domain interfaces, and this results in 989 and $18,755$ clusters at complex and interface levels respectively.

ACV (Atomic Contact Vector) [MW03] is a similar bit vector-based representation for protein–protein interfaces.

Other Related Methods

There are a number of methods, such as [FTNW95, HS94a, HS98, RG88], previously proposed for clustering of 3D protein structures in general (not specifically for interface regions). Like the interface clustering methods described above, these too are based on all-against-all comparison of structures and variations hierarchical clustering.

Clustering of sub-structures of proteins was studied in [TT04]. A number of methods for discovery of sub-structure motifs (again not specifically interface motifs) have also been proposed [BKB02, HBW$^+$05, JECT02, KJ97, LFNW01].

CHAPTER 4

Detailed Protein Structure Alignment

Summary

In this chapter, we propose a detailed protein structure alignment method named "MatAlign". It is a two-step algorithm. Firstly, we represent 3D protein structures as 2D distance matrices, and align these matrices by means of dynamic programming in order to find the initially aligned residue pairs. Secondly, we refine the initial alignment iteratively into the optimal one according to an objective scoring function. We compare our method against DALI [HS93] and CE [SB98], which are among the most accurate and the most widely used of the existing structural comparison tools. On the benchmark set of 68 protein structure pairs by Fischer *et al.*, MatAlign provides better alignment scores, according to four different criteria, than both DALI and CE in a majority of cases. MatAlign is about 3 times faster than DALI, and has about the same speed as CE.

4.1 Introduction

Comparison/alignment of 3D protein structures plays a central role in structural bioinformatics [ZK03]. Several applications of structural comparison/alignment include analysis of conformational changes on ligand binding, detection of distant evolutionary relationships, inferring functional characteristics of new proteins, assigning folds to new proteins, analysis of structural variation in protein families, identification of common structural motifs, assessment of sequence alignment methods, evaluation of structural prediction methods, etc. [Bou05, God96, LI03, OJT03].

In this chapter, we propose a new protein structure comparison method named **MatAlign** (**Mat**rix **Ali**gnment) based on the alignment of distance matrices. It can provide precise results, and can be used for the detailed comparative structural analysis of proteins.

4.2 Structural Comparison Framework

4.2.1 Structural Alignment

When comparing two proteins, researchers usually try to find the corresponding pairs (i.e. alignment) of AA residues that provides the optimum similarity score with respect to the scoring scheme used. Thus, the terms "structural comparison" and "structural alignment" are often used interchangeably. (Still, there exist some structural comparison methods that do not depend on any alignment but on various statistical measures such as [CP02, AKKS99], etc.)

There are several ways to measure the similarity between two protein structures. Among them, *root mean square deviation* (RMSD) is the most commonly used [Koe01]. Under this scheme, the aligned residues in one structure are superimposed onto those of another structure so as to yield the minimum RMSD value. The superimposition process involves translation and rotation of one structure with respect to the other. Mathematically, given two sets of aligned residues A_{al} and

B_{al} from two proteins A and B respectively, we have to minimize the RMSD value $\Delta(A_{al}, B_{al})$ between them:

$$\Delta(A_{al}, B_{al}) = \sqrt{\frac{1}{N}\sum_{i=1}^{N}(A_{al}[i] - (\mathbf{R} \cdot B_{al}[i] + \mathbf{T}))^2} \tag{4.1}$$

where N is the number of aligned residues (i.e. $|A_{al}| = |B_{al}| = N$), and $\mathbf{R}$ and $\mathbf{T}$ are the rotation matrix and translation vector applied on B_{al} in order to yield the minimum RMSD value.

The most difficult part protein structure alignment is finding the corresponding (aligned) residues in two proteins with subject to the scoring function of choice, of which RMSD is a component. This problem is known to be NP-hard, and all the existing methods use various kinds of heuristics to tackle it (as discussed in Section 3.1). Given two set of aligned residues, the RMSD value itself can be calculated in $O(N)$ time by the least square fitting method [AHB87].

In most cases, RMSD alone cannot be used to determine the quality of an alignment. A smaller RMSD value does not always imply a better alignment quality. The length of alignment (i.e. the number aligned residue pairs) is also needed to be considered. Suppose we have two structural comparison methods for aligning two protein structures with 100 residues each. If the first method can produce 30 aligned residue pairs with RMSD value 2.0Å, and the second method can generate 60 pairs with RMSD 2.1Å, the latter can be considered more significant.

Different groups of researchers have proposed different scoring schemes or functions to balance the RMSD value (Δ) and the number of aligned residue pairs (N). Each scheme calculate a "single-value" score by manipulating Δ and N in some manner so as to measure the quality of an alignment in its own way. There is no universal consensus on measuring the alignment quality by a single value [Koe01, WFB03].

In this thesis, we use the following four scoring schemes. The first one is used as the native scoring function for our proposed MatAlign method. The other three are used as the quality criteria in performance evaluation of MatAlign in comparison with the other methods. They were also used recently as the criteria

in a comprehensive evaluation of various structural comparison methods [KKL05].

1. Alexandrov and Fischer's *alignment score* [AF96] (denoted as S here). An alignment with the larger S value is considered to be a better one (i.e. S is to be maximized).

$$S = \frac{3 \times N}{1 + \Delta} \tag{4.2}$$

2. Kleywegt and Jones' *similarity index* (SI) [KJ94] (to be minimized).

$$SI = \frac{\Delta \times \min(|A|, |B|)}{N} \tag{4.3}$$

where $|A|$ and $|B|$ are the lengths or the number of residues in the original proteins A and B respectively.

3. Kleywegt and Jones' *match index* (MI) [KJ94] (to be maximized).

$$MI = \frac{1 + N}{(1 + \Delta/w_0) \times (1 + \min(|A|, |B|))} \tag{4.4}$$

where we use $w_0 = 1.5$ as a default value [KKL05].

4. Subbiah *et al.*'s *structural alignment score* (SAS) [SLL93] (to be minimized).

$$SAS = \frac{\Delta \times 100}{N} \tag{4.5}$$

4.2.2 Aligning Distance Matrices for Structural Alignment

A 3D protein structure can be represented as a 2D distance matrix. (See Section 2.4 for details.) In order to structurally align two proteins, we can align their distance matrices instead of their original 3D structures. The idea of distance matrix alignment was previously used in the DALI method [HS93]. It employs the strategy of submatrix matching and assembly to achieve the alignment.

Here, we use a different strategy. Our approach of the alignment of distance matrices is based on the observation that any two structurally matched residues, one from each protein, have the similar *distance profiles* represented as rows in their respective distance matrices.

For example, suppose we have two protein structures P and Q which are identical except for the inserted residue 3 in P, as shown in Figure 4.1. For simplicity,

let us denote the distances between residues as symbols: A for d^P_{12} (C_α–C_α distance between residue 1 and 2 in P), B for d^P_{13}, C for d^P_{14}, etc. Since the two proteins are identical except for one residue, their corresponding C_α–C_α distances are the same; i.e. $d^P_{12} = d^Q_{ab} = A$; $d^P_{14} = d^Q_{ac} = C$, etc.

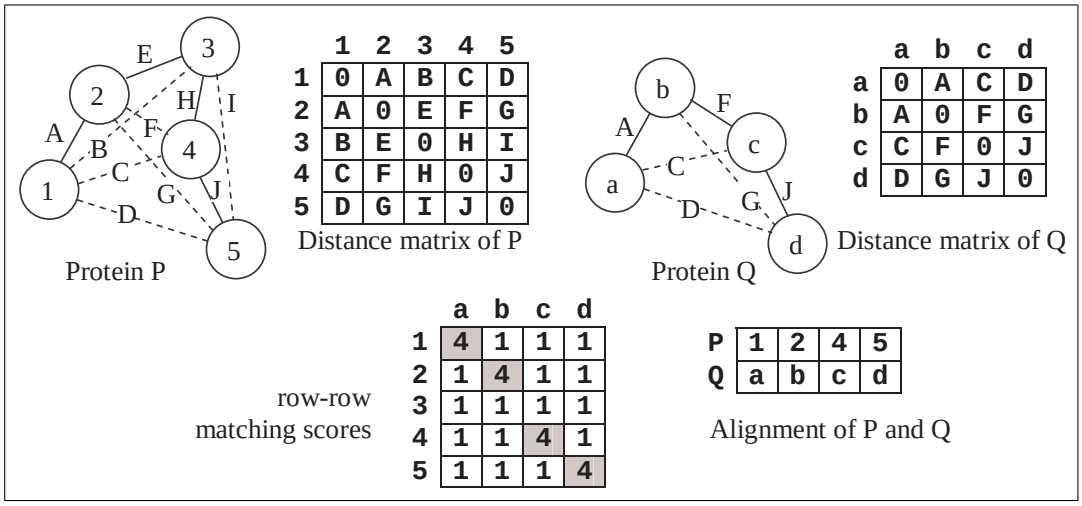

Figure 4.1: Alignment of distance matrices.

When we observe the distance matrices $\mathcal{DM}_P$ and $\mathcal{DM}_Q$ of proteins P and Q respectively, we can see that row $\mathcal{DM}_P[1]$ (i.e. the distance profile of residue 1 in protein P) is more similar to row $\mathcal{DM}_Q[a]$ (the distance profile of residue a) than any other rows in $\mathcal{DM}_Q$. The row–row matching score of $\mathcal{DM}_P[1]$ and $\mathcal{DM}_Q[a]$ is 4. The pairs $(0-0), (A-A), (C-C)$ and $(D-D)$ are the matching ones. The row–row matching score of $\mathcal{DM}_P[1]$ and any other row in $\mathcal{DM}_Q$ is at most 1. For example, if we take $\mathcal{DM}_Q[b]$, there can be only one match: either $(0-0)$ or $(A-A)$. (Both matches cannot be achieved at the same time, because of their different sequence orders: $0, A$ and $A, 0$.) Similarly, we can observe that $\mathcal{DM}_P[2]$ is most similar to $\mathcal{DM}_Q[b]$; $\mathcal{DM}_P[4]$ to $\mathcal{DM}_Q[c]$; and $\mathcal{DM}_P[5]$ to $\mathcal{DM}_Q[d]$ as shown in Figure 4.1. Thus, we finally have the alignment of residue pairs: $(1-a), (2-b), (4-c)$ and $(5-d)$.

4.3 The MatAlign Method

We propose a protein structure comparison method in the conventional framework of structural alignment, RMSD, and alignment score, using the principles of distance matrix representation and alignment as described above. From the experimental results, it is observed that MatAlign can offer the precise alignment results. It is ideal for the detailed comparative analysis of protein structures.

The basic MatAlign algorithm works in two steps. In the first step, we represent 3D protein structures as 2D distance matrices, and align them. We use the simple and well-known Needleman-Wunsch *dynamic programming* algorithm [NW71] to align the rows from two matrices all-against-all, and store the row–row matching scores in a score matrix. Then, we apply dynamic programming again on this score matrix to find the initial aligned residue pairs (one from each protein). In the second step, we calculate the RMSD value from the two sets of residues involved in the initial alignment by superimposing one onto another. Then, we refine the alignment by removing the farthest aligned residue pair from the superimposed structures, and iterate the process until the alignment score cannot be further improved. We also do some enhancements on this basic algorithm in order to improve both speed and accuracy.

MatAlign can be easily parallelized. The most time consuming part of MatAlign is the all-against-all alignments of rows from two matrices. Since we have to perform multiple mutually-independent dynamic programming procedures in this step, we can reduce the running time by parallelizing them. Several parallel systems for aligning DNA and protein sequences based on dynamic programming have been successfully implemented [SSS02]. Thus, it is highly possible for us to adopt the same idea and parallelize MatAlign in the future.

Now, we will discuss the details of the basic MatAlign algorithm and the enhancements on top of it.

4.3.1 Step 1: Finding Initial Alignment

The algorithm for generating the initial alignment between two protein structures A and B is described in Figure 4.2.

function **GetInitAlignment** $(\mathcal{DM}_A, \mathcal{DM}_B) \rightarrow (A_{al}, B_{al}, N)$
input: (1) $\mathcal{DM}_A[1 \ldots |A|, 1 \ldots |A|]$ (distance matrix of protein A)
(2) $\mathcal{DM}_B[1 \ldots |B|, 1 \ldots |B|]$ (distance matrix of protein B)
output: (1) N (number of aligned residue pairs)
(2) $A_{al}[1 \ldots N]$ (residues from A that involve in alignment)
(3) $B_{al}[1 \ldots N]$ (residues from B that involve in alignment)
procedure:
1. `for` $i = 1$ `to` $|A|$
2. `for` $j = 1$ `to` $|B|$
3. $\mathcal{SM}[i, j] =$ **AlignRow** $(\mathcal{DM}_A[i], \mathcal{DM}_B[j])$
/* row–row matching score of i^{th} row of $\mathcal{DM}_A$ and j^{th} row of $\mathcal{DM}_B$ */
4. $GS = 0$ /* Gap score */
5. `for` $i = 0$ `to` $|A|$ $F[i, 0] = i \times GS$ /* F is dynamic programming's matrix */
6. `for` $i = 0$ `to` $|B|$ $F[0, i] = i \times GS$
7. `for` $i = 1$ `to` $|A|$
8. `for` $j = 1$ `to` $|B|$
9. $F[i, j] = \max\{ (F[i-1, j] + GS),\ (F[i-1, j-1] + \mathcal{SM}[i, j]),\ (F[i-1, j] + GS) \}$
10. $(A_{al}, B_{al}, N) =$ **GetAlignedPair** $(\mathcal{DM}_A, \mathcal{DM}_B, F)$
11. `return` (A_{al}, B_{al}, N)

Note: Throughout this thesis, we use the format: function $\mathbf{X}(\mathcal{Y}) \rightarrow (\mathcal{Z})$ which means that the function $\mathbf{X}$ maps the input parameter set $\mathcal{Y}$ into the output result set $\mathcal{Z}$.

Figure 4.2: Initial alignment generation algorithm.

As discussed in Section 4.2.2, we first have to compare all rows (representing distance profiles of residues) from $\mathcal{DM}_A$ against all rows from $\mathcal{DM}_B$, and stores the row–row matching scores in the score matrix $\mathcal{SM}$. Row–row comparison algorithm **AlignRow** (line 3 in the initial alignment algorithm) is an adaptation of the classical Needleman-Wunsch dynamic programming algorithm [NW71] used for sequence alignment. The detailed algorithm is described in [SM97, p. 52]. We use the linear gap penalty model with the default gap penalty value of 0. We use the function $Match(\bullet, \bullet)$ to determine the degree of match between two C_α–C_α

distance values $d1$ and $d2$.

$$Match(d1, d2) = \begin{cases} \frac{\alpha}{|d1-d2|+\alpha} & \text{if} \quad |d1 - d2| \leq T_{Match} \\ 0 & \text{otherwise} \end{cases} \tag{4.6}$$

where α is a score adjusting weight, and T_{Match} is a difference threshold of the distances. We use the empirically chosen values $\alpha = 0.75$ and $T_{Match} = 1.6$Å for it. The function $Match(\bullet, \bullet)$ is used in the dynamic programming's selection step. After executing the dynamic programming, we get the matching score of the two given rows.

Suppose we have two proteins structures A and B whose distance matrices $\mathcal{DM}_A$ and $\mathcal{DM}_B$ are as shown in Figure 4.3. As an example, the alignment of row $\mathcal{DM}_A[1]$ (the first row of A's distance matrix) and row $\mathcal{DM}_B[1]$ (the first row of B's distance matrix) is shown in Figure 4.4. The alignment path is shown in gray. The matching score of $\mathcal{DM}_A[1]$ and $\mathcal{DM}_B[1]$ is stored in cell $[1, 1]$ of the score matrix $\mathcal{SM}$. In this manner, we align each row from $\mathcal{DM}_A$ and each row from $\mathcal{DM}_B$ all-against-all, and fill their respective matching scores in the score matrix $\mathcal{SM}$ as shown in Figure 4.5 (Left).

Then, we apply another Needleman-Wunsch style dynamic programming algorithm on $\mathcal{SM}$ to generate the initially aligned residue pairs. In fact, the score matrix stores the degrees of matching of A's residues to B's residues, and dynamic programming effectively solves the *ordered bipartite matching* problem of maximizing the number and total degree of residue–residue matchings.

Figure 4.5 (Right) shows the dynamic programming's matrix on $\mathcal{SM}$ and the initial alignment of A and B. In this alignment, we can observe that the residues whose matching partners cannot be successfully found are aligned with the gaps. Such a residue usually have a distance profile which is quite different from the others' in its counterpart protein. (The distance profiles of such residues are highlighted in gray in Figure 4.3.) Since we use the ordered bipartite matching strategy, even though the distance profile of residue 2 in protein A is similar to that of residue 5 in protein B, they are not aligned together. This is because aligning $(2 - 5)$ will forbid the alignments of other good pairs $(3 - 2), (4 - 3)$ and $(5 - 4)$, and hence

	1	2	3	4	5	6	7
1	0.00	11.00	1.00	2.00	3.00	4.00	16.00
2	11.00	0.00	12.00	13.00	14.00	15.00	17.00
3	1.00	12.00	0.00	5.00	6.00	7.00	18.00
4	2.00	13.00	5.00	0.00	8.00	9.00	19.00
5	3.00	14.00	6.00	8.00	0.00	10.00	20.00
6	4.00	15.00	7.00	9.00	10.00	0.00	21.00
7	16.00	17.00	18.00	19.00	20.00	21.00	0.00

Distance Matrix of Protein *A*

	1	2	3	4	5	6
1	0.00	1.05	2.10	3.15	11.05	4.20
2	1.05	0.00	5.05	6.10	12.10	7.15
3	2.10	5.05	0.00	8.20	13.15	9.05
4	3.15	6.10	8.20	0.00	14.20	10.10
5	11.05	12.10	13.15	14.20	0.00	15.05
6	4.20	7.15	9.05	10.10	15.05	0.00

Distance Matrix of Protein *B*

Figure 4.3: Two sample distance matrices of proteins A and B.

Row #1 from B's Distance Matrix ($\mathcal{DM}_B[1]$)

Row #1 from A's Distance Matrix ($\mathcal{DM}_A[1]$)		1	2	3	4	5	6
		0.00	1.05	2.10	3.15	11.05	4.20
	0.00	0.00	0.00	0.00	0.00	0.00	0.00
1	0.00	0.00	1.00	1.00	1.00	1.00	1.00
2	11.00	0.00	1.00	1.09	1.10	1.11	1.95
3	1.00	0.00	1.00	1.95	1.95	1.95	1.95
4	2.00	0.00	1.00	1.95	2.86	2.86	2.86
5	3.00	0.00	1.00	1.95	2.86	3.73	3.73
6	4.00	0.00	1.00	1.95	2.86	3.73	3.86
7	16.00	0.00	1.00	1.95	2.86	3.73	3.90

$\mathcal{DM}_A[1]$	0.00	11.00	1.00	2.00	3.00	——	4.00	16.00
$\mathcal{DM}_B[1]$	0.00	——	1.05	2.10	3.15	11.05	4.20	——

Figure 4.4: Alignment of first row from distance matrix of A and that from B.

will result in a smaller total degree of residue–residue matchings.

The actual aligned residue pairs are traced back from the dynamic programming's matrix F by a simple recursive algorithm **GetAlignedPair** (line 10 in the initial alignment algorithm). The detailed algorithm is described in [SM97, p. 53].

4.3.2 Step 2: Refining Alignment

We use the alignment score S defined in Equation 4.2 as MatAlign's native score. The function S balances the RMSD value and the number of aligned residue pairs [AF96]. Our objective is to maximize S as much as possible.

The initial alignment generated in Step 1 is usually not an optimal one in terms of S. Thus, we refine the alignment iteratively until S cannot be further improved. The refinement algorithm is given in Figure 4.6. In order to calculate the alignment score S, we first have to superimpose the set of aligned residues in one protein onto their counterparts in the other protein, and calculate the value of Δ (RMSD)

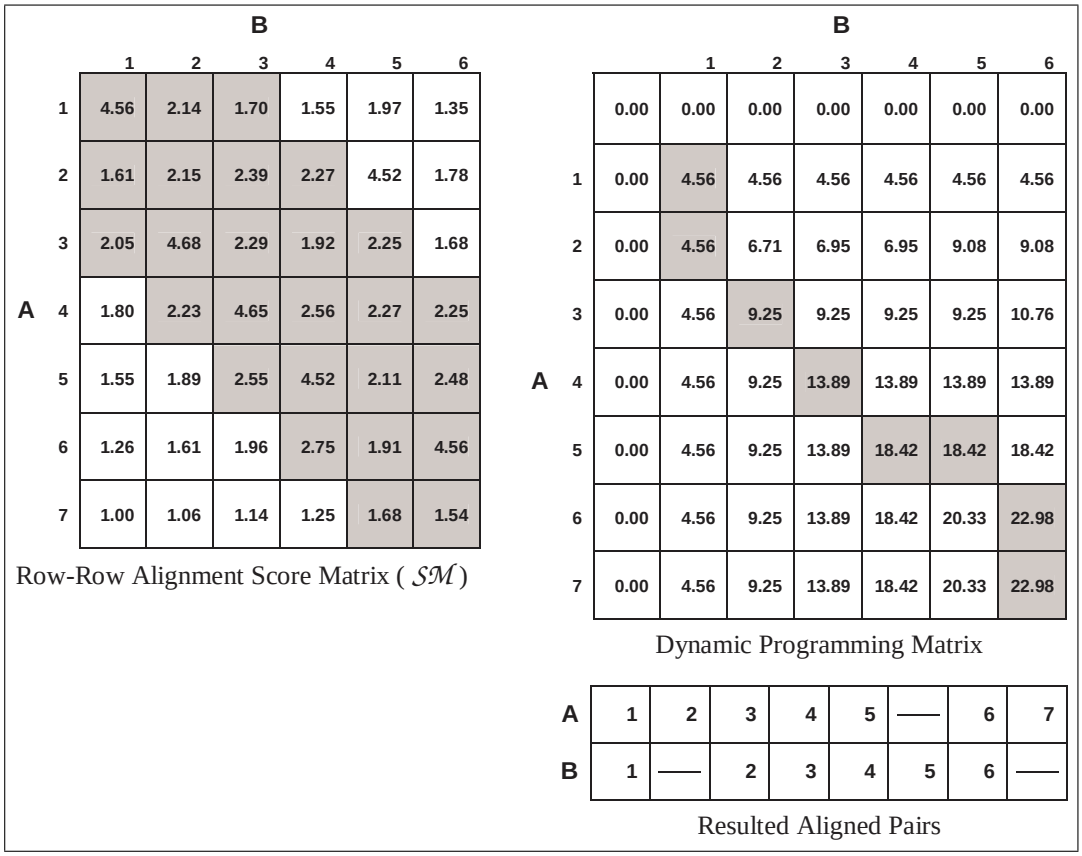

Figure 4.5: Generating initial alignment of protein A and B.

between them. The RMSD calculation algorithm **GetRMSD** (referred to in line 3 of the refinement algorithm) is explained in detail in Figure 4.7. It is adapted from the one given in [Wu03]. The calculation of RMSD can be carried by the least square fitting using the *singular value decomposition* (SVD) method [Kab78] (invoked in line 6 of the RMSD calculation algorithm). We use the software library by de Hoon *et al.* [dHINM04] for SVD.

During the process of calculating RMSD, we can easily pick up the pair of residues that are farthest. We remove this pair from our alignment, and iterate the processes of superimposition and calculating RMSD as long as the alignment score S converges (i.e. keeps increasing). We stop the iteration when S cannot be further improved (line 5 in the alignment algorithm).

The distribution of the RMSD values and the alignment lengths of 68 test protein pairs before and after the refinement step are depicted in Figures 4.8 and 4.9

function **RefineAlignment** $(N, A_{init}, B_{init}) \rightarrow (N', A_{final}, B_{final}, \Delta)$
input: (1) N (number of initially aligned residue pairs)
(2) $A_{init}[1 \ldots N]$ (3D coordinates of residues from A that involve in initial alignment)
(3) $B_{init}[1 \ldots N]$ (3D coordinates of residues from B that involve in initial alignment)
output: (1) N' (number of finally aligned residue pairs)
(2) $A_{final}[1 \ldots N']$ (residues from A involving in final alignment)
(3) $B_{final}[1 \ldots N']$ (residues from B involving in final alignment)
(4) Δ (RMSD between A_{final} and B_{final})
procedure:

```
1.  S_old = 0; N' = N; A_final = A_init; B_final = B_init   /* initialize */
2.  while (TRUE)
3.      Δ = GetRMSD (N', A_final, B_final)                 /* see detailed algo. in fig. 4.7 */
4.      S = 3 · N'/(1 + Δ)                                 /* Eq. 4.2 */
5.      if (S < S_old) then exit while                     /* if the score diverges, then stop */
6.      S_old = S                                          /* mark the last best score */
7.      Remove the farthest residue pair from A_final and B_final
8.      N' = N' − 1                                        /* reduce number of aligned pairs */
9.  end while
10. return (N', A_final, B_final, Δ)
```

Figure 4.6: Refining initial alignment into final alignment.

respectively. (Both results are after being subject to the accuracy enhancement described in the next sub-section.) It can be observed that there are many alignments that are not well-fitted (i.e. large RMSD values) before the refinement. The number of such bad alignments is much reduced after the refinement.

4.3.3 Enhancements on Basic Algorithm

The following enhancements are done on top of the basic MatAlign algorithm in order to achieve better speed and greater accuracy.

- **Reduced rows**: In the row–row alignment step, it is observed that the large C_α–C_α distance values are not very important in determining the row–row matching scores, and hence can be ignored. These distance values are removed from the rows of the distance matrix, and the resultant reduced rows can be used for alignment. For example, in Figure 4.3, if we use the cutoff

function **GetRMSD** $(N, A_{al}, B_{al}) \rightarrow (\Delta)$

input: (1) N (number of aligned residue pairs)

(2) $A_{al}[1 \ldots N]$ (3D coordinates of residues from A that involve in alignment)

(3) $B_{al}[1 \ldots N]$ (3D coordinates of residues from B that involve in alignment)

output: Δ (RMSD value between A_{al} and B_{al})

procedure:

1. $A_c = (\sum_{i=1}^{N} A_{al}[i])/N$ /* get center of geometry of A_{al} and B_{al} */
2. $B_c = (\sum_{i=1}^{N} B_{al}[i])/N$ /* get center of geometry of A_{al} and B_{al} */
3. $A_{ori} = A_{al} - A_c$ /* move A_{al} to the origin */
4. $B_{ori} = B_{al} - B_c$ /* move B_{al} to the origin */
5. $C = B_{ori}^{\mathrm{T}} \times A_{ori}$
6. $[U, S, V^{\mathrm{T}}] = \mathbf{SVD}(C)$ /* decompose C into two orthogonal matrices U and V^{T}, and diagonal matrix S */
7. $Q = UV$ /* calculate rotation matrix Q from U and V */
8. $B_{ori}^{Q} = B_{ori} \times Q$ /* superimposition of B_{ori} onto A_{ori} */
9. $\Delta = \sqrt{1/N \times \sum_{i=1}^{N} (A_{ori} - B_{ori}^{Q})^2}$ /* Eq. 4.1 */
10. `return` Δ

Figure 4.7: RMSD calculation algorithm.

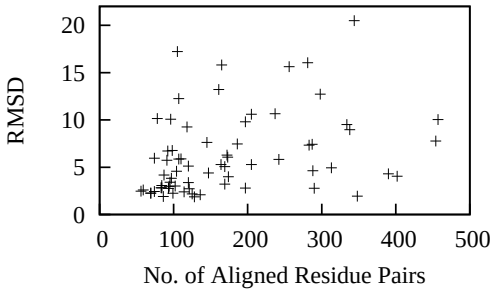

Figure 4.8: Distribution of RMSD and alignment length before refinement.

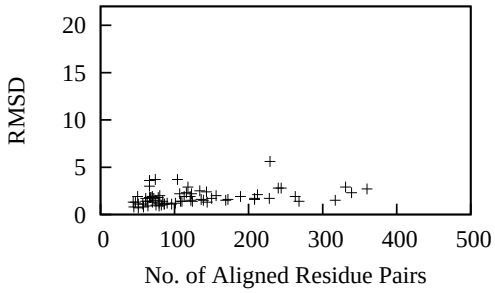

Figure 4.9: Distribution of RMSD and alignment length after refinement.

distance of 10Å, the reduced version of the first row of A's distance matrix will become: $\{0.00, 1.00, 2.00, 3.00, 4.00\}$. In our actual implementation, we use the cutoff value 21Å which is empirically determined.

- **Alignment within a band**: Both in the alignment of rows and alignment of the score matrix, it can be observed that the two residues whose ordinal

positions are quite different rarely align. For example, in Figures 4.3 and 4.4, when we align the first two rows of A and B, A's cell #2 and B's cell #5 are not likely to be aligned although their values are quite close. So, we define a *band*, and only the residue pairs that fall into the band are considered for alignment. In other words, for residue i and j to be aligned, the condition $(i - Bandwidth \leq j \leq i + Bandwidth)$ must be satisfied. The $Bandwidth$ can be calculated as:

$$Bandwidth = \#Gaps + abs(|A| - |B|) \tag{4.7}$$

where $\#Gaps$ is the number of allowable gaps and $abs(|A| - |B|)$ is the length difference between A and B. In Figure 4.5, the residue pairs falling into the bandwidth of 2 are shown as gray. In our implementation, we use $\#Gaps = 50$. The use of reduced rows and bands significantly improves the speed of the scheme as discussed later in Section 4.4.

- **Application of weights to row–row matching scores**: In the cases of distantly related protein structures, for a row in one protein's distance matrix, there are several rows in the other distance matrix which give the very similar row–row matching scores. As such, the initial alignment path based on these not-too-different scores may sometimes be incorrect. To reduce this effect, we multiply the row–row matching scores with the percent of the aligned residues. For example, in Figure 4.5, $\mathcal{SM}[1,1]$ will now be $4.56 \times (5/6)$, because the alignment of A's row #1 and B's row #1 results in 5 aligned residue pairs out of 6 pairs which is maximally possible. This heuristics improves the accuracy of the scheme.

- **Use of multiple initial alignment seeds**: Sometimes the default initial alignment produced from the first step may not lead to the optimal final alignment in the second step. To explore the possibilities for a better final alignment, we have to try multiple initial alignments. When extracting the initial alignment path from the dynamic programming's matrix, we set a threshold and if the value in a matrix's cell is lower than the threshold,

we avoid this cell in our alignment path. We generate 100 different initial alignment paths using 100 different threshold values, refine each path, and select the one that gives us the best score S. This approach substantially improves the scheme's accuracy although it slightly affects the scheme's run-time efficiency. The combined effect of the use of row–row matching weights and the use of multiple alignment seeds on the accuracy is discussed later in Section 4.4.5.

4.3.4 Time Complexity

The worst-case time complexity for finding the initial alignment of two proteins A and B with $|A|$ and $|B|$ residues respectively is $O(|A|^2|B|^2)$. (Every row in A's distance matrix has to be compared against every row in B's distance matrix, and each comparison using dynamic programming costs $O(|A||B|)$.) Nonetheless, because of the utilization of reduced rows and bands as mentioned in the above sub-section, the actual running time is reasonably fast.

The worst-case time complexity for the refinement step is $O(\min(|A|, |B|)^2)$. (The maximum possible length of the initial alignment is $\min(|A|, |B|)$, and thus at most $\min(|A|, |B|)$ refinement steps will be required. Each refinement step involves the calculation of RMSD which can be carried out in linear time, i.e., $O(\min(|A|, |B|))$ time.)

4.4 Experimental Results

In order to assess the performance of our proposed MatAlign method, we compare it against DALI [HS93] (DaliLite implementation [HP00]), and CE [SB98], which are among the most accurate and the most widely used of the existing structural alignment methods [NMK04, SP04]. We use the benchmark of 68 protein pairs selected by Fischer *et al.* [FERE96] in our experiment.

4.4.1 RMSD and Alignment Length

In Figure 4.10, it can be observed that MatAlign generally tends to produce a smaller RMSD value (which means better fitted alignment) than DALI and CE do. The average RMSD of MatAlign for 68 benchmark protein pairs is 1.81Å, and those of DALI and CE are 2.77Å and 2.88Å respectively.

On the other hand, MatAlign's alignment length is relatively shorter than those of DALI and CE as can be seen in Figure 4.11. For simplicity of presentation in the figure, the alignment length is converted to the *percent of aligned residue pairs*, which is a ratio of the number of aligned residue pairs to the length of the shorter protein. (The length of the shorter protein is the maximum possible length of the alignment.) The average percent of aligned residue pairs of MatAlign is 67%, and those of DALI and CE are 82% and 83% respectively.

Nonetheless, MatAlign's alignment length is significantly large enough. It covers over at least 50% of the maximum possible alignment length in 91% (62 out of 68) of the cases, and at least 35% of the maximum length in all of the 68 cases. Thus, it can be concluded that MatAlign is able to detect the highly conserved yet significantly large structural cores in proteins.

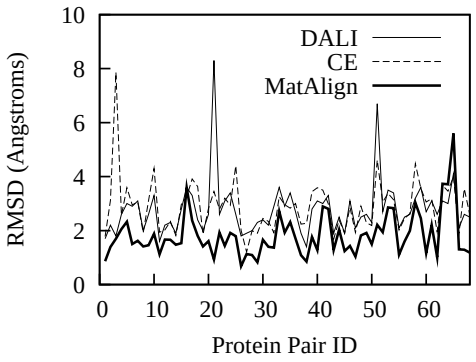

Figure 4.10: Distribution of RMSD values.

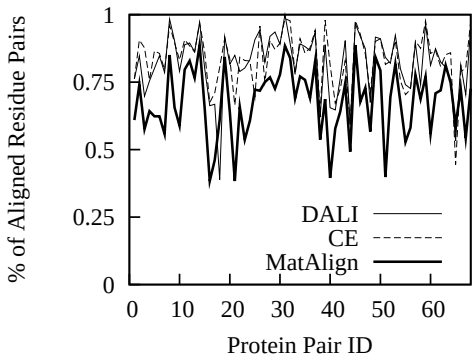

Figure 4.11: Distribution of percents of aligned residue pairs.

4.4.2 Accuracy Assessment by Different Criteria

It is observed that in terms of the alignment score criterion S by Alexandrov and Fischer [AF96] described in Equation 4.2, MatAlign can achieve better (higher) alignment scores than DALI in 55 out of 67 cases[1] (i.e. 81%), and better scores than CE in 54 out of 67 cases[2] (79%). We show the distributions of the score values for DALI, CE and MatAlign in Figure 4.12. Again, for convenience of presentation, the alignment score (S) is translated into the *normalized score* (NS), which is the ratio of S to the maximum possible alignment length. The average NS value of MatAlign is 0.77 whilst those of DALI and CE are 0.68 each.

However, this result may not be very convincing of the better accuracy achievement of MatAlign, because the scoring criterion S is also used as the native score of MatAlign. On the other hand, DALI and CE use their respective Z-scores as their native scores. This means that while the score of MatAlign is optimized in terms of S, those of DALI and CE are not.

Thus, we also compare MatAlign with DALI and CE using the other 3 scoring criteria which are not the native scores of any of these 3 methods. These are similarity index (SI) [KJ94] (Equation 4.3), match index (MI) [KJ94] (Equation 4.4), and structural alignment score (SAS) [SLL93] (Equation 4.5). These three have also been used in a recent evaluation study on various structural alignment methods by Kolodny *et al.* [KKL05].

It is observed that MatAlign can provide better results than both DALI and CE in a majority of cases in terms of all these three criteria!

With SI scoring criterion, MatAlign is better (achieves lower score values) in 58 out of 67 cases (85%) than DALI, and in 60 out of 67 cases (88%) than CE. The average SI value of MatAlign is 2.82, and those of DALI and CE are 3.48 and 3.56 respectively.

According to MI, MatAlign is better (higher values) in 52 cases (76%) than DALI, and in 53 cases (78%) than CE. The average MI value of MatAlign is 0.32,

[1] DALI cannot produce any alignment result for `1mdc` vs `1ifc`.

[2] CE cannot produce any alignment result for `1bbt1` vs `2plv1`.

while those of DALI and CE are both 0.30.

In terms of SAS, MatAlign is better (lower values) in 58 cases (85%) than DALI, and in 60 cases (88%) than CE. The average SAS value of MatAlign is 1.78, and those of DALI and CE are 2.27 and 2.40 respectively.

The distributions of the values of SI, MI and SAS on the 68 benchmark protein pairs are shown in Figures 4.13, 4.14 and 4.15 respectively.

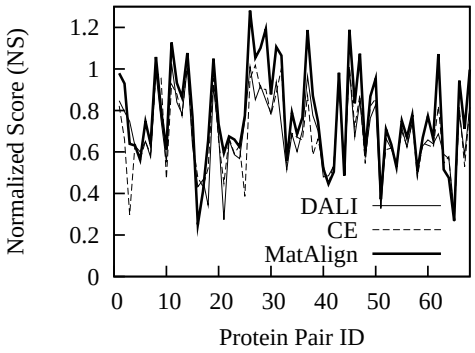

Figure 4.12: Distribution of normalized score (NS) values. (Higher values mean better alignments.)

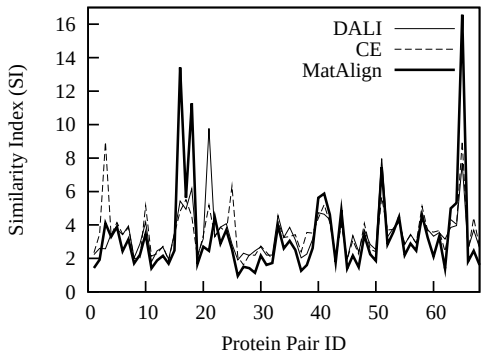

Figure 4.13: Distribution of similarity index (SI) values. (Lower values mean better alignments.)

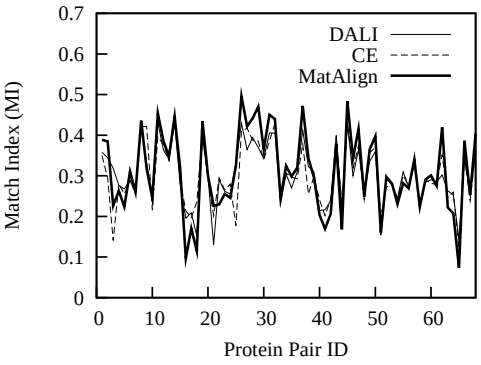

Figure 4.14: Distribution of match index (MI) values. (Higher values mean better alignments.)

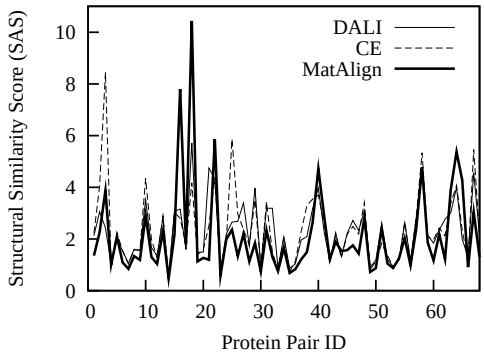

Figure 4.15: Distribution of structural similarity score (SAS) values. (Lower values mean better alignments.)

The details of the comparative accuracy evaluation of DALI, CE and MatAlign are shown in Tables 4.1 and 4.2.

Table 4.1: Detailed comparison of DALI, CE and MatAlign in terms of 4 alignment quality criteria.

Pair	Protein 1		Protein 2		DALI							CE							MatAlign							*S*		*SI*		*MI*		*SAS*	
ID	PDBID	#AA	PDBID	#AA	RMSD	#Pair	Pair%	*S*	*SI*	*MI*	*SAS*	RMSD	#Pair	Pair%	*S*	*SI*	*MI*	*SAS*	RMSD	#Pair	Pair%	*S*	*SI*	*MI*	*SAS*	C1	C2	C1	C2	C1	C2	C1	C2
1	1aaj_	105	1paz_	120	1.7	80	0.76	88.9	2.23	0.36	2.13	1.8	80	0.76	86.3	2.34	0.35	2.23	0.9	64	0.61	102.8	1.42	0.39	1.36	+	+	+	+	+	+	+	+
2	1aba_	87	1ego_	85	2.2	72	0.85	67.5	2.60	0.34	3.06	3.1	77	0.91	56.1	3.44	0.29	4.05	1.4	63	0.74	79.0	1.88	0.39	2.21	+	+	+	+	+	+	+	+
3	1aep_	153	256bA	106	1.8	74	0.70	79.3	2.58	0.32	2.43	7.9	93	0.88	31.5	8.96	0.14	8.45	1.7	61	0.58	67.8	2.95	0.27	2.79	-	+	-	+	-	+	-	+
4	1afnA	330	1aozA	552	2.6	249	0.75	207.5	3.45	0.28	1.04	2.6	250	0.76	210.1	3.39	0.28	1.03	2.1	212	0.64	208.2	3.20	0.27	0.97	+	-	+	+	-	-	+	+
5	1ak3A	214	1gky_	186	3	149	0.80	111.8	3.74	0.27	2.01	3.6	161	0.87	105.2	4.15	0.26	2.23	2.3	116	0.62	104.7	3.73	0.25	2.00	-	-	+	+	-	-	+	+
6	1arb_	263	4ptp_	223	2.9	189	0.85	145.4	3.42	0.29	1.53	3.0	191	0.86	145.1	3.44	0.29	1.54	1.5	139	0.62	166.5	2.41	0.31	1.08	+	+	+	+	+	+	+	+
7	1atnA	373	1atr_	383	3.1	293	0.79	214.4	3.95	0.26	1.06	3.1	297	0.80	219.5	3.84	0.26	1.03	1.6	208	0.56	238.1	2.91	0.27	0.78	+	+	+	+	+	+	+	+
8	1bbhA	131	2ccyA	127	2	125	0.98	125.0	2.03	0.42	1.60	1.9	122	0.96	125.3	2.00	0.42	1.57	1.4	108	0.85	134.3	1.66	0.44	1.31	+	+	+	+	+	+	+	+
9	1bbt1	186	2plv1	288	2.6	168	0.90	140.0	2.88	0.33	1.55	NA	NA	NA	NA	NA	NA	NA	1.5	122	0.66	149.1	2.22	0.33	1.19	+	NA	+	NA	+	NA	+	NA
10	1bgeB	159	1gmfA	119	3.3	94	0.79	65.6	4.18	0.25	3.51	4.3	99	0.83	56.0	5.17	0.22	4.34	1.9	70	0.59	72.8	3.20	0.26	2.69	+	+	+	+	+	+	+	+
11	1c2rA	116	1ycc_	108	1.6	96	0.89	110.8	1.80	0.43	1.67	1.9	98	0.91	100.0	2.14	0.40	1.98	1.1	86	0.80	121.7	1.41	0.46	1.30	+	+	+	+	+	+	+	+
12	1cauB	184	1cauA	181	2.2	162	0.90	151.9	2.46	0.36	1.36	2.0	160	0.88	158.9	2.29	0.38	1.26	1.7	150	0.83	168.7	2.01	0.39	1.11	+	+	+	+	+	+	+	+
13	1cewI	108	1molA	94	2.3	81	0.86	73.6	2.67	0.34	2.84	2.3	81	0.86	72.8	2.72	0.34	2.89	1.7	72	0.77	81.2	2.17	0.36	2.31	+	+	+	+	+	+	+	+
14	1chrA	370	2mnr_	357	1.9	347	0.97	359.0	1.95	0.43	0.55	1.8	346	0.97	368.1	1.88	0.44	0.53	1.5	317	0.89	384.4	1.66	0.45	0.47	+	+	+	+	+	+	+	+
15	1cid_	177	2rhe_	114	2.8	91	0.80	71.8	3.51	0.28	3.08	3.0	98	0.86	74.1	3.45	0.29	3.03	1.5	74	0.65	87.6	2.36	0.32	2.07	+	+	+	+	+	+	+	+
16	1cpcL	172	1colA	197	3.6	114	0.66	74.3	5.43	0.20	3.16	3.3	116	0.67	81.9	4.82	0.21	2.80	3.6	66	0.38	43.1	9.37	0.11	5.45	-	-	-	-	-	-	-	-
17	1crl_	534	1ede_	310	3.3	207	0.67	144.4	4.94	0.21	1.59	3.9	220	0.71	134.4	5.51	0.20	1.78	2.4	143	0.46	127.1	5.15	0.18	1.66	-	-	-	+	-	-	-	+
18	1dsbA	188	2trxA	108	2.4	42	0.39	37.1	6.17	0.15	5.71	3.6	87	0.81	56.4	4.51	0.24	4.17	1.8	66	0.61	70.6	2.95	0.28	2.73	+	+	+	+	+	+	+	+
19	1dxtB	147	1hbg_	147	2	135	0.92	135.0	2.18	0.39	1.48	1.9	134	0.91	140.6	2.04	0.41	1.39	1.4	124	0.84	154.3	1.67	0.44	1.14	+	+	+	+	+	+	+	+
20	1eaf_	243	4cla_	213	2.6	174	0.82	145.0	3.18	0.30	1.49	2.8	178	0.84	139.8	3.37	0.29	1.58	1.6	136	0.64	156.4	2.52	0.31	1.18	+	+	+	+	+	+	+	+
21	1fc1A	206	2fb4H	229	8.3	175	0.85	56.5	9.77	0.13	4.74	3.5	137	0.67	92.4	5.19	0.20	2.52	0.9	79	0.38	122.7	2.43	0.24	1.18	+	+	+	+	+	+	+	+
22	1fxiA	96	1ubq_	76	2.6	60	0.79	50.0	3.29	0.29	4.33	2.8	64	0.84	50.7	3.31	0.30	4.36	1.9	50	0.66	51.3	2.93	0.29	3.85	+	+	+	+	+	-	+	+
23	1gal_	581	3cox_	500	3.1	401	0.80	293.4	3.87	0.26	0.77	3.2	415	0.83	296.4	3.86	0.27	0.77	1.4	268	0.54	330.2	2.68	0.27	0.54	+	+	+	+	+	+	+	+
24	1gky_	186	3adk_	194	3.4	155	0.83	105.7	4.08	0.26	2.19	2.9	154	0.83	117.3	3.55	0.28	1.91	1.9	113	0.61	116.3	3.15	0.27	1.69	+	-	+	+	+	-	+	+
25	1gp1A	183	2trxA	108	2.6	98	0.91	81.7	2.87	0.33	2.65	4.4	75	0.69	41.7	6.34	0.18	5.87	1.8	78	0.72	83.7	2.49	0.33	2.30	+	+	+	+	-	+	+	+
26	1hip_	85	2hipA	71	1.8	67	0.94	71.8	1.91	0.43	2.69	2.0	68	0.96	67.8	2.10	0.41	2.96	0.7	51	0.72	91.0	0.95	0.50	1.34	+	+	+	+	+	+	+	+
27	1hom_	68	1lfb_	77	1.9	56	0.82	57.9	2.31	0.36	3.39	1.2	51	0.75	69.2	1.61	0.42	2.37	1.1	51	0.75	71.7	1.51	0.43	2.23	+	+	+	+	+	+	+	+
28	1hrhA	125	1rnh_	148	2	115	0.92	115.0	2.17	0.39	1.74	2.0	113	0.90	113.0	2.21	0.39	1.77	1.1	96	0.77	137.6	1.42	0.45	1.14	+	+	+	+	+	+	+	+
29	1isuA	62	2hipA	71	2.3	58	0.94	52.7	2.46	0.37	3.97	1.9	54	0.87	55.9	2.18	0.39	3.52	0.8	45	0.73	73.9	1.14	0.47	1.84	+	+	+	+	+	+	+	+
30	1lgaA	343	2cyp_	293	2.4	261	0.89	230.3	2.69	0.34	0.92	2.5	262	0.89	227.8	2.74	0.34	0.94	1.7	228	0.78	257.1	2.13	0.37	0.73	+	+	+	+	+	+	+	+
31	1ltsD	103	1bovA	69	2.2	69	1.00	64.7	2.20	0.41	3.19	2.3	68	0.99	61.1	2.37	0.39	3.44	1.4	61	0.88	76.3	1.58	0.46	2.29	+	+	+	+	+	+	+	+
32	1mdc_	131	1ifc_	131	NA	NA	NA	NA	NA	NA	NA	1.9	128	0.98	131.5	1.97	0.43	1.50	1.4	110	0.84	139.4	1.63	0.44	1.24	NA	+	NA	+	NA	+	NA	+
33	1mioC	525	1minB	522	3.6	411	0.79	268.0	4.57	0.23	0.88	3.3	406	0.78	285.9	4.19	0.25	0.80	2.7	360	0.69	290.8	3.94	0.25	0.75	+	+	+	+	+	+	+	+
34	1mup_	157	1rbp_	174	2.9	140	0.89	107.7	3.25	0.30	2.07	3.0	143	0.91	108.3	3.25	0.31	2.07	1.9	121	0.77	124.0	2.50	0.34	1.59	+	+	+	+	+	+	+	+
35	1npx_	447	3grs_	461	3.4	394	0.88	268.6	3.86	0.27	0.86	2.8	383	0.86	300.0	3.30	0.30	0.74	2.3	339	0.76	306.8	3.05	0.30	0.68	+	+	+	+	+	+	+	+
36	1omf_	340	2por_	301	2.7	261	0.87	211.6	3.11	0.31	1.03	3.0	264	0.88	198.0	3.42	0.29	1.14	1.7	208	0.69	230.5	2.47	0.32	0.82	+	+	+	+	+	+	+	+
37	1onc_	104	7rsa_	124	1.9	97	0.93	100.3	2.04	0.41	1.96	2.2	98	0.94	90.7	2.38	0.38	2.29	1.1	86	0.83	123.5	1.32	0.48	1.27	+	+	+	+	+	+	+	+
38	1osa_	148	4cpv_	108	1.4	67	0.62	83.8	2.26	0.32	2.09	2.3	69	0.64	63.3	3.55	0.26	3.29	0.8	58	0.54	94.1	1.58	0.35	1.46	+	+	+	+	+	+	+	+
39	1pfc_	111	3hlaB	99	2.8	88	0.89	69.5	3.15	0.31	3.18	3.4	97	0.98	65.5	3.51	0.30	3.55	1.8	68	0.69	73.9	2.56	0.32	2.59	+	+	+	+	+	+	+	+
40	1rcb_	129	1gmfA	119	3.1	78	0.66	57.1	4.73	0.21	3.97	3.6	97	0.82	63.4	4.40	0.24	3.70	1.3	47	0.39	61.9	3.23	0.22	2.72	+	-	+	+	+	-	+	+

Table 4.2: Detailed comparison of DALI, CE and MatAlign in terms of 4 alignment quality criteria (contd.).

Pair	Protein 1		Protein 2		DALI							CE							MatAlign							*S*		*SI*		*MI*		*SAS*	
ID	PDBID	#AA	PDBID	#AA	RMSD	#Pair	Pair%	*S*	*SI*	*MI*	*SAS*	RMSD	#Pair	Pair%	*S*	*SI*	*MI*	*SAS*	RMSD	#Pair	Pair%	*S*	*SI*	*MI*	*SAS*	C1	C2	C1	C2	C1	C2	C1	C2
41	1sacA	204	1ayh_	214	3	132	0.65	99.0	4.64	0.22	2.27	3.5	137	0.67	91.3	5.21	0.20	2.55	2.9	118	0.58	90.9	5.01	0.20	2.45	-	-	-	+	-	-	-	+
42	1sim_	381	1nsbA	390	3.3	291	0.76	203.0	4.32	0.24	1.13	3.0	276	0.72	207.5	4.13	0.24	1.08	2.8	244	0.64	192.3	4.38	0.22	1.15	-	-	-	-	-	-	-	-
43	1stfI	98	1molA	94	1.9	85	0.90	87.9	2.10	0.40	2.24	1.7	78	0.83	87.3	2.02	0.39	2.15	1.3	70	0.74	92.3	1.71	0.40	1.82	+	+	+	+	+	+	+	+
44	1tahA	318	1tca_	317	2.5	188	0.59	161.1	4.22	0.22	1.33	2.4	188	0.59	166.4	4.03	0.23	1.27	2.0	156	0.49	154.2	4.14	0.21	1.30	-	-	+	-	-	-	+	-
45	1ten_	89	3hhrB	195	1.9	86	0.97	89.0	1.97	0.43	2.21	1.9	87	0.98	90.0	1.94	0.43	2.18	1.2	79	0.89	105.7	1.40	0.49	1.57	+	+	+	+	+	+	+	+
46	1tie_	166	4fgf_	124	3.1	114	0.92	83.4	3.37	0.30	2.72	2.9	115	0.93	89.4	3.08	0.32	2.49	1.4	84	0.68	103.5	2.12	0.35	1.71	+	+	+	+	+	+	+	+
47	1tlk_	103	2rhe_	114	2.1	90	0.87	87.1	2.40	0.36	2.33	1.9	88	0.85	90.1	2.26	0.37	2.19	1.0	75	0.73	110.6	1.42	0.43	1.38	+	+	+	+	+	+	+	+
48	2azaA	129	1paz_	120	2.5	81	0.68	69.4	3.70	0.25	3.09	2.9	85	0.71	65.4	4.09	0.24	3.41	1.8	68	0.57	72.4	3.21	0.26	2.67	+	+	+	+	+	+	+	+
49	2cmd_	312	6ldh_	329	2.6	286	0.92	238.3	2.84	0.34	0.91	2.3	281	0.90	256.2	2.54	0.36	0.81	1.9	263	0.84	270.8	2.27	0.37	0.73	+	+	+	+	+	+	+	+
50	2fbjL	213	8fabB	214	2.3	194	0.91	176.4	2.53	0.36	1.19	2.2	194	0.91	182.4	2.40	0.37	1.13	1.5	169	0.79	203.0	1.89	0.40	0.89	+	+	+	+	+	+	+	+
51	2gbp_	309	2liv_	344	6.7	260	0.84	101.3	7.96	0.15	2.58	4.6	252	0.82	134.8	5.65	0.20	1.83	2.2	123	0.40	114.9	5.56	0.16	1.80	+	-	+	+	+	-	+	+
52	2hhmA	272	1fbpA	316	2.7	223	0.82	180.8	3.29	0.29	1.21	3.1	225	0.83	166.3	3.70	0.27	1.36	1.9	189	0.69	192.9	2.79	0.30	1.03	+	+	+	+	+	+	+	+
53	2hpdA	457	2cpp_	405	3.5	374	0.92	249.3	3.79	0.28	0.94	3.4	366	0.90	250.7	3.74	0.28	0.92	2.9	331	0.82	257.7	3.49	0.28	0.86	+	+	+	+	+	+	+	+
54	2mnr_	357	4enl_	436	3.4	285	0.80	194.3	4.26	0.24	1.19	3.1	269	0.75	194.9	4.17	0.24	1.17	2.8	240	0.67	188.1	4.21	0.23	1.18	-	-	+	-	-	-	+	-
55	2mtaC	147	1ycc_	108	2.1	80	0.74	77.4	2.84	0.31	2.63	2.0	76	0.70	75.5	2.87	0.30	2.66	1.1	57	0.53	81.1	2.10	0.31	1.95	+	+	+	+	-	+	+	+
56	2pia_	321	1fnr_	296	2.5	215	0.73	184.3	3.44	0.27	1.16	2.5	214	0.72	186.1	3.39	0.27	1.14	1.6	172	0.58	198.6	2.75	0.28	0.93	+	+	+	+	+	+	+	+
57	2pna_	104	1shaA	103	2.6	92	0.89	76.7	2.91	0.33	2.83	2.6	93	0.90	76.9	2.91	0.33	2.83	2.0	80	0.78	80.2	2.57	0.33	2.49	+	+	+	+	+	+	+	+
58	2sarA	96	9rnt_	104	3.2	71	0.74	50.7	4.33	0.24	4.51	4.5	84	0.88	46.0	5.12	0.22	5.33	3.0	66	0.69	49.1	4.42	0.23	4.60	-	+	-	+	-	+	-	+
59	2sas_	185	2scpA	174	3.6	168	0.97	109.6	3.73	0.28	2.14	3.6	170	0.98	111.8	3.64	0.29	2.09	2.5	134	0.77	116.4	3.19	0.29	1.83	+	+	+	+	+	+	+	+
60	2sga_	181	4ptp_	223	2.7	147	0.81	119.2	3.32	0.29	1.84	3.1	155	0.86	114.5	3.57	0.28	1.97	1.2	101	0.56	139.8	2.09	0.32	1.16	+	+	+	+	+	+	+	+
61	2snv_	151	4ptp_	223	3.1	132	0.87	96.6	3.55	0.29	2.35	3.2	131	0.87	94.0	3.67	0.28	2.43	2.2	107	0.71	100.1	3.11	0.29	2.06	+	+	+	+	+	+	+	+
62	3cd4_	178	2rhe_	114	2.6	94	0.82	78.3	3.15	0.30	2.77	2.0	92	0.81	93.6	2.42	0.35	2.12	1.0	82	0.72	122.2	1.41	0.43	1.24	+	+	+	+	+	+	+	+
63	3chy_	128	4fxn_	138	3.1	103	0.80	75.4	3.85	0.26	3.01	3.7	109	0.85	69.9	4.32	0.25	3.38	3.7	104	0.81	65.9	4.60	0.23	3.59	-	-	-	-	-	-	-	-
64	3hlaB	99	2rhe_	114	3	75	0.76	56.3	3.96	0.25	4.00	3.5	85	0.86	57.2	4.03	0.26	4.07	3.7	74	0.75	47.1	4.97	0.22	5.02	-	-	-	-	-	-	-	-
65	3rubL	441	6xia_	387	4.1	206	0.53	121.2	7.70	0.14	1.99	4.0	172	0.44	103.2	9.00	0.12	2.33	5.6	229	0.59	104.1	9.46	0.13	2.45	-	+	-	-	-	+	-	-
66	4sbvA	199	2tbvA	285	2.1	162	0.81	156.8	2.58	0.34	1.30	1.9	157	0.79	162.4	2.41	0.35	1.21	1.3	144	0.72	187.7	1.80	0.39	0.90	+	+	+	+	+	+	+	+
67	5fd1_	106	2fxb_	81	2.6	57	0.70	47.5	3.69	0.26	4.56	3.6	65	0.80	42.9	4.42	0.24	5.46	1.3	44	0.54	57.6	2.38	0.29	2.94	+	+	+	+	+	+	+	+
68	8i1b_	146	4fgf_	124	2.5	118	0.95	101.1	2.63	0.36	2.12	2.6	121	0.98	101.1	2.65	0.36	2.14	1.2	90	0.73	123.6	1.63	0.41	1.32	+	+	+	+	+	+	+	+

+/- difference	43	41	49	53	37	39	49	53
No. of cases in which MatAlign is better	55	54	58	60	52	53	58	60
Percentage in which MatAlign is better	80.9	79.4	85.3	88.2	76.5	77.9	85.3	88.2

S = Alexandrov and Fischer's alignment score [AF96] (to maximize)
SI = Kleywegt and Jone's similarity index [KJ94] (to minimize)
MI = Kleywegt and Jone's match index [KJ94] (to maximize)
SAS = Subbiah, Laurents and Levitt's structural alignment score [SLL93] (to minimize)
C1 = MatAlign vs DALI
C2 = MatAlign vs CE
\+ = instances in which MatAlign is better than DALI or CE
\- = instances in which DALI or CE is better
NA = no results available

4.4.3 Accuracy Assessment by Adjusted RMSD

In addition to comparing the alignment accuracies of DALI, CE and MatAlign in terms of the above 4 criteria, it will be interesting to compare these methods in terms of their "adjusted" RMSD values at a fixed alignment length. For a given alignment case, from the three different alignment results by the three methods, we choose the one with the shortest alignment length as the benchmark. The other two longer alignments are iteratively refined by removing the furthest pair in each step (as described in Section 4.3.2) until their alignment lengths become equal to the shortest one. Then, the resulting adjusted RMSD values of the three methods are compared.

It is observed that MatAlign achieves better (smaller) adjusted RMSD values than DALI in 36 out of 67 cases (i.e. 54%), and better values than CE in 35 out of 55 cases[3] (64%). The average adjusted RMSD values for MatAlign is 1.794, and those for DALI and CE are 1.799 and 1.891 respectively. The distributions of the adjusted RMSD values for the three methods are shown in Figure 4.16, and the detailed information is given in Table 4.3.

4.4.4 Speed

In terms of speed, MatAlign is about 3 times faster than DALI, and about as fast as CE on Sun Ultra Sparc II with two 480 MHz CPUs and 4 GB main memory, running Sun OS 5.7. Figure 4.17 shows the execution times of the three methods. The average time per pairwise alignment for MatAlign is 24.8 sec, and those for DALI and CE are 78.1 sec and 28.1 respectively.

4.4.5 Significance of Enhancements

The significance of the speed and the accuracy enhancements (as described in Section 4.3.3) are shown in Figures 4.18 and 4.19 respectively. It is observed that

[3]We are not able to extract the detailed residue–residue alignment information from 12 of the CE alignment results.

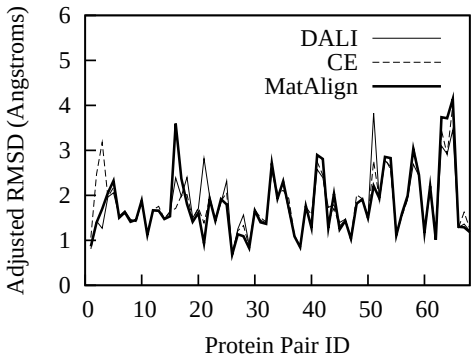

Figure 4.16: Distribution of adjusted RMSD values. (Curve smoothing is used for the missing values.)

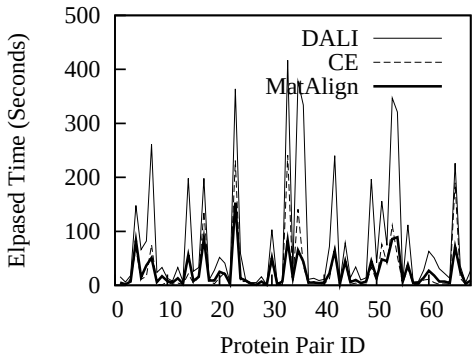

Figure 4.17: Distribution of alignment times in seconds.

the speed enhancement reduces the average running time from 225.9 sec to 24.8 sec (9 fold speedup). Similarly, the accuracy enhancement improves the average normalized score NS from 0.67 to 0.77 (15% improvement).

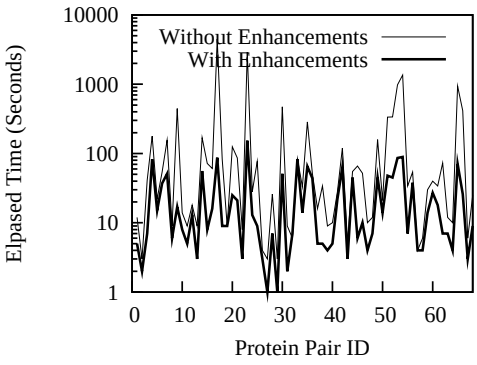

Figure 4.18: Effect of speed enhancement (use of reduced rows and bands).

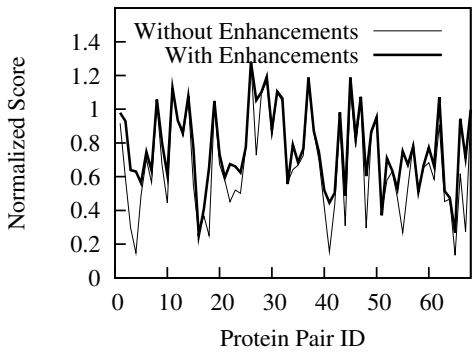

Figure 4.19: Effect of accuracy enhancement (weighting of row–row matching scores and use of multiple initial alignment seeds.)

Table 4.3: Detailed comparison of DALI, CE and MatAlign in terms of adjusted RMSD values.

Sr.	Protein 1		Protein 2			DALI	CE	MatAlign	DALI vs	CE vs
	PDBID	#AA	PDBID 2	#AA	**#Pair**	RMSD			MatAlign	MatAlign
1	1aaj_	105	1paz_	120	**64**	0.811	1.061	0.867	-	+
2	1aba_	87	1ego_	85	**63**	1.426	2.471	1.392	+	+
3	1aep_	153	256bA	106	**61**	1.269	3.180	1.700	-	+
4	1afnA	330	1aozA	552	**212**	1.963	1.966	2.055	-	-
5	1ak3A	214	1gky_	186	**116**	2.056	2.174	2.325	-	-
6	1arb_	263	4ptp_	223	**139**	1.541	1.515	1.504	+	+
7	1atnA	373	1atr_	383	**208**	1.655	1.615	1.621	+	-
8	1bbhA	131	2ccyA	127	**108**	1.466	1.450	1.413	+	+
9	1bbt1	186	2plv1	288	**122**	1.415	C.A.F.	1.455	-	N.A.
10	1bgeB	159	1gmfA	119	**70**	1.865	P.F.	1.885	-	N.A.
11	1c2rA	116	1ycc_	108	**86**	1.124	1.113	1.120	+	-
12	1cauB	184	1cauA	181	**150**	1.665	1.680	1.667	-	+
13	1cewI	108	1molA	94	**72**	1.641	1.756	1.661	-	+
14	1chrA	370	2mnr_	357	**317**	1.480	1.476	1.474	+	+
15	1cid_	177	2rhe_	114	**74**	1.630	1.641	1.535	+	+
16	1cpcL	172	1colA	197	**66**	2.389	1.709	3.594	-	-
17	1crl_	534	1ede_	310	**143**	1.976	1.998	2.375	-	-
18	1dsbA	188	2trxA	108	**42**	2.400	2.017	1.804	+	+
19	1dxtB	147	1hbg_	147	**124**	1.497	1.470	1.411	+	+
20	1eaf_	243	4cla_	213	**136**	1.703	1.724	1.609	+	+
21	1fc1A	206	2fb4H	229	**79**	2.819	1.384	0.931	+	+
22	1fxiA	96	1ubq_	76	**50**	1.972	1.930	1.925	+	+
23	1gal_	581	3cox_	500	**268**	1.444	P.F.	1.435	+	N.A.
24	1gky_	186	3adk_	194	**113**	1.831	P.F.	1.915	-	N.A.
25	1gp1A	183	2trxA	108	**78**	2.319	P.F.	1.796	+	N.A.
26	1hip_	85	2hipA	71	**51**	0.691	0.682	0.682	+	-
27	1hom_	68	1lfb_	77	**51**	1.251	1.212	1.135	+	+
28	1hrhA	125	1rnh_	148	**96**	1.564	P.F.	1.093	+	N.A.
29	1isuA	62	2hipA	71	**45**	0.892	P.F.	0.828	+	N.A.
30	1lgaA	343	2cyp_	293	**228**	1.683	1.678	1.660	+	+
31	1ltsD	103	1bovA	69	**61**	1.448	1.504	1.399	+	+
32	1mdc_	131	1ifc_	131	**110**	D.A.F	1.409	1.367	N.A.	+
33	1mioC	525	1minB	522	**360**	2.554	2.641	2.714	-	-
34	1mup_	157	1rbp_	174	**121**	1.952	2.049	1.928	+	+
35	1npx_	447	3grs_	461	**339**	2.275	2.111	2.314	-	-
36	1omf_	340	2por_	301	**208**	1.655	1.928	1.707	-	+
37	1onc_	104	7rsa_	124	**86**	1.110	1.102	1.089	+	+
38	1osa_	148	4cpv_	108	**58**	0.860	P.F.	0.849	+	N.A.
39	1pfc_	111	3hlaB	99	**68**	1.723	P.F.	1.762	-	N.A.
40	1rcb_	129	1gmfA	119	**47**	1.308	P.F.	1.276	+	+
41	1sacA	204	1ayh_	214	**118**	2.578	2.749	2.896	-	-
42	1sim_	381	1nsbA	390	**244**	2.393	2.450	2.808	-	-
43	1stfI	98	1molA	94	**70**	1.734	1.429	1.276	+	+
44	1tahA	318	1tca_	317	**156**	1.791	1.711	2.035	-	-
45	1ten_	89	3hhrB	195	**79**	1.398	P.F.	1.241	+	N.A.
46	1tie_	166	4fgf_	124	**84**	1.468	P.F.	1.434	+	N.A.
47	1tlk_	103	2rhe_	114	**75**	1.018	1.064	1.034	-	+
48	2azaA	129	1paz_	120	**68**	1.818	2.012	1.817	+	+
49	2cmd_	312	6ldh_	329	**263**	1.922	1.923	1.913	+	+
50	2fbjL	213	8fabB	214	**169**	1.518	P.F.	1.497	+	N.A.
51	2gbp_	309	2liv_	344	**123**	3.830	2.765	2.211	+	+
52	2hhmA	272	1fbpA	316	**189**	1.895	P.F.	1.939	-	N.A.
53	2hpdA	457	2cpp_	405	**331**	2.773	2.822	2.854	-	-
54	2mnr_	357	4enl_	436	**240**	2.642	2.575	2.828	-	-
55	2mtaC	147	1ycc_	108	**57**	1.120	1.136	1.109	+	+
56	2pia_	321	1fnr_	296	**172**	1.572	1.534	1.598	-	-
57	2pna_	104	1shaA	103	**80**	1.933	1.914	1.993	-	-
58	2sarA	96	9rnt_	104	**66**	2.691	3.095	3.036	-	+
59	2sas_	185	2scpA	174	**134**	2.430	2.458	2.453	-	+
60	2sga_	181	4ptp_	223	**101**	1.167	1.241	1.167	+	+
61	2snv_	151	4ptp_	223	**107**	2.125	2.219	2.207	-	+
62	3cd4_	178	2rhe_	114	**82**	1.092	1.173	1.013	+	+
63	3chy_	128	4fxn_	138	**104**	3.100	3.445	3.735	-	-
64	3hlaB	99	2rhe_	114	**74**	2.918	2.911	3.715	-	-
65	3rubL	441	6xia_	387	**172**	3.455	4.000	4.142	-	-
66	4sbvA	199	2tbvA	285	**144**	1.281	1.281	1.301	-	-
67	5fd1_	106	2fxb_	81	**44**	1.364	1.625	1.291	+	+
68	8i1b_	146	4fgf_	124	**90**	1.206	1.259	1.185	+	+
			Total no. of valid comparisons						67	55
			+/- Difference						5	15
			No. of cases in which MatAlign is better						36	35
			% of cases in which MatAlign is better						53.73%	63.64%

Legends

D.A.F. = DALI alignment failure (No DALI alignment result available.)
C.A.F. = CE alignment failure (No CE alignment result available.)
P.F. = Parsing failure (We cannot successfully parse the CE alignment result.)
N.A. = Comparison not applicable.
\+ = MatAlign's RMSD is smaller (better) than that of DALI/CE.
\- = MatAlign's RMSD is larger (worse) than that of DALI/CE.

4.5 Discussions

4.5.1 Accuracy Advantage of MatAlign

The accuracy advantage of MatAlign over DALI and CE may be because of MatAlign uses all individual residues as the basic elements to be matched. On contrary, both DALI and CE use residue "fragments" as the basic elements for matching. DALI matches a 6×6 submatrix (encoding the relationship between two 6-residue fragments) from one protein against a 6×6 submatrix from another protein. CE tries to find the aligned fragment pairs (AFPs) of two matching 8-residue fragments. Thus, both of these methods may miss the good seed alignments that are shorter than their minimum fragment lengths of 6 and 8 respectively. MatAlign's alignment is more fine-grained, and it cannot miss out these good but short alignments.

4.5.2 MatAlign vs DALI and SSAP

MatAlign can be considered similar to DALI [HS93], and SSAP [TO89] in some aspects. But, in fact, it is significantly different from both of them in overall.

MatAlign vs DALI

MatAlign uses 2D distance matrix representation of 3D protein structures as in DALI. But their algorithmic approaches are diverse in that:

1. DALI sub-divides a distance matrix into 6×6 overlapping submatrices, finds the matching submatrix pairs from two proteins, and assemble these matching pairs into the final alignment by means of Monte Carlo optimization. On the other hand, MatAlign uses dynamic programming at two levels: first for row–row alignment and second for consolidating row–row scores into the initial alignment; and the iteratively refining the initial alignment into the final one based on the objective alignment scoring function.

2. Unlike DALI (and many other methods such as VAST [GMB96] and LOCK [SB97]),

MatAlign method does not use any secondary structure information at all. Thus, the alignment results produced by MatAlign will not be affected by the choice of the secondary structure annotation method.

MatAlign vs SSAP

MatAlign uses double dynamic programming as in SSAP. But, their data representation and detailed procedures are quite different in that:

1. SSAP uses a complex representation called the "view" (encoding direction, orientation, sequence distance, and spatial distance components) and the local reference frames for each residue. On the other hand, MatAlign uses a simple representation of the distance profile (a row in distance matrix) for each residue.

2. SSAP requires a relatively expensive superimposition of two residues' reference frames for each of the exhaustive pairs of residues. It means that $|A|\times|B|$ superimpositions (where $|A|$ and $|B|$ are the lengths of two proteins respectively) are required. MatAlign only has to perform at most $\min(|A|, |B|)$ superimpositions in its iterative refinement procedure.

3. In calculating the entries of the overall scoring matrix $\mathcal{SM}$, SSAP accumulates (adds up) the relevant intermediate scores from the individual residue pair's dynamic programming matrices, whereas MatAlign only uses the final score of the individual alignments. Because of this feature, together with the first feature, MatAlign is able to use the reduced distance profiles (rows) which leads to a great speed improvement. Such a condensed representation cannot be achieved in SSAP.

According to [KKL05], SSAP is about twice slower than DALI. From our experiments, DALI is found to be about 3 times slower than MatAlign. So, it can be expected that SSAP will be about 6 times slower than MatAlign. We are not able to directly compare the relative performances of MatAlign and SSAP, because we cannot successfully port the latter to our computing platform.

4.6 Conclusion

In this chapter, we have presented a new scheme for comparing 3D protein structures based on the alignment of distance matrices. MatAlign produces the alignment results that are alternative to those of the established DALI and CE methods. According to four different quality criteria, MatAlign's alignment results are better (more accurate) than those of DALI and CE in a majority of cases. In particular, MatAlign's alignment is tighter (smaller in RMSD) albeit a little shorter than the alignments of DALI and CE. Thus, MatAlign can be useful in detecting the highly conserved structural cores of the related proteins. It can also be used in combination with DALI, CE, or other existing alignment methods in order to achieve a more comprehensive result for a given task of detailed structural alignment. For example, a user can study the different candidate alignments for a particular pair of proteins using both DALI and MatAlign, and choose the better alignment according to his/her own criteria. The running time for MatAlign is reasonable fast with an average of 24.8 sec per alignment.

CHAPTER 5

Rapid Protein Structure Database Retrieval

Summary

As the sizes of 3D protein structure databases are growing rapidly nowadays, exhaustive database searching, in which a query protein structure is compared or aligned to each and every structure in the database, becomes inefficient. We propose a rapid protein structure database retrieval system named "ProtDex2", in which we adopt the techniques used in information retrieval (IR) systems in order to perform rapid database searching without having to access every structure in the database. The retrieval process is based on the inverted index constructed on the feature vectors of the relationships between the secondary structure elements (SSEs) of all the protein structures in the database. The experimental results show that ProtDex2 is very much faster than two commonly used detailed structural comparison methods, DALI and CE, yet not much sacrificing on the accuracy of the comparison. When comparing with a fast database scan method, Topscan, ProtDex2 is much faster and still slightly more accurate.

5.1 Introduction

Similarity searching in protein structure databases is a natural extension of pairwise structural comparison. Usually, a protein structure is required to be compared against a database of other protein structures to find and retrieve the structures that are similar to it. Structural database searching/retrieval is useful for a variety of purposes such as protein function inference, motif discovery, drug target selection, structural classification, etc. [Bre01, GFH03, HS94c].

Because of the advancements in the laboratory methods to determine the 3D structures of proteins, the sizes of the protein structure databases such as PDB [BWF+00] are growing at a very rapid rate. When the databases were of small size, in order to search a protein structure against a database, we could comfortably use exhaustive searching. That is, we had to compare the query structure against each and every structure in the database using any detailed or coarse structural comparison method. But, when the database sizes grow to the order of ten's of thousands, such an exhaustive searching approach cannot provide a satisfactory response time — even with a very fast coarse comparison (database scan) method [CKS04, CHTY05]. This is because the response time grows "linearly" with the number of proteins in the database. Therefore, researchers have been starting to look at the *indexing* approach to cope with this database searching problem.

In this chapter, we propose a protein structure database searching and retrieval scheme named **ProtDex2** (**Prot**ein In**dex**ing version **2**). Our design objective is to develop an index-based search method using on an abstract representation scheme and the *information retrieval* (IR) methodologies in order to speed up the process of database searching. We first build an inverted index based on the feature vectors of the relationships among the SSEs from all the protein structures in the database. When evaluating a query, we use this index to collectively determine the overall similarities (ranks) of all the proteins in the database with respect to the query, and then retrieves and reports those that are most similar. If required, we can optionally perform detailed pairwise comparisons of the query to some selected

candidates using any of the existing structural alignment methods.

5.2 Index-based Structural Database Searching

Due to the inscalability of exhaustive searching, researchers have started to look at more economical strategies, typically based on indexing. Use of indexes effectively reduces the search space when evaluating a query. Indexing has been widely used in the areas of document, image, spatial and multi-dimensional database searchings and retrievals [BOSD+97]. It has started to emerge in the area of 3D protein structure database searching recently [AKKS99, CHTY05, CKS04, GZ05, HZS05, WKHK04].

In our work, we employ an indexing system based on the IR approach. In this approach, the objects in a database are represented in their abstract formats, and an index (typically an inverted index or a signature file) is constructed from them. When evaluating a query, the overall similarity measures of the objects in the database to the query object are computed by using this pre-constructed index. The original objects in the database are not needed to be processed in query evaluation at all. Thus, the speed of searching is generally very fast. However, using this approach, we may need to sacrifice accuracy to some acceptable extent. We have to allow some amounts of both false positives and false negatives during the index searching process.

Here, we adopt a particular IR technique called "inverted indexing" and its related similarity ranking mechanism, which have been successfully used in the area of document/text retrieval for a long time. Our work is inspired by the methods such as CAFE [WZ02] that uses the IR techniques to index and retrieve genome sequences, and VIPER [MSMP99] that uses the IR techniques for content-based image retrieval.

5.3 Index Construction

The inverted index of ProtDex2 is based on SSEs. As discussed in Section 2.2.1, SSEs are the well-defined sub-structures within the protein structures. Two common types of SSEs are helix (H) and sheet (E). In our approach, we treat SSEs as the "basic elements", as we can roughly, though not precisely, determine the overall shape of a protein structure through the forms and the arrangement (topology) of its SSEs. The number of SSEs in a protein is only an order of tens, while the number of AA residues is an order of hundreds. Thus, storing and handling SSEs as the basic structural elements is much more cost effective than handling the individual AA residues as the basic elements.

We perform global similarity searching of a given query protein against the proteins in the database based on the feature vectors of the inter-SSE relationships (called the contact patterns) that are indexed.

The steps involved in constructing the index are described below.

5.3.1 Contact Pattern (CP) Representation

We represent a 3D protein structure as a 2D distance matrix (see Section 2.4 for the definition). In a distance matrix, the forms and arrangement of the SSEs are captured in submatrices called the *inter-SSE contact patterns* or simply the *contact patterns* (CPs). A CP is formed by the interaction of two SSEs. A CP formed by the SSEs of lengths m and n respectively is a submatirx of size $m \times n$. If we have $|S|$ SSEs in a protein, there will be $|S|^2$ CPs.

Suppose we have a sample imaginary protein with 10 residues, where residues 2–3 form a sheet, 5–6 a helix, and 8–10 another sheet. (This is for demonstration purpose only. In reality, an SSE normally contains at least four residues.)

Let $S = S_1 S_2 S_3 \ldots S_{|S|}$ be the SSE sequence of a protein where $|S|$ is the number of SSEs in that protein. Then, the SSE sequence S of our sample protein will be: **E H E**.

There will be 9 CPs in the distance matrix for the our protein. These are shown

as the light and dark gray blocks in Figure 5.1.

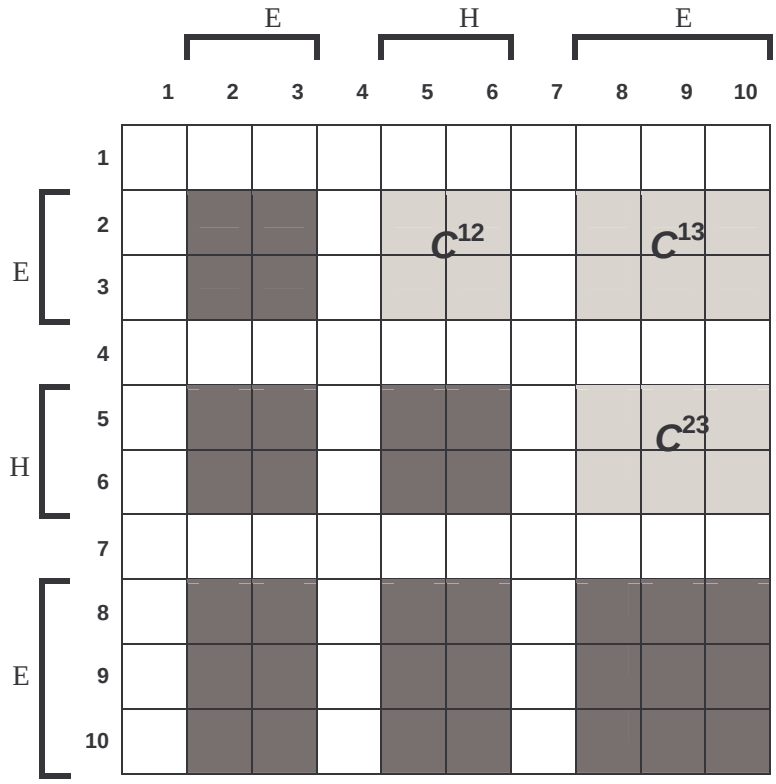

Figure 5.1: Contact patterns (CPs) in a distance matrix.

Among the CPs in a distance matrix, only those above the main diagonal are sufficient to capture the forms and arrangement information of the SSEs. This is because the CPs below the main diagonal are just the mirror images of those above the main diagonal, and those on the main diagonal are merely the self-interactions of the single SSEs. In our example, only the CPs C^{12}, C^{13}, and C^{23} (shown as the light gray blocks in Figure 5.1) are needed to be taken into account. The number of such CPs is $|S|(|S|-1)/2$.

5.3.2 Extracting CP Feature Vectors

Now, we extract the important properties from a CP and represent them as a *feature vector*. There are 8 attributes (properties) in the feature vector we use to represent a CP. These feature vector attributes are designed to effectively determine

the similarity or dissimilarity of the CPs they represent. For example, the two CPs with very different mean C_α–C_α distance values cannot be similar in anyway. CP feature vector representation is rotation and translation invariant, as it is based on distance matrix.

The feature vector of a CP C^{ab}, which is formed by the interaction of s_a (first SSE) and s_b (second SSE), where $b > a$, consists of 8 attributes as shown in Table 5.1. It is observed that all these 8 attributes are more or less important on their own, because dropping any of them more or less degrades the accuracy of the system as shown in Section 5.6.3.

Table 5.1: Attributes of CP feature vector.

Sr.	Attribute	Sym-bol	Equa-tion	Upper Bound (c_r)	#Girds in Hash Table (m_r)
1	Type of C^{ab}	CT	(5.1)	3	4
2	Position of s_a in SSE sequence S	SS	(5.2)	48	12
3	Position difference of s_a and s_b in SSE sequence S	SD	(5.3)	48	20
4	Torsion angle between $\mathbf{V}_a$ and $\mathbf{V}_b$ (-180.0 to $+180.0$)	Ω	[Sfy04]	360.0	16
5	Closest segment–segment distance of $\mathbf{V}_a$ and $\mathbf{V}_b$	ND	[Sun04]	64.0	16
6	Nearest vertex pair distance of $\mathbf{V}_a$ and $\mathbf{V}_b$	VD	(5.6)	64.0	4
7	Mean of C_α–C_α distances in C^{ab}	MD	(5.7)	64.0	4
8	Contact density of C^{ab}	CD	(5.8)	1.0	4

Attribute no. 1–3 simply correspond to the types and the positions of the SSEs that make up the CP. The attributes CT (CP type); SS (SSE sequence position of the first SSE); and SD (SSE sequence position difference of two SSEs) can be

simply calculated/extracted respectively as follows.

$$CT(s_a, s_b) = \begin{cases} 0 & \text{if } (s_a \text{ is H}) \wedge (s_b \text{ is H}) \\ 1 & \text{if } (s_a \text{ is H}) \wedge (s_b \text{ is E}) \\ 2 & \text{if } (s_a \text{ is E}) \wedge (s_b \text{ is H}) \\ 3 & \text{if } (s_a \text{ is E}) \wedge (s_b \text{ is E}) \end{cases} \tag{5.1}$$

$$SS(a) \; = \; a \tag{5.2}$$

$$SD(s_a, s_b) \; = \; b - a \tag{5.3}$$

where a and b are the positions of s_a and s_b respectively in SSE sequence S.

Attribute no. 4–6 correspond to the *3D vector representation* of the SSEs. An SSE can be roughly approximated by its representative vector or line segment in 3D space. Since a CP represents the interaction between the two SSEs, we can logically associate it with the spatial relationship (torsion angle and two types of distances) between the two SSE vectors.

Let $\mathbf{V}_a$ denote the 3D vector of s_a, and $\mathbf{V}_b$ that of s_b. We can calculate the vertex points $(\mathbf{V}_a^{start}, \mathbf{V}_a^{end})$ and $(\mathbf{V}_b^{start}, \mathbf{V}_b^{end})$ of the vectors using the equations proposed by Singh and Brutlag [SB97]. For vector $\mathbf{V}$ representing a "helix" beginning at AA residue i and ending at residue j, its start and end points are calculated as:

$$\begin{aligned} \mathbf{V}^{start} &= (0.74 \times \mathbf{V}_i + \mathbf{V}_{i+1} + \mathbf{V}_{i+2} + 0.74 \times \mathbf{V}_{i+3}) \,/\, 3.48 \\ \mathbf{V}^{end} &= (0.74 \times \mathbf{V}_j + \mathbf{V}_{j-1} + \mathbf{V}_{j-2} + 0.74 \times \mathbf{V}_{j-3}) \,/\, 3.48 \end{aligned} \tag{5.4}$$

The start and end points for vector $\mathbf{V}$ for a "sheet", beginning at residue i and ending at residue j, are calculated as:

$$\begin{aligned} \mathbf{V}^{start} &= (\mathbf{X}_i + \mathbf{V}_{i+1}) \,/\, 2 \\ \mathbf{V}^{end} &= (\mathbf{X}_j + \mathbf{V}_{j+1}) \,/\, 2 \end{aligned} \tag{5.5}$$

In our implementation, we use the STRIDE algorithm [FA95] to identify the SSEs. For both helix and sheet, we assume the minimum length (number of AA residues) of an SSE to be 4. Any SSE with length shorter than 4, as annotated by STRIDE,

is not regarded as an SSE. In the case of helices, if the length of a helix is exactly 4, it is extended by a single residue on either end in order to avoid a zero vector.

Now, using the SSE vectors, we can calculate the torsion angle attribute (Ω) using the formula given in [Sfy04], and the closest segment-to-segment distance attribute (ND) using the algorithm described in [Sun04]. The nearest vertex pair distance (VD) can be calculated as follows.

$$VD(\mathbf{V}_a, \mathbf{V}_b) = \min \begin{cases} Dist(\mathbf{V}_a^{end}, \mathbf{V}_b^{start}) \\ Dist(\mathbf{V}_a^{start}, \mathbf{V}_b^{end}) \\ Dist(\mathbf{V}_a^{end}, \mathbf{V}_b^{end}) \\ Dist(\mathbf{V}_a^{start}, \mathbf{V}_b^{start}) \end{cases} \tag{5.6}$$

where $Dist$ is the Euclidean distance between two points in space.

Figure 5.2 shows Vector representation of SSEs and the attributes Ω, ND and VD between two vectors. Various angle and distance attributes are the natural and most commonly used properties for the relationship between two SSE vectors, and are also used in many structural comparison methods such as VAST [GMB96] and LOCK [SB97].

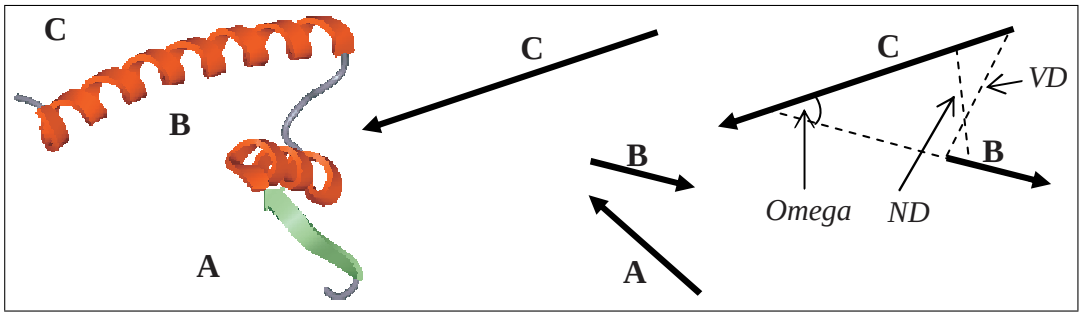

Figure 5.2: Vector representation of SSEs and relationships between two vectors.

The remaining two attributes for a CP are derived directly from the distance matrix $\mathcal{DM}$. They are related to the C_α–C_α interaction patterns within a CP. The functions to calculate these attribute values, MD (mean of C_α–C_α distances) and CD (contact density), are defined as follows.

$$MD(s_a, s_b) = \frac{\sum_{i=0}^{|s_a|-1} \sum_{j=0}^{|s_b|-1} \mathcal{DM}[s_a^{start} + i, s_b^{start} + j]}{|s_a|\,|s_b|} \tag{5.7}$$

$$CD(s_a, s_b) = \frac{\sum_{i=0}^{|s_a|-1} \sum_{j=0}^{|s_b|-1} (t_{ij})}{|s_a|\,|s_b|} \qquad \text{where}$$
$$t_{ij} = \begin{cases} 1 & \text{if} \quad \mathcal{DM}[s_a^{start} + i, s_b^{start} + j] \leq 5.0\text{Å} \\ 0 & \text{otherwise} \end{cases} \tag{5.8}$$

where 5.0Å is the threshold distance to define whether two C_α atoms are in contact (i.e. close enough to each other) or not.

Now, let

$$\mathbf{K} = (\, k_{CT},\, k_{SS},\, k_{SD},\, k_{\Omega},\, k_{ND},\, k_{VD},\, k_{MD},\, k_{CD}\,)$$

be a feature vector. We can generate feature vector $\mathbf{K}^{ab}$ for CP C^{ab} as follows.

$$\begin{aligned} \mathbf{K}^{ab} = (\quad & CT(s_a, s_b),\, SS(s_a),\, SD(s_a, s_b),\, \Omega(\mathbf{V}_a, \mathbf{V}_b), \\ & ND(\mathbf{V}_a, \mathbf{V}_b),\, VD(\mathbf{V}_a, \mathbf{V}_b),\, MD(s_a, s_b),\, CD(s_a, s_b) \quad) \end{aligned} \tag{5.9}$$

In generating CP feature vectors, when a feature vector has one or more attribute values which are greater than their respective predefined upper bounds (as given in Table 5.1), it is regarded as an outlier and discarded. These upper bound values are determined empirically. It is observed in our experiments that only about 1% of the CP feature vectors are dropped because they are outliers.

The CP feature vector we use is sequence-order dependent (referring to attribute no. 1–4). Since the cases of re-arrangement of SSEs are rarer than those of insertion and deletion throughout evolution [Kar03], it will be better to take the sequence order information into account in our nearest neighbor search. This prevents false matchings of CPs which have very different relative sequence orders of their constituent SSEs. For example, if we have two proteins each having 9 SSEs, we will not allow C^{12} from one protein and C^{19} from the other to be matched, because there is only a little chance that SSE #2 from the first protein is re-arranged as SSE #9 in the second protein during evolution. Also, it is not much possible that all the 7 SSEs between SSE #1 and #9 are deleted in the second protein. It is observed that restricting the sequence order of the SSEs (rather than allowing to float freely in any order) helps improve the accuracy of the scheme.

It should be noted that the feature vector we use is only a good approximation of the original CP in an abstract form. There may be some cases in which the two

feature vectors are similar even though their original CPs are not similar.

5.3.3 Building Inverted Index

For every protein structure in the database, we generate the 8-dimensional feature vectors as described above. After that, we hash these feature vectors into a hash table of 8 dimensions, together with their Protein IDs. We finally build an inverted index based on the hash table.

Feature Vector Hashing

An n-dimensional hash table $\mathcal{H}$ is an n-dimensional array of size $m_1 \times m_2 \times \ldots \times m_n$ where m_i $(1 \leq i \leq n)$ is the length of each dimension. Each cell $\mathcal{H}[d_1, d_2, \ldots, d_n]$ $(1 \leq d_i \leq m_i, 1 \leq i \leq n)$ in the array corresponds to a feature vector having exactly the "discrete" attribute values of $(d_1, d_2, \ldots, d_n)$.

We have to hash the original 8-dimensional CP feature vector $\mathbf{K}$ with continuous attribute values into a 8-dimensional hash table with the hash function $Hash$. The idea is similar to that of hashing points into 3D grid cells in geometric hashing [NW91].

Let us define a *discretized feature vector* $\mathbf{T}$.

$$\mathbf{T} = (\, t_{CT},\, t_{SS},\, t_{SD},\, t_{\Omega},\, t_{ND},\, t_{VD},\, t_{MD},\, t_{CD}\,)$$

$\mathbf{T}$ can be calculated from $\mathbf{K}$ by the function $Hash$.

$$\mathbf{T} = Hash(\mathbf{K}) \tag{5.10}$$

where $Hash$ is a collection of partial *discretization* functions $Hash_r$ on each continuous attribute value k_r (where $r \in \{CT, SS, SD, \Omega, ND, VD, MD, CD\}$).

$$t_r = Hash_r(k_r) = \begin{cases} floor(k_r \times m_r / c_r) & \text{if } k_r = c_r \\ floor(k_r \times m_r / c_r) + 1 & \text{otherwise} \end{cases} \tag{5.11}$$

where c_r and m_r are the maximum possible values of attribute r in the original continuous space and the new discretized space respectively. In fact, the discretization

function $Hash_r$ performs a *space-based* or equal-size partitioning of the continuous data space of the attribute r.

The parameter values for c_r and m_r for each attribute r are given in Table 5.1. As a result, we have a hash table of size $(4 \times 12 \times 20 \times 16 \times 16 \times 4 \times 4 \times 4)$.

Inverted Index

The idea of inverted indexing is borrowed from the area of text and document retrieval. An inverted index is basically a list of "words", each pointing to a *posting list* of "documents" in which it occurs. In our case, we can treat the discretized feature vectors as our words, and the proteins in which they occur as our documents.

In our implementation, each cell in the hash table $\mathcal{H}$ stores a pointer to a posting list consisting of Protein IDs together with their occurrence counts. After we have hashed an original feature vector $\mathbf{K}$ into a discretized feature vector $\mathbf{T} = Hash(\mathbf{K})$, we update the posting list pointed by the cell $\mathcal{H}[\mathbf{T}]$. We insert the Protein ID, in which $\mathbf{K}$ occurs, into the posting list if it does not exist in the list yet. Otherwise, its occurrence count is increased.

After processing all the CP feature vectors from all the proteins in the database in this way, we finally come up with our inverted index, in which each cell in the hash table points to the posting list of Protein IDs and their number of occurrences. Obviously, some of the cells in the hash table may have empty pointers. Figure 5.3.3 illustrates an excerpt from a sample inverted index.

5.4 Query Evaluation and Database Retrieval

In order to evaluate the *similarity score* between a query protein structure a protein structure in the database, we adopt and modify the well-known $\Sigma(tf \times idf)$ scoring scheme commonly used in document retrieval systems. Given a query protein structure Q and a protein structure P in the database, their overall similarity

Hash Table Cell	Posting List (Protein ID, #Occurrence)
...	...
$\mathcal{H}[1,1,5,10,3,3,1,1]$	(`d1eu3a1`, 3), (`d1f86a_`, 1)
$\mathcal{H}[3,4,9,10,5,4,4,1]$	(`d1tph1_`, 2), (`d1dzka_`, 1)
$\mathcal{H}[3,5,5,14,5,3,2,3]$	(`d1eal__`, 1), (`d1ej8a_`, 3), (`d1ep3b1`, 2)
...	...

Figure 5.3: An excerpt from a sample inverted index.

score ψ can be calculated as:

$$\psi(Q,P) = \frac{\sum_{\phi(\mathbf{T}\in Q,\mathbf{T}'\in P)\neq 0}(\, w(Q,\mathbf{T}) \cdot w(P,\mathbf{T}') \cdot \phi(\mathbf{T},\mathbf{T}')\,)}{W_Q \cdot W_P} \tag{5.12}$$

Given two discretized feature vectors $\mathbf{T}$ and $\mathbf{T}'$, we can determine their *matching or compatibility score* ϕ as:

$$\phi(\mathbf{T},\mathbf{T}') = \prod_{r\in\{CT,SS,SD,\Omega,ND,VD,MD,CD\}} \phi_r(t_r,t'_r) \tag{5.13}$$

where ϕ_r is the partial matching score for attribute r (where $r \in \{CT, SS, SD, \Omega, ND, VD, MD, CD\}$), which is in turn defined as:

$$\phi_r(t_r,t'_r) = \begin{cases} \sigma_r \cdot e^{-\frac{|t_r - t'_r|}{\xi_r}} & \text{if } |t_r - t'_r| \leq \xi_r \\ 0 & \text{otherwise} \end{cases} \tag{5.14}$$

where ξ_r is the threshold value for the allowable difference between two attribute values t_r and t'_r, and σ_r is the relative weight of attribute r. In our current implementation, we set $\xi_r = 2$ for $r \in \{SS, SD, \Omega, ND\}$, set $\xi_r = 1$ for $r \in \{VD, MD, CD\}$, and $\xi_r = 0$ for $r \in \{CT\}$, and $\sigma_r = 1$ for all $r \in \{CT, SS, SD, \Omega, ND, VD, MD, CD\}$.

$w(Q,\mathbf{T})$ is the weight of discretized feature vector $\mathbf{T}$ from query Q, which is calculated as:

$$w(Q,\mathbf{T}) = (\lg f_{Q,\mathbf{T}} + 1) \cdot (\lg \frac{N}{f_{\mathbf{T}}} + 1) \tag{5.15}$$

and $w(P, \mathbf{T}')$ is the weight of discretized feature vector $\mathbf{T}'$ from database protein P, which is calculated as:

$$w(P, \mathbf{T}') = (\lg f_{P,\mathbf{T}'} + 1) \tag{5.16}$$

where N is the total number of protein structures in the database, $f_{\mathbf{T}}$ is the number of proteins in which $\mathbf{T}$ occurs, $f_{Q,\mathbf{T}}$ is the number of occurrences of $\mathbf{T}$ in Q, and $f_{P,\mathbf{T}'}$ is the number of occurrences of $\mathbf{T}'$ in P.

W_x is the size of protein $x \in \{Q, P\}$ in terms of the number of discretized feature vectors it contains.

$$W_x = \sqrt{\sum_{\mathbf{T} \in x} (w(x, \mathbf{T}))^2} \tag{5.17}$$

All the information required to calculate similarity score ψ can be easily extracted from the inverted index. We use a modified version of a textbook algorithm [BOSD+97, p. 171] to calculate the similarity scores of all the proteins in the database, with respect to a query, by using the inverted index. The scores are then normalized into the range of 0 to 100. After that, all the database proteins are ranked according to their similarity scores, and are reported to the user. (ProtDex2 does not provide the actual alignment and RMSD for each database protein, but rather its "relative rank" among the other database proteins with respect to the query. If required, we can carry out the actual alignment of the query and the top-ranking database proteins using any detailed structural alignment method such as DALI, CE or MatAlign.)

Calculations of the similarity scores for all the potentially matching proteins (those which have matching CPs with the query's) are done "simultaneously" and "incrementally" during the process of searching through the index. The scheme is scalable, because the index structure we need to search through is only a fixed-size hash table which will not grow with the growth of the database itself. However, the lengths of the posting lists will apparently increase in sizes with the growth of the database. There will still be some sub-linear increases in cost for handling them when the database grows.

5.5 Experimental Results

In order to assess the relative performance of ProtDex2, we compare it against the two widely used detailed structural alignment schemes DALI [HS93] (DaliLite implementation [HP00]) and CE [SB98] — which are also used in performance studies of the previous chapter. In addition, we include a fast database scan method named Topscan [Mar00] as well as an index-based database search method named ProtDex [AFT03], which is ProtDex2's predecessor, in our performance studies.

All the experiments are conducted on Sun Ultra Sparc II with two 480 MHz CPUs and 4 GB main memory, running Sun OS 5.7. The databases we use in our experiments are the subsets of ASTRAL v1.59 [BKL00]. (The 3D structures stored in ASTRAL are not the whole proteins, but the SCOP domains. However, we will hereafter refer to them as proteins for simplicity.)

We conducted two experiments: one involving a small database and a limited number of queries, and the other involving a large database and a greater number of queries.

5.5.1 Experiment on Small Database

We randomly select 10 proteins from *Globins* Family (`a.1.1.2` in SCOP) and 10 proteins from *Serine/Threonin Kinases* Family (`d.144.1.1` in SCOP) from the representative ASTRAL data set with less than 40% sequence homology. These 20 proteins are designated as the query proteins.

We again randomly select 180 proteins, other than Globins and Serine/Threonin Kinases, from four major classes (All-α, All-β, α/β and $\alpha + \beta$) of the same representative data set. We combine these 180 proteins with the aforementioned 20 query proteins to form the target database of 200 proteins.

We run 20 queries – taken from the Globins and Serine/Threonin Kinases Families – against the target database. For DALI (DaliLite) and CE, the similarity scores of each query protein to all the database proteins are calculated using pair-

wise comparisons. (Although DaliLite has a specialized database searching facility, it is not flexible enough to be used in our experiment.) For Topscan, the symbolic topology strings for the database proteins are preconstructed. For each query, the similarity scores are calculated by comparing the query's topology strings to all of the database's topology strings. A comprehensive comparison mode is used taking into account the information on neighbors, accessibility, element length and loop length. For both ProtDex and ProtDex2, the indexes are preconstructed from the database. The similarity scores of each query protein to the database proteins are calculated with the help of the index.

In all methods, for each query, all the proteins in the database are ranked according to their similarity scores with respect to the query, and are retrieved in this ranking order. If a retrieved protein and the query protein belong to the same "Family", which is the most detailed level in SCOP classification, it is regarded as a "relevant" retrieval. For example, for a Globins Family query protein, if a retrieved protein also belongs to Globins Family, it is regarded as a relevant retrieval. For each query, there are 10 relevant proteins in the database of 200 proteins. If retrieved randomly, the probability of selecting a relevant protein is only 0.05.

The speed comparison of the selected methods for this experiment is shown in Table 5.2. The accuracy comparison is shown in Table 5.3, where row i represents the ranking under the various methods to retrieve i relevant answers. For example, row 2 says that when 2 answers are required, the top 2 ranked answers from DALI, CE, Topscan and ProtDex2 are relevant retrievals from the same Family as the query; while ProtDex ranks the 2 relevant answers among the top 3 retrievals.

5.5.2 Experiment on Large Database

We conduct another experiment using a large database containing $34,055$ proteins which cover about 90% of the entire ASTRAL database. From them, we select 108 query proteins which belongs to 108 medium-size Families (with ≥ 40 members and ≤ 180 members) from four major classes, and which have less than 40% sequence

Table 5.2: Running times for 20 queries on the database of 200 proteins.

Method	Total Time (hh:mm:ss)	Average Time per Query (hh:mm:ss.mm)	Average Time per Comparison (hh:mm:ss.mmmm)
DALI	52:36:08	02:37:48.40	00:00:47.3420
CE	10:23:03	00:31:09.15	00:00:09.3458
Topscan	00:00:59	00:00:02.95	00:00:00.0148
ProtDex	00:00:43	00:00:02.15	00:00:00.0108
ProtDex2	00:00:15	00:00:00.75	00:00:00.0038

Table 5.3: Accuracy comparison for 20 queries (10 from Globins Family and 10 from Serine/Threonin Kinases Family) on the database of 200 proteins.

No. of Relevant Retrievals	Average No. of Retrievals Required			
	DALI/CE	Topscan	ProtDex	ProtDex2
1	1	1	1	1
2	2	2	3	2
3	3	3	5	3
4	4	5	7	4
5	5	6	10	5
6	6	8	12	6
7	7	10	15	7
8	8	14	21	9
9	9	20	37	10
10	10	29	79	15

homology to each other.

DALI and CE are excluded from this experiment because it is impractical to run them given their very high computational costs. It can be estimated that

DALI will take over 5 years, and CE will take over 1 year respectively to run this experiment on the given machine. Only Topscan, ProtDex and ProtDex2 are included in this experiment.

It should be noted that the sizes of the Families (40 to 180) are quite small with respect to the size of the entire database (34, 055) and the probability of selecting a relevant protein by chance is quite low (0.0012 to 0.0053).

The speed comparison of the selected methods for this database searching task is shown in Table 5.4.

Table 5.4: Running times for 108 queries on the database of 34, 055 proteins.

Method	Total Time (hh:mm:ss)	Average Time per Query (hh:mm:ss.mm)	Average Time per Comparison (hh:mm:ss.mmmm)
Topscan	26:15:51	00:14:35.47	00:00:00.0257
ProtDex	05:44:35	00:03:11.46	00:00:00.0056
ProtDex2	00:13:54	00:00:07.72	00:00:00.0002

The accuracy comparison is shown in Figure 5.4. Again, a "relevant" retrieval is defined as an event of retrieving a protein from the database that belongs to the same "Family" as the query. The results are shown as average *precision-recall curves*, which are commonly used in the IR experiments. *Precision* and *recall* can be defined as:

$$\text{Precision} = \frac{\text{Number of relevant retrievals}}{\text{Total number of proteins retrieved}} \tag{5.18}$$

$$\text{Recall} = \frac{\text{Number of relevant retrievals}}{\text{Total number of proteins in the same Family}} \tag{5.19}$$

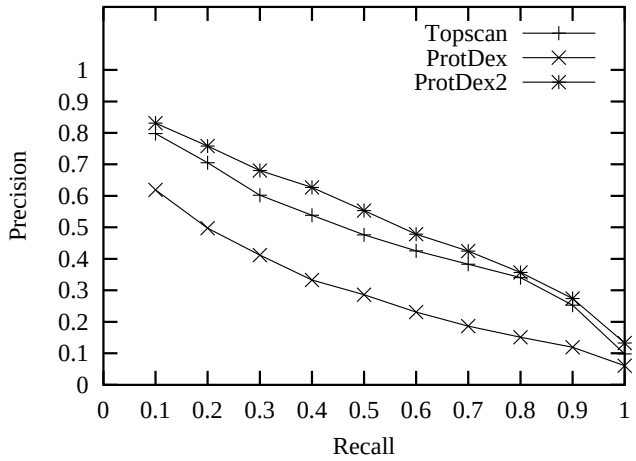

Figure 5.4: Average precision-recall curves for 108 queries on the database of 34,055 proteins.

5.6 Discussions

5.6.1 Analysis on Speed

The fast speed of ProtDex2 is attributed to the conciseness of the CP feature vector representation scheme, and the query evaluation scheme that uses the inverted index to collectively rank the database proteins simultaneously. The running time of ProtDex increases only "sub-linearly" as the database size grows. The cost incurred on each virtual pairwise comparison decreases significantly (from 3.8 milliseconds to 0.2 milliseconds) as the size of the database grows (from 200 proteins to 34,055 proteins).

Although its predecessor method, ProtDex, also uses inverted based query evaluation, the feature vectors are based on fixed-size overlapping sliding windows. Thus the number of feature vectors per protein is much more than that in ProtDex2, and the query evaluation is relatively slower as it involves comparisons of a huge number of feature vector pairs.

DALI and CE are apparently much slower than ProtDex2 as they are detailed alignment schemes, and they perform database searching by exhaustive pairwise comparisons.

Topscan is much faster than DALI and CE, but still slower than ProtDex2. It has to perform exhaustive searching of each query against the whole database. The disadvantage of this exhaustive searching scheme is magnified when the database size grows. Topscan is only about 4 times slower than ProtDex2 for the small database of 200 proteins, but about 113 times slower for the large database with 34,055 proteins. In addition, Topscan requires 24 rotations of one structure for each pairwise comparison. Since ProtDex2 is based on inter-SSE CPs of the distance matrix, such rotations are not required.

5.6.2 Analysis on Accuracy

As shown in Table 5.3, in order to obtain all the relevant answers, ProtDex2 has to retrieve more proteins than the detailed comparison methods of DALI and CE. In this experiment, ProtDex2 needs to retrieve the top 16 answers on the average, whereas DALI and CE need to retrieve only the top 10 answers, in order to obtain all of the 10 relevant answers. However, we can achieve the same level of accuracy as DALI and CE by retrieving these top 16 answers, which is only 8% of the entire database in this case, and refining them with DALI or CE. Given the very fast speed of ProtDex2, this filter-and-refine strategy can reduce the running time by about 12 folds while maintaining the good accuracy of the detailed comparison methods.

ProtDex2 is more accurate than its predecessor ProtDex method. In ProtDex method, the feature vectors are extracted from the fixed-size sliding windows sub-divided from the CPs. This approach leads to the poorer results due to the cross-matchings of the sliding windows from the different CPs. This weaknesses is avoided in ProtDex2 method by using only the feature vectors of the CPs in their entirety.

The accuracy of ProtDex2 is slightly better that of Topscan. Both methods are based on SSEs. Topscan uses symbolic linear representation of SSE vectors using the various properties such as SSE type, direction, length, proximity, etc. On the other hand, ProtDex2 uses feature vector representation of 2D inter-SSE

CPs using their various properties.

5.6.3 Importance of Feature Vector Attributes

We conduct a test on the expressive powers of the attributes in the CP feature vector in order to determine their relative importance. We run the large database searching test (108 queries on 34,055 database proteins) described above for 8 times, with excluding one attribute from the feature vector at a time. It turns out that all the attributes are more or less important. In Figure 5.5, we can see that every the precision-recall curve for excluding any attribute falls below the curve for including all the attributes. However, some attributes such as CP type (CT) and torsion angle (Ω) are found to be relatively more important than the others.

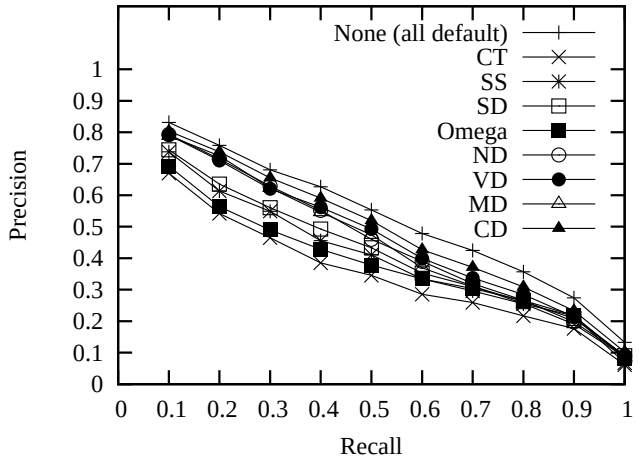

Figure 5.5: Average precision-recall curves for excluded attributes.

5.6.4 Interpreting Similarity Scores

For each query, ProtDex2 assigns a similarity score between 0 to 100 to every database protein. For the experiment of 108 queries on 34,055 proteins, we conduct a frequency analysis of the scores of the relevant retrievals (intra-Family matches) and those of the irrelevant retrievals (inter-Family mismatches). Then, we calculate the average percentage of errors and misses for each score checkpoint yielding

Figure 5.6. It can be observed that if we set the similarity score threshold as 15, we can have an optimal result with about 10% errors and 17% misses. If we set the score threshold as 30, we can achieve 99% accuracy rate (1% errors) with 53% coverage (47% misses).

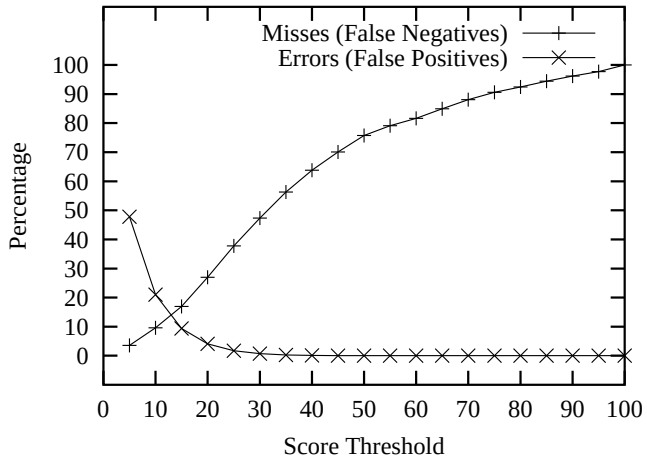

Figure 5.6: Errors and Misses percentages for various score thresholds.

5.6.5 Indexing Costs

For the aforementioned database of 34,055 protein structures, the construction of the inverted index from scratch (from PDB-format files) takes a total of 3 hr 51 min 20 sec (i.e. 0.40 sec per protein on average). Out of this total time, 3 hr 20 min 15 sec (about 86%) is incurred in running the STRIDE external program for SSE annotation, and only 31 min 05 sec is for ProtDex2's actual index building. Anyhow, unlike indexes used in other applications, the index for a protein structure database does not require online updating. The original database (such as PDB) may be updated daily, with 10s of new structures added per day. But, the updating of its index can only be done in batch on a regular basis (e.g. once per week) without much affecting the quality of service. Thus, the index construction time of ProtDex2 is affordable.

In terms of space requirement, while the size of the original database for 34,055

proteins in PDB format (3D coordinates only, without annotations) is 6.17 GB, that of the entire inverted index is only 51.8 MB (i.e. less than 1% of the original database's size).

5.7 Conclusion

In this chapter, we have proposed a new SSE-based indexing scheme for efficient retrieval of protein structures from the large databases. We conducted an experiment on the retrieval efficiency and effectiveness of the scheme in comparison with the other methods by using a small database and some query proteins from the well-known Globins and Serine/Threonin Kinases SCOP Families. We also conducted another experiment using a larger database and several query proteins from diverse SCOP Families so as to observe the more general behavior of the scheme.

The experimental results showed that our method is very much faster than two popular protein structure comparison methods, DALI and CE, yet not much sacrificing on the accuracy of the comparison. When comparing with an SSE-based database scan method, Topscan, our scheme is much faster even with a slightly better accuracy. In filter-and-refine framework, it can be ideally used as a filtering tool to reduce the search space before running a slow detailed structural comparison method.

Finally, it can become a very useful scheme in the near future when the protein structure database sizes become too large to be searched through exhaustively.

CHAPTER 6

Protein Structure Classification

Summary

In this chapter, we present a new scheme named "ProtClass" for automatic classification of 3D protein structures. It is a dedicated and unified multi-class classification scheme. Neither detailed structural alignment nor multiple binary classifications are required in this scheme. We adopt a nearest-neighbor classification strategy with a filter-and-refine scheme. In the first step, we filter out the most improbable by a coarse search. In the second, we perform a relatively more detailed search on the remaining answers. We also incorporate the pre-learned parameters from the training data in searching the nearest neighbors. We employ very concise and effective encoding schemes of the 3D protein structures in both steps. We compare our proposed method against two other dedicated protein structure classification schemes, namely SGM [RF03] and CPMine [AT04a]. The experimental results show that ProtClass is slightly better in accuracy than SGM, and much faster than it. In comparison with CPMine, ProtClass is much more accurate, while their running times are about the same. We also compare ProtClass against a detailed structural alignment-based classification scheme named DALI [HS93], which is found to be slightly more accurate, but extremely slower.

6.1 Introduction

Categorization of protein structures allows us to study the structural properties of proteins more easily through reductionism. Other benefits of structural categorization include provision of knowledge on sequence–structure relationships, reduction of search space functional prediction, etc. [Bou05, Ore99]. Protein structure categorization encompasses two different yet related topics: (1) clustering or building structural groups (classes) of proteins from scratch, and (2) classification or adding a new protein into the most appropriate of the existing structural classes.

We will study the automatic classification of protein structures in this chapter. In order to build an automatic classifier, we must have a database of protein structures whose class labels — in terms of a standard (usually a manual) class annotation system such as SCOP [HAB+97] and CATH [OMJ+97] — are already known. We use this database as the *training data* for the classifier. The classifier learns the relationships between the structural properties of the proteins and their structural class labels, and stores this knowledge in some abstract form. When a new protein (a query) is to be classified, the classifier reapplies the learned knowledge to predict its structural class label.

As discussed in Section 1.1.3, nearest neighbor, support vector machines, decision trees, hidden Markov model and fingerprinting are the methods for protein structure classification (and classification in general as well). Nearest neighbor classification is the most common used method for structural classification. Any detailed or coarse structural alignment tool or any explicit index-based search method can be used to find the protein(s) in the database that is/are most similar to the query, and derive the query's class label from its/their label(s).

Nearest neighbor classification is simple and generally effective. But it is generally inefficient — particularly in the present age of large structural databases. In addition, it usually lacks an active learning, and hence, fails to exploit the knowledge of the existing classes (unlike other classification methods such as support vector machines).

In this chapter, we propose a new protein structure classification system named

ProtClass (**Prot**ein **Class**ification), which rectifies the above weaknesses of the traditional nearest neighbor systems. Our objective is to develop an efficient and effective learning-based nearest neighbor classifier that do not have to perform any detailed structural comparison/alignment.

Suppose we have a database (training data) of protein structures together with their SCOP class labels. We train our classifier by encoding each protein structure in a concise format with two levels of abstraction, and extracting some important pieces of information from each distinct class. In this way, we can explore the prior knowledge of human expert judgement in classifying protein structures, and exploit this knowledge for classifying the new proteins in the future.

When we want to classify a query protein structure whose class is not known yet, we also represent it in its concise format, and conduct a filter-and-refine search. Firstly, we filter out the database proteins which are quite unrelated to the query using the first-level abstract representation. Secondly, for refinement, we employ a more detailed nearest-neighbor search based on the second-level abstract representation. In the both steps, we utilizes the pre-learned parameters of the distinct classes. Finally, we report the class label(s) of the nearest neighbor protein(s) as the possible class designation(s) for the query.

6.2 Encoding Protein Structures

In this section, we will discuss how ProtClass concisely and effectively represents a 3D protein structure in its encoded formats, namely *PA* and *CPset*; and how it measures the similarities between these encoded structures.

6.2.1 Protein Abstract (PA)

Let P be a 3D protein structure. Let $A = a_1a_2a_3 \ldots a_{|A|}$ be the amino acid (AA) residue sequence of P where $|A|$ is the number of residues in P. Let $S = s_1s_2s_3 \ldots s_{|S|}$ be the SSE sequence of P where $|S|$ is the number of SSEs in P. As an example, let us assume we have a 10 residue protein P with the following AA

sequence A.

K F A V N H I T R S

Let us also assume that we have 3 SSEs in the protein where residue 2–3 forms a sheet, 5–6 a helix, and 8–10 a sheet. Then we have the SSE sequence S of P as follows.

E H E

Here we formulate a concise encoding format named *Protein Abstract* (PA). It is a simple tuple featuring 6 attributes regarding the overall structure of a 3D protein structure as shown in Table 6.1.

Table 6.1: Attributes in a Protein Abstract (PA).

Sr	Description	Symbol	Equation	Example for protein P
1	No. of AA residues	$\|A\|$		10
2	No. of SSEs	$\|S\|$		3
3	Total length of all SSEs as a percentage of no. of residues	SL	(6.1)	0.7
4	Total length of all helices as a percentage of total SSE length	HL	(6.2)	0.29
5	No. of helices as a percentage of no. of SSEs	HN	(6.3)	0.33
6	SSE sequence	S		E H E

Attribute no. 1, 2 and 6 are readily available from the PDB file and the STRIDE output. Attribute no. 3–5 can be calculated using the following equations.

$$SL = \left(\sum_{i=1}^{|S|} |s_i|\right) / |A| \tag{6.1}$$

where $|s_i|$ is the length of SSE s_i. Here, the length of an SSE is an integer in terms of the number of AA residues it constitutes (rather than its physical length

in Angstroms (Å)).

$$HL = (\sum_{i=1}^{|S|} t_i) \,/\, SL \quad \text{where} \quad t_i = \begin{cases} |s_i| & s_i \text{ is H (helix)} \\ 0 & \text{otherwise} \end{cases} \tag{6.2}$$

$$HN = (\sum_{i=1}^{|S|} t_i) \,/\, |S| \quad \text{where} \quad t_i = \begin{cases} 1 & s_i \text{ is H} \\ 0 & \text{otherwise} \end{cases} \tag{6.3}$$

All the abovementioned six attributes in a PA are designed to capture the overall sequence and structure information of a protein. They can be used to roughly distinguish a protein from one class to that from another class. The differences of the attribute values in the PAs of two proteins from the same class tend to be lower than those from different classes. For example, the proteins belonging to the All-α Class usually have very high HL and HN values as opposed to the All-β Class proteins which usually have very low HL and HN values. In a big enough class, there almost always exists another protein whose PA attributes are very similar to those of a protein in question. We use this property of the protein structure classes to filter out the proteins which have very different PA attribute values from the query protein.

We can formally define a PA as the following hexa-tuple.

$$\mathcal{PA} = \{ \quad |A|,\, |S|,\, SL,\, HL,\, HN,\, S \quad \}$$

Given a query protein Q and a database protein P, we can represent them as two PAs: $\mathcal{PA}_Q$ and $\mathcal{PA}_P$. Let b be any attribute in $\mathcal{PA}$. The normalized distance or difference Δ_b between two attribute values (for the first 5 attributes) belonging to $\mathcal{PA}_Q$ and $\mathcal{PA}_P$ respectively can be defined as follows.

$$\Delta_b(\mathcal{PA}_Q, \mathcal{PA}_P) = \frac{|\, b_Q - b_P \,|}{b_Q} \quad \text{where} \quad b \in \{|A|, |S|, SL, HL, HN\} \tag{6.4}$$

For the last SSE sequence attribute S, we use ΔS as its SSE *edit distance* which is defined as follows.

$$\Delta_S(\mathcal{PA}_Q, \mathcal{PA}_P) = 1.0 - \frac{\mathbf{NW}(S_Q, S_P)}{|S_Q|} \tag{6.5}$$

where **NW** is the pairwise SSE alignment score for S_Q and S_P using Needleman-Wunsch algorithm [SM97, p. 52].

Suppose we have the pre-calculated difference (or distance) threshold values δ_b for all the 6 PA attributes. (The threshold value for each attribute is different from class to class. We will discuss how to calculate these threshold values for each of the distinct classes from the training data in Section 6.3.1.) When comparing a pair of PAs (one from Q and one from P), they are deemed similar if and only if $\Delta_b \leq \delta_b$ for every b. The similarity between two PAs can be formally defined as:

$$Similar(\mathcal{PA}_Q, \mathcal{PA}_P, \delta) = \begin{cases} \text{TURE} & \text{if } \Delta_b(\mathcal{PA}_Q, \mathcal{PA}_P) \leq \delta_b \\ & \text{for } \forall\, b \in \{|A|, |S|, SL, HL, HN, S\} \\ \text{FALSE} & \text{otherwise} \end{cases} \quad (6.6)$$

where δ is the set of PA attributes' distance thresholds for the class to which the database protein P belongs.

After we have determined that a pair of PAs is similar, we can calculate the *overall distance PADist* between them as a simple Euclidean distance as follows. (We do not have to calculate *PADist* for the two PAs that are not similar. On average, for a PA of a query protein, about 71% of the PAs in the database are dissimilar and can be discarded right away.)

$$PADist(\mathcal{PA}_Q, \mathcal{PA}_P, \delta) = \Big(\sum_{b \in \{|A|,|S|,SL,HL,HN,S\}} \big(\frac{\Delta_b(\mathcal{PA}_Q, \mathcal{PA}_P)}{\delta_b}\big)^2 \Big)^{0.5} \quad (6.7)$$

in which dividing the actual distance Δ_b with distance threshold δ_b maps the normalized distance into the range of 0 to 1 for all attributes. We assume equal weights for all the attributes.

Now, we can derive the matching score *PAMatch* between two PAs as based on *PADist*:

$$PAMatch(\mathcal{PA}_Q, \mathcal{PA}_P, \delta) = \frac{\sqrt{6} - PADist(\mathcal{PA}_Q, \mathcal{PA}_P, \delta)}{\sqrt{6}} \quad (6.8)$$

where $\sqrt{6}$ is the maximum possible Euclidean distance between two PAs, since a PA has 6 attributes whose values are between 0 and 1.

PA representation is simple yet powerful. As discussed later, it helps improve both the efficiency and effectiveness of the scheme. A similar concept of representing a protein structure in a concise high-level format was also put forward in [HSZK03].

6.2.2 Discrete Contact Pattern Feature Vector Set (CPset)

In this sub-section we will discuss how a 3D protein structure can be represented as another abstract structure called CPset, which is a set of integer-valued contact pattern feature vectors.

Contact Pattern (CP) Feature Vector

As discussed in Sections 5.3.1 and 5.3.2 of the ProtDex2 method, we can represent a 3D protein structure as a 2D distance matrix; define contact patterns (CPs); and represent them as feature vectors. Here we use a similar feature vector representation with 10 attributes (instead of 8 attributes as in ProtDex2) as given in Table 6.2. The two additional attributes are marked with asterisks. (In fact, we first tried these two attributes in ProtDex2. But they did not help improve its accuracy, and we later dropped them from it.)

The two new attributes AS (starting position of s_a in AA sequence) and AD (difference between starting positions of s_a and s_b in AA sequence) are defined as:

$$AS \;=\; s_a^{start} \tag{6.9}$$

$$AD(s_a, s_b) \;=\; s_b^{start} - s_a^{start} \tag{6.10}$$

where s_a^{start} and s_b^{start} are the starting positions of s_a and s_b respectively in AA sequence A. Since $b > a$, $s_b^{start} > s_a^{start}$.

The equations for the other attributes can be referred to in the previous chapter. Now we can define the CP feature vector $\mathbf{K}^{ab}$ for CP C^{ab} as:

$$\begin{aligned} \mathbf{K}^{ab} = \;\; (\;\; & CT(s_a, s_b),\, AS(s_a),\, SS(s_a),\, AD(s_a, s_b),\, SD(s_a, s_b), \\ & \Omega(\mathbf{V}_a, \mathbf{V}_b),\, ND(\mathbf{V}_a, \mathbf{V}_b),\, VD(\mathbf{V}_a, \mathbf{V}_b), \\ & MD(s_a, s_b),\, CD(s_a, s_b) \quad) \end{aligned} \tag{6.11}$$

Discrete CP Feature Vector

Now, we encode/discretize the CP feature vector so that it can be represented as a compact 4-byte integer value. In order to do this, we map each attribute value

Table 6.2: Attributes of CP feature vector for ProtClass.

Sr.	Attribute	Sym-bol	Equa-tion	Upper Bound	Discret-ization	
					Bins	Bits
1	Type of C^{ab}	CT	(5.1)	3	4	2
2*	Starting position of s_a in AA sequence A	AS	(6.9)	800	2	1
3	Position of s_a in SSE sequence S	SS	(5.2)	48	12	4
4*	Starting position difference of s_a and s_b in AA sequence A	AD	(6.10)	800	4	2
5	Position difference of s_a and s_b in SSE sequence S	SD	(5.3)	48	20	5
6	Torsion angle between $\mathbf{V}_a$ and $\mathbf{V}_b$ (-180.0 to $+180.0$)	Ω	[Sfy04]	360.0	16	4
7	Closest segment–segment distance of $\mathbf{V}_a$ and $\mathbf{V}_b$	ND	[Sun04]	64.0	16	4
8	Nearest vertex pair distance of $\mathbf{V}_a$ and $\mathbf{V}_b$	VD	(5.6)	64.0	4	2
9	Mean of C_α–C_α distances in C^{ab}	MD	(5.7)	64.0	4	2
10	Contact density of C^{ab}	CD	(5.8)	1.0	2	1
	Total					27

in the feature vector into a discrete number of bins, and concatenate all the bits representing these bins into a bit string which can naturally be interpreted as an integer. (The idea of discretization is similar to that of ProtDex2 in the previous chapter. But, discretization here is done by physical encoding and no hash table is used as in ProtDex2.)

The objectives of this encoding are (1) to enable efficient handling of the CP feature vectors, and (2) to allow approximate matching of the original CP feature

vectors by simply performing exact matching of their discrete versions. The idea of encoding a multi-dimensional feature vector into a bit string for efficient and effective processing is inspired by that of VA-File method [WSB98].

The disadvantage of discretization is that there may be false matches (when the attributes values are near the upper and lower boundaries of the same bin), and false mismatches (when the attribute values are near the upper and lower boundaries of the adjacent bins). However, the degree of accuracy provided by the discretization scheme is well sufficient for our purpose of finding the nearest neighbors of proteins in terms of the number of common CP feature vectors they include — as demonstrated in our experimental results.

The possible ranges for the original space (upper bound) and the discretized space (number of bins and bits) for each attribute are given in Table 6.2. Some attributes are allocated larger discretized spaces (i.e. more number of bins) than the others because they are found to be relatively more important.

As an example, for the closest segment-segment distance (ND) attribute, we map an original real number distance value between 0.0 to 64.0 into one of the discrete *bins* numbered between 0 to 15 (i.e. 4 bit space). We use simple *equal partition discretization* which is informally defined as follows.

$$bin(Value) = \begin{cases} floor(\frac{Value \times \#Bins}{UpperBound}) - 1 & \text{if } Value = UpperBound \\ floor(\frac{Value \times \#Bins}{UpperBound}) & \text{otherwise} \end{cases} \tag{6.12}$$

For instance, we can calculate the discretized value of 14.1 Å distance as: $floor(14.1 \times 16/64.0) = 3$.

Now, we can define a 27-bit *discrete CP feature vector* $\mathbf{T}$ as follows.

$$\begin{aligned} \mathbf{T}^{ab} = (\quad & bin(CT(s_a, s_b)) \,|\, bin(AS(s_a)) \,|\, bin(SS(s_a)) \,|\, bin(AD(s_a, s_b)) \,| \\ & bin(SD(s_a, s_b)) \,|\, bin(\Omega(\mathbf{V}_a, \mathbf{V}_b)) \,|\, bin(ND(\mathbf{V}_a, \mathbf{V}_b)) \,| \\ & bin(VD(\mathbf{V}_a, \mathbf{V}_b)) \,|\, bin(MD(s_a, s_b)) \,|\, bin(CD(s_a, s_b)) \quad) \end{aligned} \tag{6.13}$$

where *bin* is the discretization function (Eq. 6.12) and | is the concatenation operator for bit strings.

CPset

Now, we can encode an entire 3D protein structure as a set of discrete CP feature vectors it contains. We call this set a *CPset*, and denote it as $\mathcal{CPS}$. $\mathcal{CPS}_P$ of protein structure P with $|S|$ SSEs can be defined as:

$$\mathcal{CPS}_P = \{\mathbf{T}^{12}, \mathbf{T}^{13}, \ldots, \mathbf{T}^{1|S|}, \mathbf{T}^{23}, \ldots, \mathbf{T}^{(|S|-1)\,|S|}\} \tag{6.14}$$

where $\mathbf{T^{ij}}$ (where $1 \leq i \leq (|S|-1)$ and $(i+1) \leq j \leq |S|$) is a discrete CP feature vector.

The cardinality of a CPset with $|S|$ SSEs is at most $|S|(|S|-1)/2 = O(|S|^2)$. (There may be some outlier CPs which are excluded from the CPset.)

We sort the discrete CP feature vectors (which can be regarded as integers) in the CPset in ascending order to enable linear-time comparison of them in the later classification step. Sorting alters the original order of these discrete feature vectors in the CPset. However, since the discretized attributes AS (position of first SSE in AA sequence), SS (position of first SSE in SSE sequence), AD (AA position difference between first and second SSEs), and SD (SSE position difference between first and second SSEs) are stored in the discrete CP feature vector, the positions and relative order of the original CPs in the distance matrix can still be roughly known.

We can calculate the matching score between two CPsets $\mathcal{CPS}_Q$ and $\mathcal{CPS}_P$ with a simple linear-time algorithm described in Figure 6.1. It is based on the merging algorithm for two sorted arrays. Being a linear-time algorithm working on integers, it is very fast.

Both PA and CPset are compact and efficient means of encoding a 3D protein structure. The average sizes of a PA and a CPset are 160 and 782 bytes respectively, whereas the average size of an original PDB format file (3D coordinates only, without any annotation) is about 261 KB (261,000 bytes).

function $CPsetMatch(\mathcal{CPS}_Q, \mathcal{CPS}_P) \rightarrow (MatchScore)$
input: Two CPsets to compare: $\mathcal{CPS}_Q$ and $\mathcal{CPS}_P$
output: Their matching score $MatchScore$
procedure:
1. $x = 1$, $y = 1$, $MatchCount = 0$
2. `while` $(x \leq |\mathcal{CPS}_Q| \wedge y \leq |\mathcal{CPS}_P|)$
3. `if` $(\mathbf{T}_{Qx} == \mathbf{T}_{Py})$ `then` $MatchCount$ ++, x ++, y ++
4. `else if` $(\mathbf{T}_{Qx} < \mathbf{T}_{Py})$ `then` x ++
5. `else` y ++
6. `end while`
7. $MatchScore = MatchCount \,/\, |\mathcal{CPS}_Q|$ /* Normalize */
8. `return` $MatchScore$

Figure 6.1: Similarity score function for two CPsets.

6.3 The ProtClass Method

In this section, we will discuss the *preprocessing step* and the *querying (classification) step* of the ProtClass method.

In the preprocessing step, the system first generates the database of protein abstracts (PAs), and the database of sets of discrete contact pattern feature vectors (CPsets) from the training data set (the database of protein structures with known structural class labels). Then, it learns two types of parameters from the members and classes of the training data. It computes:

1. The **PA distance thresholds** of 6 PA attributes for each class by all-against-all comparison of the PAs in the given class.

2. The **membership weight** for each member in each class by calculating its matching scores to the other proteins in the same class and the different classes. The membership weight of a protein is positive if it is similar to its fellow class members, and is negative if it is an outlier to its own class.

In the querying step, the system generates the query's PA and CPset in the same manner. Then, in the first filtering sub-step, it prunes away the unpromising answers by comparing the PA of the query against those of the database proteins,

using the PA distance thresholds learned in the preprocessing step. Then, in the refinement sub-step, the system conducts a nearest-neighbor search of the query's CPset against the remaining database proteins' CPsets, and returns the class label(s) of the protein(s) that are best matched. The membership weights learned from the preprocessing step are also taken into account in selecting the candidate nearest neighbors.

The overview of the method is illustrated in Figure 6.2. The algorithmic details of the preprocessing and querying steps are described in the following two sub-sections.

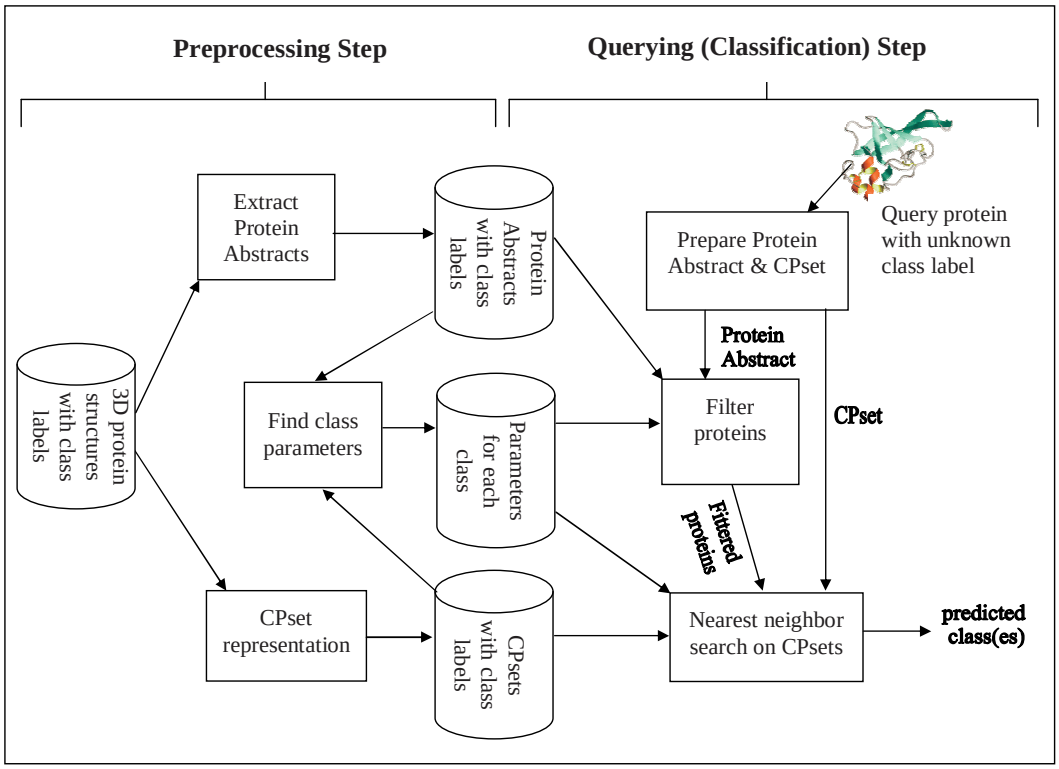

Figure 6.2: Overview of ProtClass method.

6.3.1 Preprocessing Algorithm

Given a database of protein structures with known class labels, we can generate the databases of PAs, CPsets, and the two class parameters using the preprocessing algorithm shown in Figures 6.3 and 6.4. For each distinct class, we generate the

PAs and CPsets for the proteins belonging to this class, and store them in the database (line 4–10).

We calculate the membership weight for each protein with respect to its class (line 15). We use the *silhouette width* measure [KR90] for the membership weight. For a protein j in class i, its silhouette width is defined as:

$$SilhouetteWidth(i,j) = \frac{b(j) - a(j)}{\max(a(j), b(j))} \tag{6.15}$$

where $a(j)$ is the average distance of j to its fellow class members in class i, and $b(j)$ is the average distance of j to the members in its nearest neighbor class other than i. The distance between two proteins Q and P is calculated based on their PA matching score and CPset matching score as follows:

$$Dist(Q,P) = 1.0 - (PAMatch(\mathcal{PA}_Q, \mathcal{PA}_P, \delta_{default}) \cdot CPsetMatch(\mathcal{CPS}_Q, \mathcal{CPS}_P)) \tag{6.16}$$

where *PAMatch* and *CPsetMatch* are defined in Equation 6.8 and Figure 6.1 respectively. $\delta_{default}$ is described in the last paragraph of the current sub-section.

In calculating the silhouette width, if $b(j) > a(j)$, the result will be a positive value. Otherwise, it will be a negative value. In other words, if a member protein in a class is closer to its fellow members than to the members in other class, its membership weight (silhouette width) will be positive, This protein is useful in predicting the class of a query protein by nearest neighbor search in the future. On the other hand, if a member protein is closer to the members of other classes than to its own fellow members, it is an outlier and its membership weight will be negative. This protein should not be taken into account in determining the nearest neighbor of the query protein. The use of membership weights can help improve the accuracy of classification [BM03].

Again, for each class, we calculate the farthest PA attribute distances $max\delta_b$ that are exhibited in the PA pairs belonging to this class. (line 18–21). For each PA attribute, its farthest distance value is multiplied with a $CoverageFactor$ to obtain the distance threshold value of this attribute (line 25).

The empirically determined value, $CoverageFactor = 0.80$, is used in our im-

plementation. The objective of setting the threshold distances is to ensure that at least one nearest proteins belonging to the same class as a given query protein will pass the filtering step (see the next sub-section), whilst the dissimilar proteins are discarded straight away. It means that for each PA attribute, we expect to find the nearest neighbor(s) to a query protein within 80% of the distance of the two farthest proteins (with respect to this attribute) belonging to this particular class in the existing database. If the number of trained proteins in a class is too few (say less than 20), this condition may not be always true. We use the default threshold values $\delta_{default} \equiv (\delta_{|A|} = 0.4,\ \delta_{|S|} = 0.4,\ \delta_{SL} = 0.3,\ \delta_{HL} = 0.2,\ \delta_{HN} = 0.3,\ \delta_{S} = 0.5)$ in this case.

6.3.2 Querying Algorithm

The algorithm in Figure 6.5 describes how unpromising answers with respect to a given query can be filtered out using PAs, and how the class of the query protein can be predicted by using the nearest-neighbor search based on the PA similarity and the CPset similarity, together with the membership weights.

First of all, if the membership weight of a particular member protein in a class is negative, it is regarded as an outlier, and is neglected in selecting the query's nearest neighbors (line 9–10).

In the *filtering step*, the algorithm first filters out the unpromising answers using the PA of the query and those of the database proteins (line 11–12). For a protein that passes the filtering test, the matching score of its PA to the query PA ($PAScore$) is calculated (line 13).

Our experimental results show that an average of 71% of the database proteins are discarded in the filtering step, as they are not close enough to the query. An average of 38% of the classes are entirely discarded. It should be noted that the proteins that are in the same class as the query but not similar enough (the distantly related ones) are also discarded. But the similar ones in the correct class pass the test. So, there is no chance of discarding the correct class as a whole.

In the second *refinement step*, the matching score of the protein's CPset to that

function **ProtClass_Preprocess** $(\mathcal{D}) \rightarrow (\mathcal{PA}, \mathcal{CPS}, \delta, \mathcal{MW})$
input: Protein structure database $\mathcal{D} = \{\mathcal{D}_1, \mathcal{D}_2, \ldots, \mathcal{D}_n\}$ where $\mathcal{D}_i$ $(1 \leq i \leq n)$
is a set of protein structures with class label i
output: (1) PA database $\mathcal{PA} = \{\mathcal{PA}_1, \mathcal{PA}_2, \ldots, \mathcal{PA}_n\}$ where $\mathcal{PA}_i$ $(1 \leq i \leq n)$
is a set of Protein Abstracts for proteins with class label i
(2) CPset database $\mathcal{CPS} = \{\mathcal{CPS}_1, \mathcal{CPS}_2, \ldots, \mathcal{CPS}_n\}$ where $\mathcal{CPS}_i$ $(1 \leq i \leq n)$
is a set of CPsets for proteins with class label i
(3) PA distance threshold database $\delta = \{\delta_1, \delta_2, \ldots, \delta_n\}$ where δ_i $(1 \leq i \leq n)$
is a set of PA distance thresholds in class i
(4) Membership weight database $\mathcal{MW} = \{\mathcal{MW}_1, \mathcal{MW}_2, \ldots, \mathcal{MW}_n\}$
where $\mathcal{MW}_i$ $(1 \leq i \leq n)$ is a set of weights for members in class i
procedure:
1. $\mathcal{PA} = \phi$, $\mathcal{CPS} = \phi$, $\delta = \phi$, $\mathcal{MW} = \phi$
2. `for` $i = 1$ `to` n /* n is the number of distinct classes */
3. $\mathcal{PA}_i = \phi$, $\mathcal{CPS}_i = \phi$, $\delta_i = \phi$, $\mathcal{MW}_i = \phi$
4. `for` $j = 1$ `to` $|\mathcal{D}_i|$ /* $|\mathcal{D}_i|$ is the number of members in class i */
5. Let $\mathcal{D}_{ij}$ $(1 \leq j \leq |\mathcal{D}_i|)$ be an individual protein structure in $\mathcal{D}_i$
6. $\mathcal{PA}_{ij} =$ **GeneratePA**$(\mathcal{D}_{ij})$ /* See Section 6.2.1 */
7. $\mathcal{PA}_i = \mathcal{PA}_i \cup \mathcal{PA}_{ij}$
8. $\mathcal{CPS}_{ij} =$ **GenerateCPset**$(\mathcal{D}_{ij})$ /* See Section 6.2.2 */
9. **Sort**$(\mathcal{CPS}_{ij})$ /* Sort in ascending order */
10. $\mathcal{CPS}_i = \mathcal{CPS}_i \cup \mathcal{CPS}_{ij}$
11. `end for`

(continued to Figure 6.4)

Figure 6.3: ProtClass preprocessing algorithm.

of the query ($CPsetScore$) is calculated is using the function *CPsetMatch* (line 15). Since the function is a linear-time algorithm and it only has to handle integer values, the calculation is very fast. The final score of the protein with respect to the query is calculated by taking both its PA matching score ($PAScore$) and CPset matching score ($CPsetScore$) into account (line 16). Finally, we return the class label of the protein which is the nearest to the query (in terms of the final score), and optionally other information such as the best scoring protein for each class, etc. (line 23).

(continued from Figure 6.3)

```
12.     for each b ∈ {|A|, |S|, SL, HL, HN, S}   /* b is a PA attribute */
13.         maxδ_b = 0
14.     for j = 1 to |D_i|   /* |D_i| is the number of members in class i */
15.         MW_ij = SilhouetteWidth(i, j)   /* Eq. 6.15 */
16.         MW_i = MW_i ∪ MW_ij
17.         for k = 1 to |D_i|
18.             for each b ∈ {|A|, |S|, SL, HL, HN, S}
19.                 if (maxδ_b < Δ_b(PA_ij, PA_ik)) then
20.                     maxδ_b = Δ_b(PA_ij, PA_ik)   /* Eq. 6.4 and 6.5 */
21.             end for
22.         end for
23.     end for
24.     for each b ∈ {|A|, |S|, SL, HL, HN, S}
25.         δ_ib = maxδ_b × CoverageFactor
26.         δ_i = δ_i ∪ δ_ib
27.     end for
28.     PA = PA ∪ PA_i, CPS = CPS ∪ CPS_i, δ = δ ∪ δ_i, MW ∪ MW_i
29. end for   /* of line 2 */
30. return (PA, CPS, δ, MW)
```

Figure 6.4: ProtClass preprocessing algorithm (contd.).

6.4 Experimental Results

In order to assess the accuracy and efficiency of the proposed ProtClass scheme, we test it on a medium size data set with 600 protein structure in the experimental setup mentioned below. We compare ProtClass against DALI [HS93] (using DaliLite [HP00] implementation), SGM [RF03] and CPMine [AT04a] using their default settings in the same experimental setup. When running DaliLite, we use its database search option rather than its pairwise alignment option.

function **ProtClass_Query** $(Q, \mathcal{PA}, \mathcal{CPS}, \delta, \mathcal{MW})$
$\rightarrow ((MaxClass, MaxClassScore), (MaxProtein, MaxScore))$
input: (1) Query protein structure Q
(2) $\mathcal{PA}, \mathcal{CPS}, \delta, \mathcal{MW}$ /* See their definitions in above algorithm Figure 6.3. */
output: (1) Most possible class $MaxClass$ for Q and its score $MaxClassScore$
(2) Most possible proteins $MaxProtein$ and their respective scores $MaxScore$ arrays for all distinct classes /* optional */
procedure:
1. $PAQ =$ **GeneratePA**(Q) /* See Section 6.2.1 */
2. $CPSQ =$ **GenerateCPset**(Q) /* See Section 6.2.2 */
3. **Sort**$(CPSQ)$ /* Sort in ascending order */
4. Let $CPSQ = \{\mathbf{T}_{Q1}, \mathbf{T}_{Q2}, \ldots, \mathbf{T}_{Q\,|CPSQ|}\}$ where $\mathbf{T}_{Qx}$ $(1 \leq x \leq |CPSQ|)$ is a discrete CP feature vector of Q.
5. $MaxClassScore = 0$, $MaxClass = 0$
6. `for` $i = 1$ to n /* n is the number of distinct classes */
7. $MaxScore_i = 0$, $MaxProtein_i = 0$
8. `for` $j = 1$ `to` $|\mathcal{PA}_i|$ /* $|\mathcal{PA}_i|$ is the number of trained proteins in class i */
9. `if` $(\mathcal{MW}_{ij} \leq 0)$ `then` /* Check if membership weight is negative */
10. `continue`; /* outlier of its own class; skip this protein */
11. `if` $(Similar(PAQ, \mathcal{PA}_{ij}, \delta_i) ==$ `FALSE` $)$ `then` /* See Eq. 6.6 */
12. `continue`; /* filter test failed; skip this protein */
13. $PAScore = PAMatch\,(PAQ, \mathcal{PA}_{ij}, \delta_i)$ /* See Eq. 6.8 */
14. Let $\mathcal{CPS}_{ij} = \{\mathbf{T}_{P1}, \mathbf{T}_{P2}, \ldots, \mathbf{T}_{P\,|\mathcal{CPS}_{ij}|}\}$ where $\mathbf{T}_{Py}$ $(1 \leq y \leq |\mathcal{CPS}_{ij}|)$ is a discrete CP feature vector of $\mathcal{CPS}_{ij}$.
15. $CPsetScore = CPsetMatch\,(CPSQ, \mathcal{CPS}_{ij})$ /* See Fig. 6.1 */
16. $FinalScore = PAScore \times CPsetScore$
17. `if` $(FinalScore > MaxScore_i)$ `then`
18. $MaxScore_i = FinalScore$, $MaxProtein_i = j$
19. `end for`
20. `if` $(MaxScore_i > MaxClassScore)$ `then`
21. $MaxClassScore = MaxScore_i$, $MaxClass = i$
22. `end for`
23. `return` $((MaxClass, MaxClassScore), (MaxProtein, MaxScore))$

Figure 6.5: ProtClass querying (classification) algorithm.

6.4.1 Experimental Setup

We use the ASTRAL data set [BKL00] that contains proteins with less than 40% sequence homology. From this data set, we choose 15 "Folds" (according to SCOP

designation) each with 40 member proteins. (For Folds with more than 40 members, we randomly select 40 from them.) Thus, we have a pool of $15 \times 40 = 600$ protein structures whose class labels (Folds) are known. We use these 15 Folds as our target structural classes.

We conduct our experiment using 10-*fold cross validation* strategy. We split each Fold into 10 partitions each having 4 protein structures. We conduct 10 sub-experiments in each of which we build the *testing data set* by choosing a partition from each of the Folds and combining them together. In this way, we have a testing data set consisting of 60 proteins for each sub-experiment. The remaining 540 proteins are used as the *training data set*. The training data set is made up of 36 proteins from each of 15 Folds.

In other words, in each sub-experiment, we have a database of 540 protein structures whose Folds are already known, and a set of 60 query protein structures whose Folds are to be predicted. We then validate the predicted Folds of the query proteins against their actual Folds as designated by SCOP.

6.4.2 Accuracy

In the abovementioned manner, 10 sub-experiments are conducted by using the different testing sets and training sets in each cycle. Then, we consolidate the results from 10 sub-experiments and calculate the average accuracy of the scheme. We look at the top 3 scoring Folds (which is 20% of the total number of distinct Folds), and examine whether they are actually the correct classifications. The results are shown in Table 6.3. Column "Top 1" shows the accuracy of the scheme if only the topmost scorer is examined, and Column "Top 2" shows the accuracy if both top 1 and 2 scorers are examined, etc. The accuracy results of DALI, SGM and CPMine are also shown in Table 6.3.

With a large number of possible classes (15 SCOP Folds in this case), it may be more useful to report a few candidate classes rather than reporting a single but incorrect class — as long as the number of reported classes is only a small fraction of all the possible classes (20% in our case). The user can manage these

candidate classes according to his/her own requirement. For example, if only moderate accuracy in classification is required, the user can just take the topmost scoring class as the answer. If high accuracy is needed, manual inspections or detailed structural alignments can be done on the top scoring members of the top 3 scoring classes. This strategy of reporting more than one class as the possible candidates is also advocated by the authors of SGM [RF03].

From the experiments, it is observed that ProtClass performs quite accurately. In overall, it offers an average accuracy of 99.17% if we take the top 3 scorers into account and 91.17% if we take only the topmost scorer into account.

It gives the perfect results on certain Folds such as `47472`, `48370`, and `51734` with 100% accuracy even with the topmost scorer. It performs quite fairly on certain Folds such as `52171` (95% accuracy with the top 3 scorers and 85% with the topmost scorer).

As expected, DALI exhibits more accuracy than ProtClass. Its high accuracy (99.7% with the topmost and 99.2% with top 3) can be attributed to its detailed structural alignment mechanism. But, on the other hand, this approach is extremely slow (see Section 6.4.3). We can achieve the same high accuracy as DALI while reducing the running time by employing ProtClass as a rapid query preprocessor. We can run the filtering step of ProtClass before running DALI itself. The filtering step filters out the about 71% of all the database proteins as irrelevant. It is observed that the proteins that are relevant to the final answer are always retained in the remaining 29% to be processed by DALI in the next step. Therefore we do not miss out anything, but can reduce the total running time by about 73%. This means 370% improvement in speed.

The overall accuracy of ProtClass is slightly better than that of SGM. Out of 15 Folds tested, ProtClass performs better than SGM in 9 Folds, equally in 5 Folds, and poorer in 1 Fold (according to the top 3 scorer results). We can observe some similarities between the result of ProtClass and that of SGM. For example, both methods give perfect results for Folds `48370`, `48725`, `51734`, etc., but give poor topmost scorer results for Fold `52439`.

In comparison with CPMine, ProtClass is found to be much more accurate. This is because CPMine is a fingerprint-based comparison approach without using any filters. Matching a query against the fingerprints of the classes (Folds in this case) can introduce both false positives and false negatives, because the fingerprints sometimes cannot represent their respective classes uniquely and unfailingly. In ProtClass, we do not use such a fingerprinting mechanism, thus reducing the possibility of false classifications due to misrepresentation.

6.4.3 Speed

It is observed that the proposed ProtClass scheme works very efficiently. All the experiments are done on Sun Ultra Sparc II with two 480MHz CPUs and 4GB main memory, running Sun OS 5.7. The time statistics are shown in Table 6.4. It shows the time taken to run one cycle of sub-experiment (preprocessing on 540 proteins, and querying with 60 proteins) by each method. It is averaged out from the times taken by the 10 sub-experiments in 10-fold cross validation.

Although DALI is more accurate than ProtClass, it is found to be about 620 times slower! It takes an average of about 1 day and 21 hours for querying of 60 proteins on the database of 540 proteins. In fact, it may be impractical to use DALI for a real-time classification task involving a large database on an average stand-alone machine. In the previous sub-section, we have already discussed how we can improve the running time of DALI by using ProtClass as a rapid preprocessor.

In comparison with SGM, it is observed that ProtClass is about 18 times faster. This is because SGM involves a large number of floating point operations to calculate the Gauss Integrals. On the contrary, ProtClass mainly performs integer and bit-wise operations. CPMine's running time is about the same as that of ProtClass. They both use the similar integer and bit operations.

From the experiment, it is also observed that the running time of ProtClass, both for preprocessing and querying steps, is overwhelmed by that of STRIDE external algorithm used to generate the SSE information. The breakdown of the various time costs in both preprocessing and querying steps are shown in Table 6.5.

Table 6.3: Experimental results on 15 distinct Folds.

Fold	Class	Average Percentage of Correct Classifications											
		DALI			SGM			ProtClass			CPMine		
		Top1	Top2	Top3	Top1	Top2	Top3	Top1	Top2	Top3	Top1	Top2	Top3
46688	All-α	92.5	95.0	95.0	80.0	95.0	97.5	92.5	97.5	100.0	80.0	85.0	92.5
47472	All-α	100.0	100.0	100.0	80.0	90.0	97.5	100.0	100.0	100.0	47.5	97.5	100.0
48370	All-α	100.0	100.0	100.0	97.5	100.0	100.0	100.0	100.0	100.0	50.0	72.5	85.0
48725	All-β	100.0	100.0	100.0	100.0	100.0	100.0	95.0	97.5	100.0	72.5	97.5	100.0
50198	All-β	100.0	100.0	100.0	82.5	92.5	95.0	90.0	92.5	100.0	30.0	62.5	85.0
51350	α/β	100.0	100.0	100.0	77.5	92.5	97.5	97.5	97.5	100.0	47.5	65.0	77.5
51734	α/β	100.0	100.0	100.0	72.5	95.0	100.0	100.0	100.0	100.0	52.5	85.0	87.5
51904	α/β	100.0	100.0	100.0	97.5	97.5	100.0	95.0	97.5	97.5	32.5	55.0	60.0
52171	α/β	95.0	100.0	100.0	65.0	82.5	82.5	85.0	95.0	95.0	42.5	72.5	95.0
52539	α/β	100.0	100.0	100.0	50.0	72.5	85.0	72.5	90.0	100.0	32.5	60.0	82.5
52832	α/β	100.0	100.0	100.0	90.0	92.5	95.0	95.0	97.5	100.0	25.0	37.5	62.5
53066	α/β	100.0	100.0	100.0	67.5	80.0	92.5	80.0	95.0	95.0	30.0	37.5	47.5
53473	α/β	100.0	100.0	100.0	77.5	92.5	92.5	95.0	97.5	100.0	47.5	60.0	70.0
54235	$\alpha+\beta$	100.0	100.0	100.0	87.5	92.5	100.0	85.0	97.5	100.0	50.0	70.0	85.0
54861	$\alpha+\beta$	100.0	100.0	100.0	85.0	97.5	100.0	85.0	92.5	100.0	32.5	67.5	90.0
Overall		99.2	99.7	99.7	80.7	91.5	95.7	91.2	96.5	99.2	44.8	68.3	81.3

Table 6.4: Average running times for 60 queries on 540 proteins for 4 methods.

Description	Average time elapsed (in seconds)				Average time on one protein/query (in seconds)			
	DALI	SGM	ProtClass	CPMine	DALI	SGM	ProtClass	CPMine
Preprocessing (540 proteins)	1,080	4,297	235	227	2.00	7.96	0.44	0.42
Querying (60 proteins)	163,466	478	30	26	2,724.43	7.97	0.50	0.43
Total	164,546	4,775	265	253				

Table 6.5: Breakdown of costs for ProtClass based on average running times for 60 queries on 540 proteins.

Description	Average time elapsed (in seconds)	Average time on one protein/query (in seconds)
Preprocessing (540 proteins)		
- Running STRIDE	211.53	0.39
- Generating PAs, CPsets, and class parameter databases	23.78	0.04
Total	235.31	
Querying (60 queries)		
- Running STRIDE	24.05	0.40
- Preparing queries (PA and CPset)	1.31	0.02
- Filtering step	1.94	0.03
- Refinement step	2.85	0.05
Total	30.15	

6.4.4 Effect of Proportion of Training and Testing Data

In our 10-fold cross validation experiment on 600 proteins, we use 540 (90%) of them as the training data, and the remaining 60 as the testing data in each cycle. In order to explore the effect of the proportion of the training and testing data, we change it variously and observe the changes in the accuracy of the scheme. First, we conduct the leave-one-out test by using 15 proteins as the testing data (one from each distinct Fold) and the remaining 585 as the training data, and repeat the experiment 40 times. In Figure 6.6, the label on x-axis "97.5%" means that the percentage of the training proteins is 97.5% of the total proteins (i.e. 585 out of 600). The label "(39/40)" means that 39 out of 40 proteins in each distinct Fold are used as the training data. The other test cases are with 75%, 50%, and 25% training data respectively. All these are compared against our default test with 90% training data as shown in the figure.

Similar experiments are also conducted on SGM whose results are also shown in Figure 6.6. We exclude DALI and CPMine from our experiment, because the former takes a very long time to run, and the latter is clearly inferior to ProtClass.

As expected, the accuracy of the scheme gradually declines with the reduction of the training data percentage. However, there are no steep slopes in the curves. In the worst case with 25% training data, ProtClass can still provide the accuracies of 77.4%, 88.0%, and 93.2% for the topmost, top 2, and top 3 answers respectively. We can also observe a similar trend of declining accuracy in the curves of SGM. In fact, this is a general phenomenon for all classification systems — the more the training data, the better the accuracy.

6.4.5 Effect of Class Size

In our experiment, we use classes (SCOP Folds) with 40 members each, which can be considered as relatively "big" ones. In order to assess the performance of the scheme on the various sizes of Folds, we run multiple tests on various Fold sizes. In the first test, we take Folds with at least 2 members from ASTRAL data set with less than 40% sequence homology. (For Folds with more than 2 members, we

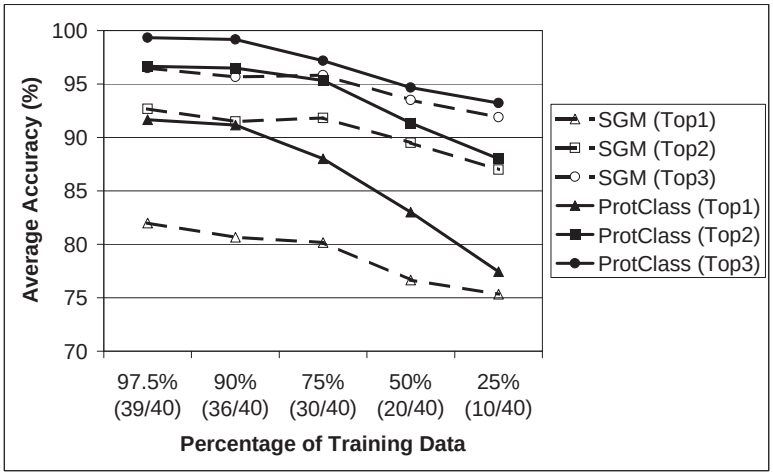

Figure 6.6: Effect of percentage of training data.

randomly choose 2 from them.) There are 350 such Folds, thus yielding a data set with $(350 \times 2 = 700)$ proteins. Then we run two test cycles, each with 350 training proteins and 350 testing proteins. The other test cases are for Folds with 5, 10, 15 members etc. up to 50 members. The results are shown in Figure 6.7. Similar experiments are also conducted on SGM.

ProtClass can only provide 50% accuracy (with the top 3 scorers) for the Folds with 2 members. However, given a very large number of possible Folds (350), this 50% accuracy is not trivial. We can observe the trend of accuracy improvement with the increased number of members in the Folds. ProtClass can provide a reasonable accuracy of at least 80% for the Folds with 10 or more members when the top 3 scorers are taken into account, and 25 or more members when only the topmost scorer is taken into account. We can also see a similar trend of accuracy improvement in the curves of SGM. The accuracy of SGM is better than ProtClass for 2-member Folds, but the latter is generally better for the rest of the Folds. It is interesting to observe a high degree of correlation between the curves of ProtClass and those of SGM.

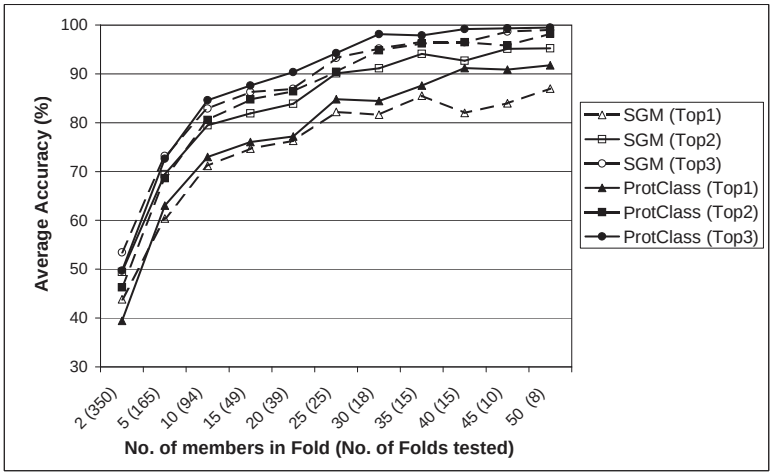

Figure 6.7: Effect of number of members in each distinct Fold.

6.5 Discussions

6.5.1 Importance of Filter and Refine Steps

With the hope to further improve the accuracy of the scheme, one may be tempted to drop the filtering step and run only the relatively more detailed refinement step on every database protein. But, unfortunately, this does not work. The accuracy of the system degrades substantially if filtering is not carried out. This is because the filtering step can prune away a lot of potential false positive proteins whose CPsets are similar to that of the query, but whose PAs are not. Our experimental results show that both filtering and refinement steps are indispensable. Figure 6.8 shows the overall accuracy of the system when both steps are included, and when each step is dropped at a time.

6.5.2 Importance of PA Attributes

In order to assess the importance of the six attributes in a PA, we drop each attribute at a time and re-run the experiment as described in Section 6.4.1. It is observed that all the attributes are more or less important on their own, because dropping any of them reduces the accuracy of the scheme — as shown in Figure 6.9.

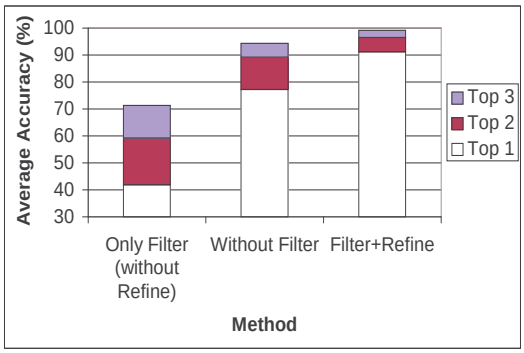

Figure 6.8: Importance of filter and refine steps.

6.5.3 Importance of CP Feature Vector Attributes

Similarly, in order to evaluate the importance of the ten attributes in a CP feature vector, we exclude each attribute at a time from the experiment as described in Section 6.4.1. Again, it is found out that all the attributes are more or less important, because dropping any of them degrades the accuracy of the scheme — as shown in Figure 6.10. Although all the attributes are important, some attributes — such as CT (contact pattern type) and Ω (torsion angle) — are found to be more important than the others, as the exclusion of these attribute affects the accuracy of the system more seriously. (This observation is consistent with that on ProtDex2 as discussed in Section 5.6.3 in the previous chapter.)

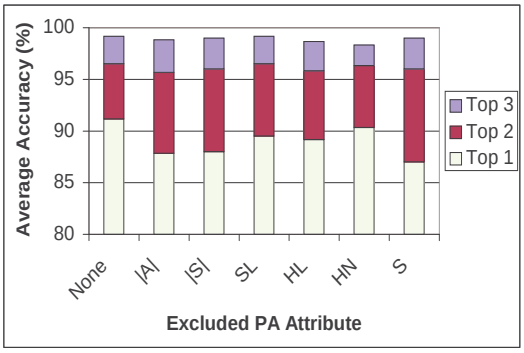

Figure 6.9: Importance of each PA attribute.

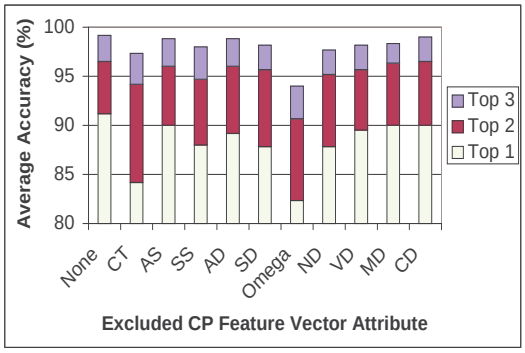

Figure 6.10: Importance of each CP feature vector attribute.

6.5.4 ProtClass vs ProtDex2

Although ProtClass also uses a CP feature vector representation as in the ProtDex2 method, it is not a trivial extension of ProtDex2. In particular:

1. ProtClass is a two-tier system using the PA representation in the upper tier and the CPset representation in the lower tier. On the other hand, ProtDex2 is a single-tier system using the hash table of CPs. ProtClass is a filter-and-refine system whereas ProtDex2 is not one by itself (although it can be used as a filtering tool in conjunction with any existing detailed comparison method).

2. The scoring function of ProtClass is a coarse one designed just enough to be able to recognize a few nearest neighbors with respect to the query. ProtDex2's scoring function is more detailed and designed to identify a number of proteins that are both closely and distantly related to the query.

3. Being a classification system, ProtClass need to know the class labels of the database proteins in advance, and utilize these class labels. In contrast, being a mere database search system, ProtDex2 neither need nor utilize any class label.

6.6 Conclusion

Nowadays, due to the high throughput methods in 3D protein structure determination, several tens of new protein structures are deposited into the structural databases such as PDB. Biologists naturally want to classify these new structures into their appropriate structural classes. But, both the manual class assignment systems (such as SCOP) and detailed alignment-based classification systems (such as DALI) becomes inefficient because of the large volume of the data involved. Thus, we are in need of a method that can quickly and effectively classify a newly determined structure into its appropriate structural class.

In this chapter, we have presented a new automatic scheme for protein structure classification. Our system is a dedicated classifier without requiring a costly

structural comparison process. The experimental results shows that our method is both accurate and efficient. We have proved its usefulness on a data set with 600 proteins belonging to 15 SCOP Folds. It is very much faster than the traditional structural alignment-based classification with the DALI method whilst only slightly less accurate. In comparison with two other purpose-built structural classification systems named SGM and CPMine, our method is much faster as well as more accurate.

Finally, we believe our scheme can become a useful tool for rapid structural classification in the age of very large and rapidly growing protein structure databases.

CHAPTER 7

Protein–Protein Interface Clustering

Summary

In this chapter, we present a new method to encode, cluster and analyze the similar 3D interface patterns among various protein complexes. We represent the protein–protein interfaces as 2D residue–residue interface matrices, and encode them as multi-dimensional feature vectors. Then, we cluster the interfaces using these feature vectors, and analyze the resultant clusters by various means. Experimental results show that we can discover a number of statistically significant clusters of interfaces. A visual inspection also confirms that the interfaces that fall into the same cluster are visually similar. We can find out the clusters of similar interface patterns in the protein complexes belonging to diverse structural fold types. We can also discover in some clusters the recurring interface patterns associated with biologically important functional motifs. Furthermore, we compare our method with the sequence-only clustering approach, and observe that ours is much better in terms of the statistical significance of the resultant clusters.

7.1 Introduction

Like structural classification discussed in the previous chapter, structural clustering is another instance of protein structure categorization. The aim of clustering is to organize a given set of objects in an orderly manner in such a way that the objects that are close to each other are in the same clusters, whilst those that are far apart are in different clusters. By definition, it is unsupervised learning in that we do not know the class or cluster labels of all the objects *a priori*; but rather we try to generate these labels [HK05].

In protein structure context, we try to organize the protein structures sharing common structural characteristics into their respective clusters. There are well-established and quite popular clustering methods such as FSSP [HS94a] for clustering protein chains, and DDD [HS98] for clustering protein domains. Therefore, we do not intend to build another protein chain or domain clustering system, but focus on a relatively less studied area of clustering protein–protein interfaces.

Any protein rarely acts alone, but rather interacts with other proteins to perform a specific function. The study of protein–protein interactions (PPI) is an important field in bioinformatics. We can acquire comprehensive knowledge on the biological functioning of cells by studying the interactions of proteins. This knowledge can be applied in many real-life applications such as drug discovery.

In this chapter, we study the 3D *protein complexes* which are formed by the interactions of proteins. In these complexes, we focus on the regions called *protein–protein interfaces* (or simply *interfaces*) where interacting proteins come in contact. We propose a method named PICluster (**P**rotein–Protein **I**nterface **Cluster**er) for finding the statistically significant clusters (groups) of interfaces.

We represent each interface as a 2D matrix of the center–center distances of AA residues that are in contact. From all the interfaces available, we choose a non-redundant set of them based on the sequence identity of their parent proteins. Then, we represent each non-redundant interface as a multi-dimensional feature vector based on the frequency of the types of submatrices they contain. The feature vector representation is designed in such a way that the similarity between the two

vectors can well reflect the structural similarity between their original interfaces. Finally, we cluster (group) these non-redundant interfaces based on their feature vector similarities.

From this study, we obtain a number of clusters each containing the interfaces that are structurally similar to each other. We ensure the quality of these clusters both by means of statistical analysis and visual verification. We also conduct a biological analysis on the clusters which results in some important findings. We discover that some interface clusters are strongly associated with the well-known motifs of important biological functions.

We also discover in many instances that the structurally similar interfaces in a same cluster sometimes belong to the parent proteins which are structurally diverse. This may probably be a clue to the existence of similar protein functions among the various structural fold types, because the interface portion of a protein is more responsible for its function than its other portions.

In addition, we highlight the usefulness of our method by comparing it against the clustering of interfaces by the AA sequence information alone. We find out that our method can detect a large number of clusters that the sequence-based method fail to detect.

7.2 Definitions

7.2.1 General Definitions

Naturally, the interacting proteins are close to each other in a cell. The co-occurring interacting proteins are usually collectively crystallized into their 3D formats as a single group, deposited as a single entity into PDB [BWF$^+$00] database, and given a unique PDB ID. Such a group of interacting proteins is referred to as a *protein complex*. The member proteins of a protein complex are called *protein chains* or *polymer chains* or simply *chains*. (See Section 2.2 for more details.)

Within a particular complex, each chain is assigned a unique chain ID. Many of the complexes are made up of only 2 or 3 chains, but some complexes contain a

large number of chains up to 60. In a protein complex, any pair of protein chains that are directly interacting with each other can be referred to as an *interacting pair*. For an interacting pair, there usually exists an *interface* region through which they actually interact. The chains between which an interface occur are named the *parent* chains of that interface.

For example, in Figure 7.1, the protein complex "gamma delta resolvase" is designated with the PDB ID `2rsl`. It has three protein chains which are assigned the chain IDs A, B, and C. Chain A of `2rsl` is referred to as `2rslA`, and so on. In this complex, there are direct interactions between chains A and B, and between chains B and C respectively. Thus, we have two interacting pairs which can be denoted as `2rslAB` and `2rslBC` [TLWN96]. (There is no direct interaction between chains A and C, and hence, `2rslAC` is not an interacting pair.) The interface for each interacting pair is highlighted in the figure. The interface for `2rslAB` is encoded as $I_{2rsl}(A, B)$, and that of `2rslBC` as $I_{2rsl}(B, C)$. A and B are the parent chains for $I_{2rsl}(A, B)$, and B and C are for $I_{2rsl}(B, C)$.

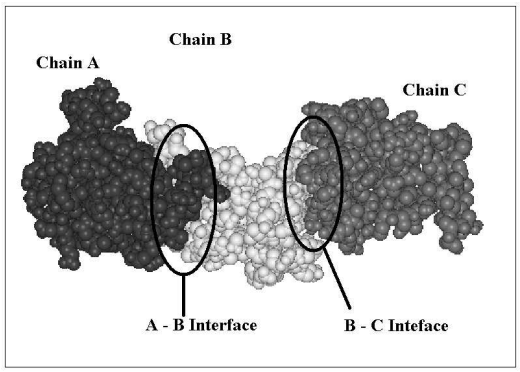

Figure 7.1: The protein complex *gamma delta resolvase* (PDB ID `2rsl`) with three protein chains A, B and C.

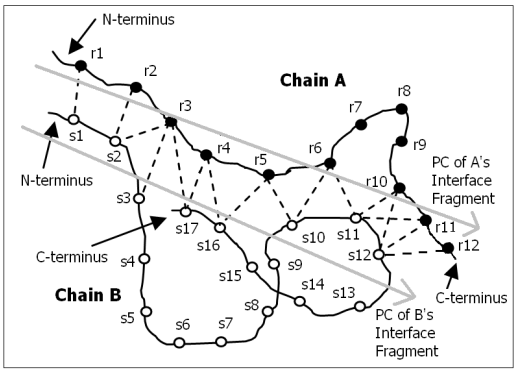

Figure 7.2: Example protein complex p with chains A and B. The dotted lines means that the two residues are in contact.

It should be noted that not all the direct protein interactions (and hence the interfaces) are pairwise in nature. In some protein complexes, there are interface regions where more than two chains come into contact. However, in our study, we divide these triple, quadruple, or higher interfaces into multiple pairwise interfaces,

for the sake of simplicity.

Now, we will formally define the terms and their symbols that are used throughout this chapter. We will also illustrate these terms with an example.

7.2.2 Interface

Let p denote a *protein complex*, and A and B the *chains* within p. Let $\{r_1, \ldots, r_{|A|}\}$ be the set of AA residues in A, where r_1 is the N-terminus residue and $r_{|A|}$ is the C-terminus residue. Similarly, let $\{s_1, s_2, \ldots, s_{|B|}\}$ be the set of AA residues in B. Let $3DDist(\bullet, \bullet)$ be the *Euclidean distance* function between any two points in 3D space.

Definition 7.1 *Contact of AA residues*
A residue r_i $(1 \leq i \leq |A|)$ *from chain* A *and a residue* s_j $(1 \leq j \leq |B|)$ *from chain* B *are in* contact*, if and only if there exists at least one pair of atoms* $(u \in r_i, v \in s_j)$ *such that* $3DDist(u, v) \leq 5$Å*.*
If r_i *and* s_j *are in contact, it is denoted as* $Contact(r_i, s_j)$*. If not, it is denoted as* $\neg Contact(r_i, s_j)$*.*

The distance threshold value 5Å is also mentioned as a default value in other studies such as [BDH+03, DBG+03, TLWN96]. Now, let us define an *interface* $I_p(A, B)$ between chains A and B of protein complex p as a *nonempty* set of pairs as follows:

$$I_p(A,B) = \{\, (r_i, s_j) \mid r_i \in A\,(1 \leq i \leq |A|) \quad \text{and} \quad s_j \in B\,(1 \leq j \leq |B|) \quad \text{such that} \quad Contact(r_i, s_j)\,\} \tag{7.1}$$

It should be noted that the set $I_p(A, B)$ can be regarded as an interface if and only if it is nonempty. For interface $I_p(A, B)$, its parent protein chain pair pAB can be defined as an *interacting pair*.

7.2.3 Interface Fragment

Let $F_p(A)$ be the set of all AA residues from chain A that participate in interface $I_p(A, B)$. We call $F_p(A)$ an *interface fragment* which is defined as:

$$F_p(A) = \{r_i \in A \mid (r_i, s_j) \in I_p(A, B) \text{ for any } s_j \in B\}$$

$F_p(A)$ is an *ordered set* in which the member AA residues are arranged by their positions along its spatial *principle component (PC)* vector. (Since the residues in an interface are not always sequential in nature, arranging them by their sequence order does not always make sense. It is observed that the PC vector ordering gives more biologically relevant results than the sequential ordering.)

The PC vector is generated by the *principle component analysis* of the spatial (x, y, z) coordinates of the member residues in $F_p(A)$. (Principle component analysis is a process of finding the general orientation of a set of points in a vector space. The detailed algorithm on it can be found in [MH87].) Now, we can rewrite $F_p(A)$ as:

$$F_p(A) = \{r_{i_1}, r_{i_2}, \ldots, r_{i_{|F_p(A)|}}\} \quad \text{where} \quad pos(r_{i_k}) \leq pos(r_{i_{k+1}}) \quad \text{for } 1 \leq k < |F_p(A)|$$

where $pos(\bullet)$ is the position of a residue along the PC vector of the interface fragment it belongs to. For simplicity, we will rewrite $F_p(A)$ again as:

$$F_p(A) = \{a_1, a_2, \ldots, a_{|F_p(A)|}\} \quad \text{where} \quad (a_k \equiv r_{i_k}, \quad 1 \leq k \leq |F_p(A)|) \tag{7.2}$$

In the same way, we can also define the interface fragment $F_p(B)$ for chain B as:

$$F_p(B) = \{b_1, b_2, \ldots, b_{|F_p(B)|}\} \tag{7.3}$$

It should be noted that an interface fragment is not necessarily contiguous, and the order of residues in it are not always from the N-terminus to the C-terminus.

7.2.4 Interface Matrix

Now let us define $rd(\bullet, \bullet)$ as the distance between the centers of two residues $a \in F_p(A)$ and $b \in F_p(B)$:

$$rd(a,b) = \begin{cases} 3DDist(a.center, b.center) & \text{if} \quad 3DDist(a.center, b.center) \leq 20\text{Å} \\ 20\text{Å} & \text{otherwise} \end{cases} \tag{7.4}$$

where *a.center* is the algebraic mean of the positions of all atoms in residue a, and *b.center* that of b. (The distances greater than 20Å are considered insignificant and just rounded off to 20Å. This cutoff value is also used in [CKK04].)

Definition 7.2 *Interface Matrix*
An interface matrix IM_{pAB} *representing the interface* $I_p(A,B)$ *in interacting pair* pAB *is a* $|F_p(A)| \times |F_p(B)|$ *matrix in which* $IM_{pAB}[i,j] \equiv rd(a_i, b_j)$ *(where* $1 \leq i \leq |F_p(A)|$ *and* $1 \leq j \leq |F_p(B)|$*).*
$|F_p(A)| \times |F_p(B)|$ *can be defined as the* interface size *of* IM_{pAB}*.*

An interface matrix is different from a normal distance matrix used in the previous chapters in that (1) it is asymmetrical, and (2) it stores the algebraic center–center distances of residues, rather than their C_α–C_α distances.

Let $IM_{pAB}^{\intercal}$ be the transposed matrix of IM_{pAB}. We can rewrite $IM_{pAB}^{\intercal}$ as IM_{pBA}. The transposed interface matrices are useful, because given two interacting pairs pAB and qXY, it may be the case that IM_{qXY} is compatible with IM_{pBA} rather than with IM_{pAB}.

7.2.5 Submatrix

The interface matrix can be cut into several overlapping square submatrices also known as sliding windows.

Definition 7.3 *Submatrix*
A submatrix $SM_{pAB}^{(i,j)}$ *is a square matrix of size* $w \times w$ *whose starting cell is* $IM_{pAB}[i,j]$ *of interface matrix* IM_{pAB} *where* $(1 \leq i + w - 1 \leq |F_p(A)|)$ *and* $(1 \leq j + w - 1 \leq |F_p(B)|)$.

Let $\mathcal{SM}_{pAB}$ be the *submatrix set* of IM_{pAB}, i.e. the set of all submatrices that belong to interface matrix IM_{pAB}.

$$\mathcal{SM}_{pAB} = \{SM_{pAB}^{(i,j)} \,|\, 1 \leq i \leq (|F_p(A)| - w + 1) \text{ and } 1 \leq j \leq (|F_p(B)| - w + 1)\} \quad (7.5)$$

The cardinality of submatrix set $\mathcal{SM}_{pAB}$ is $(|F_p(A)| - w + 1) \times (|F_p(B)| - w + 1)$.

The *submatrix distance* $sd(\bullet, \bullet)$ between any two submatrices $SM1$ and $SM2$ of size $w \times w$ can be calculated as:

$$sd(SM1, SM2) = \frac{\sqrt{\sum_{i=1}^{w} \sum_{j=1}^{w} (SM1[i,j] - SM2[i,j])^2}}{20 \cdot w} \quad (7.6)$$

where $20 \cdot w = \sqrt{\sum_{i=1}^{w} \sum_{j=1}^{w} (20 - 0)^2}$ is the maximum possible difference between the two extreme submatrices: one with all 20Å's and one with all 0Å's (although all 0Å's is actually infeasible in nature). Here $sd(\bullet, \bullet)$ can be regarded as an Euclidean distance in an $(w \times w)$-dimensional space normalized by the maximum possible distance in this space. Being based on Euclidean distance, $sd(\bullet, \bullet)$ has metric properties: isolation, symmetry and triangular inequality.

Now, let us define the *representative submatrix set* $\mathcal{SM}'$ given a submatrix set $\mathcal{SM}$ and a distance threshold sd_t:

$$\mathcal{SM}' = \{SM_i \in \mathcal{SM} \,|\, sd(SM_i\,,\, SM_j) > sd_t \quad \text{for any } SM_j \in \mathcal{SM}'\} \quad (7.7)$$

It means that all the members in $\mathcal{SM}'$ are at least sd_t distance apart from each other. So $\mathcal{SM}'$ forms a non-redundant set of submatrices that can roughly represent the overall distribution of the submatrices in $\mathcal{SM}$.

7.2.6 Nearest-Neighbor Clustering Algorithm

Clustering is an unsupervised machine learning procedure in which we try to generate the clusters/ groups of objects that are similar according to a particular

distance function. The aim of clustering is to put the objects that are close to each other in the same clusters, whilst those that are far apart in different clusters.

In this study, we use clustering in various places. We use the *threshold-based single-link nearest-neighbor clustering* algorithm as described in Figure 7.3. Our algorithm is inspired by a similar algorithm given in [Dun03]. (However, the two algorithms use different strategies on deciding the creation of new clusters.)

Given a distance threshold, we find the clusters, each of which contains the objects with distances among them not greater than the threshold. It is called *nearest-neighbor* algorithm because it assigns an object into a cluster to which it is the nearest. It is called a *single-link* algorithm because it chooses the nearest cluster by considering only the nearest member within this cluster (as opposed to the complete-link or the average-link approaches where all the members in a given cluster are taken into account [Dun03]).

For every object in the input data set, we allocate it to the cluster in which its nearest neighbor exists and all the other existing cluster members are also near enough to it, with regard to the given threshold. If we cannot detect such a cluster, we create a new cluster with this object as the first member. After allocating all objects into clusters, we find the cluster *medoids*. The medoids are the median objects of the clusters, where the total distance from each medoid to its peer cluster members is the smallest.

It should be noted that it is a heuristic algorithm, and the result may vary depending on the ordering of the input objects. The time complexity of the algorithm for $\mathcal{O}$ objects is $O(|\mathcal{O}|^2)$. But, we use some optimizations (such as early rejection of an object from a cluster by comparing it first to the extreme members in the cluster, etc.) in order to make it faster. (For simplicity, those optimizations are not shown in the algorithm.)

7.2.7 Illustration

As an example, let us consider an imaginary protein complex p with two chains A (with 12 residues represented as black circles) and B (with 17 residues represented

function $NNCluster(\mathcal{O}, d, d_t) \rightarrow (\mathcal{K}, \mathcal{H})$

input: (1) A set of objects $\mathcal{O} = \{o_1, o_2, \ldots, o_{|\mathcal{O}|}\}$

(2) Distance function $d(\bullet, \bullet)$

(3) Distance threshold d_t

output: (1) A set of clusters $\mathcal{K} = \{K_1, K_2, \ldots, K_{|\mathcal{K}|}\}$

(2) A set of cluster medoids $\mathcal{H} = \{h_1, h_2, \ldots, h_{|\mathcal{K}|}\}$

procedure:

/* Find clusters */

1. $k = 1$ /* initial number of clusters */
2. $K_1 = \{o_1\}, \quad \mathcal{K} = \{K_1\}$
3. `for` $i = 2$ `to` $|\mathcal{O}|$
4. $\quad min_d = \infty, \quad min_k = \infty$
5. $\quad$ `for each` $K_j \in \mathcal{K}$
6. $\quad\quad mindist = \min_{x \in K_j}(d(o_i, x))$
7. $\quad\quad maxdist = \max_{x \in K_j}(d(o_i, x))$
8. $\quad\quad$ `if` $(maxdist \leq d_t \wedge mindist < min_d)$ `then` $min_d = mindist$, $min_k = j$
9. $\quad$ `end for`
10. $\quad$ `if` $(min_d \neq \infty)$ `then` $K_{min_k} = K_{min_k} \cup \{o_i\}$ /* add into nearest cluster */
11. $\quad$ `else`
12. $\quad\quad k = k + 1$ /* increase the number of clusters */
13. $\quad\quad K_k = \{o_i\}, \quad \mathcal{K} = \mathcal{K} \cup \{K_k\}$ /* initialize new cluster */
14. $\quad$ `end if`
15. `end for`

/* Find cluster medoids */

16. $\mathcal{H} = \phi$
17. `for each` $K_j \in \mathcal{K}$
18. $\quad h_j = \arg\min_{x \in K_j}(\sum_{y \in K_j} d(x, y))$
19. $\quad \mathcal{H} = \mathcal{H} \cup \{h_j\}$
20. `end for`
21. `return` $(\mathcal{K}, \mathcal{H})$

Figure 7.3: Threshold-based nearest-neighbor clustering algorithm.

as white circles) as shown in Figure 7.2. That is, $A = \{r_1, r_2, \ldots, r_{12}\}$ and $B = \{s_1, s_2, \ldots, s_{17}\}$. Suppose a pair of residues connected by a dotted line are in contact (by Def. 7.1). Then, their interface $I_p(A, B)$, and interface fragments $F_p(A)$ and $F_p(B)$ will be:

$I_p(A, B) = \{(r_1, s_1), (r_2, s_2), (r_3, s_2), (r_3, s_3), (r_3, s_{17}), \ldots, (r_{11}, s_{12}), (r_{12}, s_{12})\}$ and

$F_p(A) = \{r_1, r_2, r_3, r_4, r_5, r_6, r_{10}, r_{11}, r_{12}\}$, $F_p(B) = \{s_1, s_2, s_3, s_{17}, s_{16}, s_{10}, s_{11}, s_{12}\}$

re-written as:

$F_p(A) = \{a_1, a_2, a_3, a_4, a_5, a_6, a_7, a_8, a_9\}, \quad F_p(B) = \{b_1, b_2, b_3, b_4, b_5, b_6, b_7, b_8\}$

Then, their interface matrix IM_{pAB} will be:

$$IM_{pAB} = \begin{pmatrix} rd(a_1, b_1) & rd(a_1, b_2) & \ldots & rd(a_1, b_8) \\ rd(a_2, b_1) & rd(a_2, b_2) & \ldots & rd(a_2, b_8) \\ \vdots & \vdots & \ddots & \vdots \\ rd(a_9, b_1) & rd(a_9, b_2) & \ldots & rd(a_9, b_8) \end{pmatrix}$$

The *interface size* of IM_{pAB} is $9 \times 8 = 72$.

Let us define 2×2 as the submatrix size. Then, the *submatrix set* $\mathcal{SM}_{pAB}$ will be

$$\mathcal{SM}_{pAB} = \{SM_{pAB}^{(1,1)}, \ldots, SM_{pAB}^{(1,7)}, \ldots, SM_{pAB}^{(8,1)}, \ldots, SM_{pAB}^{(8,7)}\}$$

Its size $|\mathcal{SM}_{pAB}| = (9 - 2 + 1) \times (8 - 2 + 1) = 56$.

As an example, let us choose two submatrices $SM_{pAB}^{(2,3)}$ and $SM_{pAB}^{(5,1)}$ which respectively are:

$$\begin{pmatrix} rd(a_2, b_3) & rd(a_2, b_4) \\ rd(a_3, b_3) & rd(a_3, b_4) \end{pmatrix} \quad \text{and} \quad \begin{pmatrix} rd(a_5, b_1) & rd(a_5, b_2) \\ rd(a_6, b_1) & rd(a_6, b_2) \end{pmatrix}$$

Then, their *submatrix distance* $sd(\bullet, \bullet)$ will be:

$$sd(SM_{pAB}^{(2,3)}, , SM_{pAB}^{(5,1)}) = \sqrt{(rd(a_2, b_3) - (a_5, b_1))^2 + \ldots + (rd(a_3, b_4) - rd(a_6, b_2))^2}$$

7.3 The PICluster Method

In this section, we will describe the detailed procedures we follow in the PICluster method in order to discover the clusters/groups of similar protein–protein interfaces. The three steps undertaken are:

1. Selecting representative interfaces from PDB and representing them as interface matrices.

2. Generating feature vectors for the representative interface matrices.

3. Clustering the interface feature vectors (and hence the original interfaces).

Step 1 is illustrated in Figure 7.4. Steps 2 and 3 are illustrated in Figure 7.5. (Step 2 is in turn elaborated in Figure 7.6.)

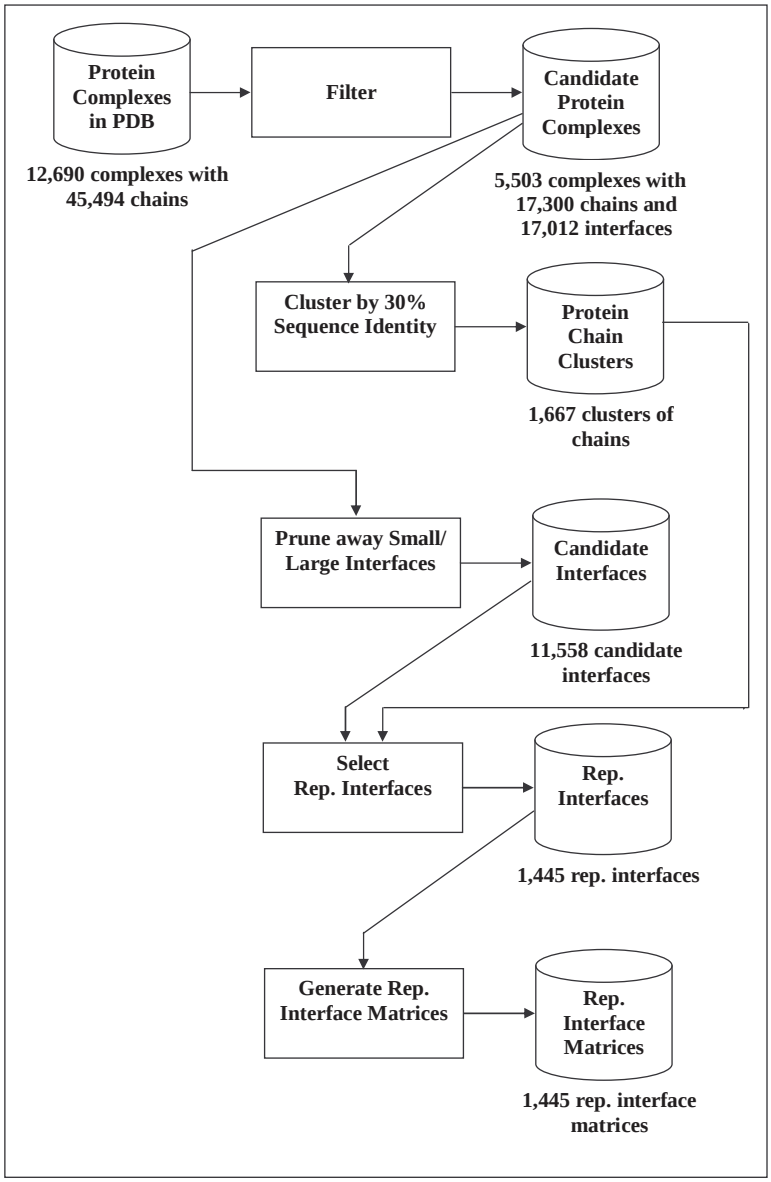

Figure 7.4: Generating representative interfaces.

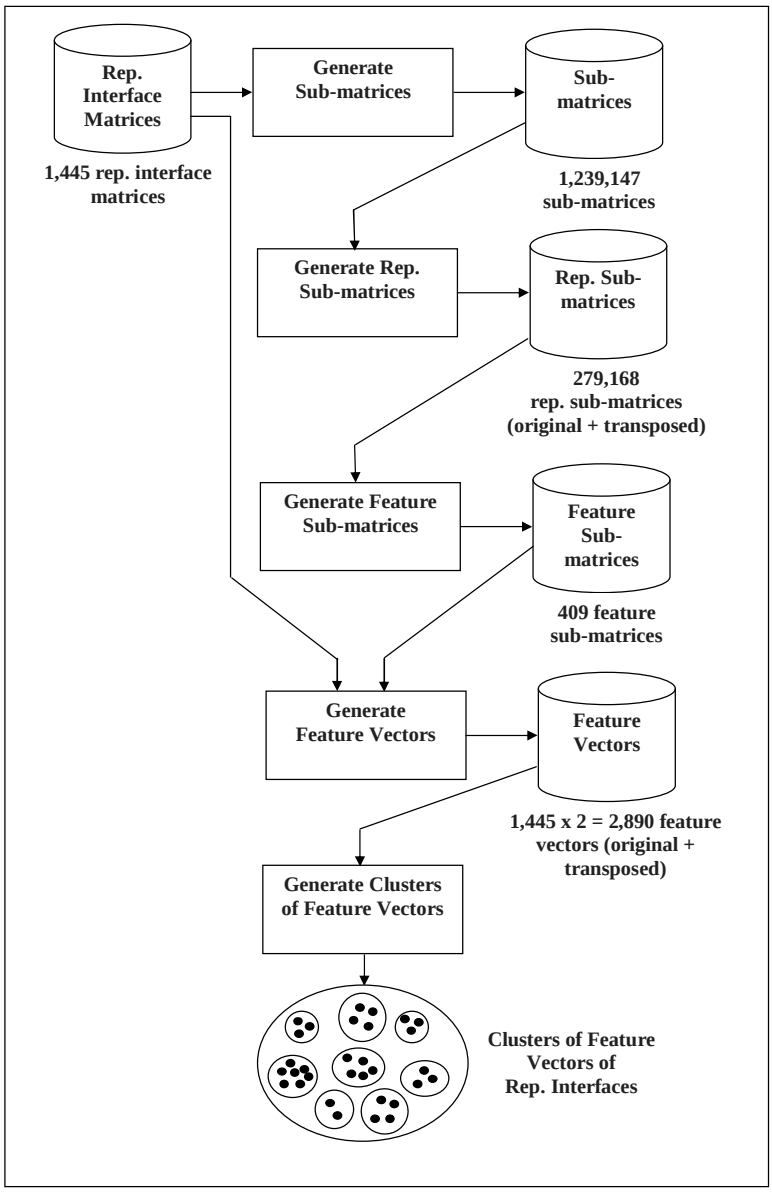

Figure 7.5: Clustering representative interfaces. (The first four steps are elaborated in Figure 7.6.)

7.3.1 Selecting Representative Interfaces from PDB

In this study we use the 3D protein complexes from PDB database [BWF+00] downloaded in July 2004. The database contains 25,882 entries among which 12,690 are protein complexes or protein–nucleic acid complexes. (From here onwards, we will also refer to the protein–nucleic acid complexes as protein complexes for simplicity.) The others are single-chain proteins, nucleic acids and carbohydrate structures, and we do not use them.

There are 45,494 protein chains belonging to the 12,690 complexes. Among these chains, we remove ones which are not suitable for our studies. These include C_α only chains, the chains with less than 10 amino acids, the chains that are not annotated in SCOP [HAB+97] database (version 1.65), the ones that belong to more than one family in SCOP (such as multi-domain chains), the ones with resolution higher than 3Å, etc. In this way, we have our clean data set of 17,300 protein chains which belongs to 5,503 protein complexes.

Then, we cluster these chains with BLAST [AGM+90] using 30% sequence identity threshold. This results in 1,667 groups (clusters) of chains where any two given proteins in a same group have more than 30% amino acid sequence identity, and those in different groups have the sequence identity of less than or equal to 30%. We choose this threshold value because the proteins with less than or equal to 30% sequence identity are assumed to be in "twilight zone" [Ros99] where no significant structural relationships among them can be inferred from their sequence similarity. This enables us to carry out a study of interfaces based on their structural similarity alone.

For a protein complex with n chains, there are $\binom{n}{2}$ possible pairs of chains. But in this study, we only take into account the *interacting pairs*, each of which has an *interface* between its constituent chains. In our data set of 5,503 protein complexes, there are 37,793 possible pairs of chains. Among them, only 17,012 are the interacting pairs, each forming an interface.

From those 17,012 interfaces, we prune away ones whose *interface fragments* are too short, with less than 10 residues, or too long, with more than 200 residues. This fragment length cutoff value 10 is also used in [KTWN04, TLWN96]. This prunes away 5,434 and 20 interfaces respectively. Thus, 11,558 interfaces remain.

Among these remaining interfaces, we choose the non-redundant *representative interfaces*. Two interfaces $I_p(A, B)$ from protein complex p and $I_q(X, Y)$ from protein complex q are considered to be redundant if A and X belong to a same group (with at least 30% sequence identity by BLAST), and B and Y belong to a same group. Alternatively, they are considered redundant if A and Y belong

to a same group, and B and X belong to a same group. From more than one redundant interfaces, we choose the one with the best resolution as the representative interface. (The smaller a resolution, the better it is. We give preference to the X-ray structures than the NMR structures.) In case of equal resolutions, we choose the one with the largest *interface size*. In this way, we come up with $1,445$ representative interfaces.

According to the observations in [TLWN96], the residues that constitute an interface are not always sequential in nature. So, arranging them according to their sequential order from the N-terminus to the C-terminus of the chain may not make sense. Thus, for the two interface fragments in an interface, we derive their respective principle component (PC) vectors by means of principle component analysis [MH87]. Then, we arrange the residues in each interface fragment by their positions along its PC vector as described in Section 7.2.3.

After that, we represent these representative interfaces as *interface matrices*, which stores the distances between the residue pairs, each from each interface fragment. Thus, we have $1,445$ *representative interface matrices* for $1,445$ representative interfaces. Representing an interface as a 2D interface matrix can capture the "interface pattern" of the interface fragments very well. Thus, processing the interface matrix as a single entity means processing its two constituent interface fragments simultaneously. This overcomes the weakness of the methods [KTWN04, SPNW04, TLWN96] that handle the two interface fragments separately.

7.3.2 Generating Interface Feature Vectors

Our objective is to group "similar" interface matrices into their respective clusters. So, we have to compare the interface matrices and determine the similarity values somehow. We cannot use the traditional structural alignment tools in this case, because they only deal with the 3D structures, and not the 2D matrices.

One option is to use DALI method [HS93] which carries out 3D structural comparison by means of aligning 2D distance matrices. But, unfortunately, DALI is

known to be a time consuming pairwise alignment method, and it may take a very long time to align $1,445$ interface matrices all-against-all. Moreover, unless specifically modified, the original DALI method cannot directly handle asymmetrical matrices like the interface matrix.

So, we look forward to a scheme in which we can encode and compare the interface matrices both efficiently and effectively. We opt for a scheme where we can represent each interface matrix as a multi-dimensional feature vector based on the frequencies of the "local features" that exhibit in the interface matrix. Then, we can simply compare the feature vectors representing two interface matrices, and determine their similarity in a very short time. Such a frequency-based approach has been extensively used in various histogram methods in the area of image processing [ZIB01]. Recently, it has also been used in the area of structural bioinformatics [CP02, CKK04].

The basic idea is to represent an interface matrix as a "bit-vector" where each bit corresponds to the presence or absence of a single type of submatrix which constitute the whole interface matrix. However, for all $1,445$ interface matrices, there are over one million submatrix types. If we use them all, our resultant bit-vector will be too long. So, we have to reduce the number of submatrix types to be used by grouping the similar ones together and selecting a representative submatrix from each group. This is done by two clustering processes: first to choose the representative submatrices from each individual interface matrix, and second to choose the higher-level representatives of the representative submatrices from all interface matrices. Finally, we can derive the *feature vector* of each interface matrix by fusing together the higher-level representative submatrices (named *feature submatrices*) that they contain.

The process of generating feature vectors from the representative interface matrices is outlined in Figure 7.6. The details of the process are described in detail in the following sub-sections.

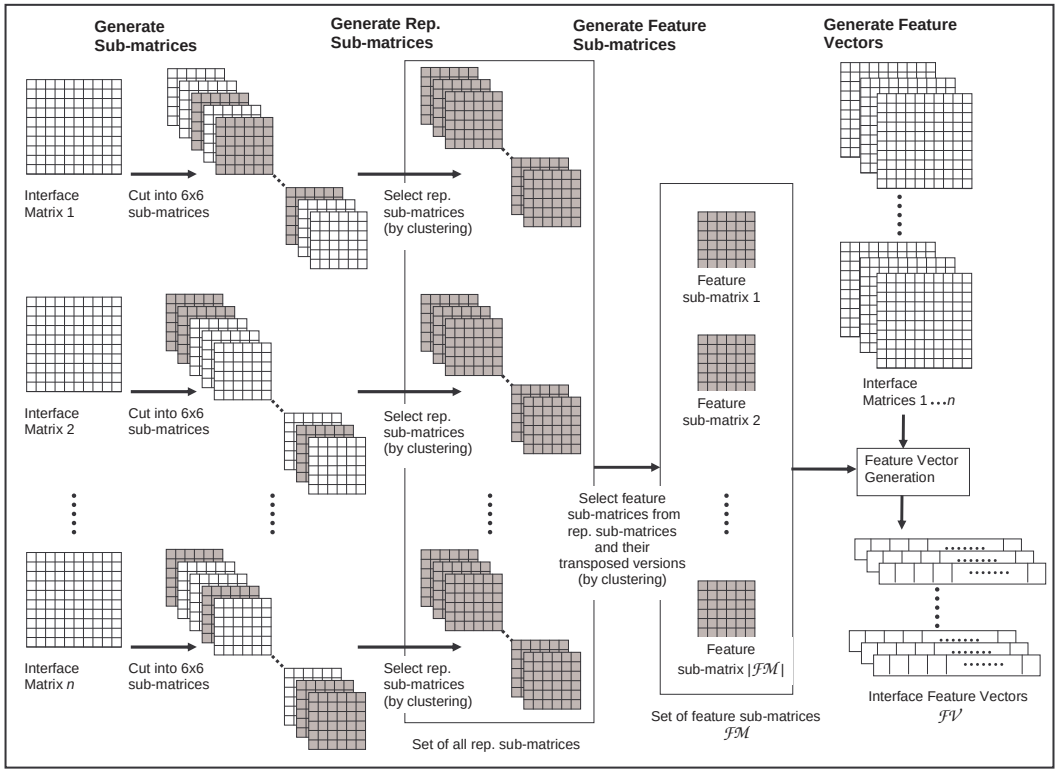

Figure 7.6: Generating feature vectors from representative interface matrices. Representative submatrices for each representative interface matrix are shown in gray.

Feature Submatrices

We cut each interface matrix into several overlapping fixed-size *submatrices* of size $w \times w$, and store them in a *submatrix set*. (We use $w = 6$ in this study. This is small enough to enable efficient processing, but still large enough to capture the distinct local patterns in interfaces. The fixed matrix size 6 was also used previously in [AFT03, HS93].) An interface matrix of size $m \times n$ has $(m-w+1) \times (n-w+1)$ submatrices. We have a total of $1,239,147$ submatrices from $1,445$ representative interface matrices.

Our objective is to select a small number of *feature submatrices*, which will later be used to encode the feature vectors of the interface matrices, from all these submatrices. Since we have to use an expensive quadratic-time clustering algorithm for this feature submatrix selection, it will take a very long time if we process all these $1,239,147$ submatrices per se.

So, as an intermediate step, we derive the *representative submatrix set* from

each *submatrix set* of an interface matrix. We apply the *nearest-neighbor clustering* algorithm as described in Section 7.2.6. We use the submatrix distance threshold value 0.2, and take the *medoids* generated by the algorithm as the representative set. More precisely, for a submatrix set $\mathcal{SM}$, we invoke the clustering function given in Figure 7.3 as follows:

$$(\texttt{NULL},\ \mathcal{SM}') \leftarrow \mathit{NNCluster}\,(\mathcal{SM},\ \mathit{sd},\ 0.2)$$

where $\mathit{sd}(\bullet, \bullet)$ is the *submatrix distance* function (Eq.7.6), and $\mathcal{SM}'$ is the output representative set. We use `NULL` for the first output parameter, because we do not need the clusters themselves, but only their medoids. We set the threshold $sd_t = 0.2$ in order to yield a reasonable number of representative submatrices. If we set this threshold value too low, we will still get a large number of representative submatrices to be processed in the next step. On the other hand, if we set this threshold value too high, we may probably miss some important submatrices.

After clustering, we have $139,584$ representative submatrices from $1,239,147$ submatrices belonging to $1,445$ representative interface matrices.

Let us denote $\mathcal{TM}$ as the set of all representative submatrices and their transposed counterparts from all the representative interface matrices.

$$\mathcal{TM} = (\mathcal{SM}'_1 \cup \mathcal{SM}'_2 \cup \ldots \cup \mathcal{SM}'_n) \cup (\mathcal{SM}'^{\mathrm{T}}_1 \cup \mathcal{SM}'^{\mathrm{T}}_2 \cup \ldots \cup \mathcal{SM}'^{\mathrm{T}}_n) \tag{7.8}$$

where $n = 1,445$ is the number of all representative interface matrices. We add the transposed submatrices into $\mathcal{TM}$ as well, because we also want to analyze the transposed interface matrices later. Thus, we have $139,584 \times 2 = 279,168$ representative submatrices.

Now, we select the *feature submatrices* that we will use to encode our interface matrices in the next step. Let us define $\mathcal{FM}$ be the set of feature submatrices. We can derive $\mathcal{FM}$ from $\mathcal{TM}$. In this instance, we can assume $\mathcal{TM}$ as a submatrix set and $\mathcal{FM}$ as a representative submatrix set, and use the same clustering function:

$$(\texttt{NULL},\ \mathcal{FM}) \leftarrow \mathit{NNCluster}\,(\mathcal{TM},\ \mathit{sd},\ \mathit{sd}_f)$$

where sd_f is the distance threshold for the feature submatrices. We set $sd_f = 0.35$ which results in $|\mathcal{FM}| = 409$. (We will show the effects of different sd_f values in

Section 7.4.5.) We will treat $\mathcal{FM}$ as an array, with $\mathcal{FM}[j]$ as the j^{th} element of $\mathcal{FM}$ $(1 \leq j \leq |\mathcal{FM}|)$.

Feature Vectors

Now, we will first encode each interface matrix as a *frequency vector*. The dimension of the frequency vector is equal to the feature submatrix set's size $|\mathcal{FM}|$. Basically, it is the frequency profile of feature submatrices in the interface matrix. For every submatrix in the interface matrix, we find its nearest feature submatrix, and increase the frequency value of this feature submatrix's dimension. Let us denote the frequency vector for interface matrix IM_{pAB} as FQ_{pAB}. The j^{th} dimension of FQ_{pAB} can be formally defined as:

$$\begin{aligned} FQ_{pAB}[j] = \; & card(\{\, SM_k \in \mathcal{SM}_{pAB} \mid \\ & sd(SM_k, \mathcal{FM}[j]) < sd(SM_k, \mathcal{FM}[j']) \quad \text{for all } j' \neq j \,\}) \end{aligned} \tag{7.9}$$

where $card(\bullet)$ is the function to count the number of elements in a set.

Now, let us denote the set $\mathcal{FQ}$ of all frequency vectors of n representative interface matrices and their transposed counterparts as:

$$\mathcal{FQ} = \{\, FQ_1, FQ_2, \ldots, FQ_n \,,\, FQ_{1^{\mathrm{T}}}, FQ_{2^{\mathrm{T}}}, \ldots, FQ_{n^{\mathrm{T}}} \,\} \tag{7.10}$$

where FQ_i is the frequency vector of i^{th} representative interface matrix, and $FQ_{i^{\mathrm{T}}}$ is that of its transposed counterpart. Here $|\mathcal{FQ}| = 2n$.

After we have $2n$ frequency vectors in $\mathcal{FQ}$, we can derive their *interface feature vectors*. An interface feature vector is a frequency vector normalized by the maximum frequencies for each dimensions. Let FV_i be the interface feature vector for i^{th} representative interface matrix. Its j^{th} dimension will be:

$$FV_i[j] = FQ_i[j] \,/\, (\max_{FQ_k[j] \in \mathcal{FQ}[j]} FQ_k[j]) \tag{7.11}$$

where $\mathcal{FQ}[j]$ is the set of all elements in j^{th} dimension of $\mathcal{FQ}$.

Finally, we can define the set $\mathcal{FV}$ of feature vectors for all n representative interface matrices and their transposed counterparts as:

$$\mathcal{FV} = \{\, FV_1, FV_2, \ldots, FV_n, FV_{1^{\mathrm{T}}}, FV_{2^{\mathrm{T}}}, \ldots, FV_{n^{\mathrm{T}}} \,\}$$

For simplicity, let us denote FV_{i^T} as FV_{i+n}. We can rewrite $\mathcal{FV}$ as:

$$\mathcal{FV} = \{ FV_1, FV_2, \ldots, FV_n, FV_{n+1}, FV_{n+2}, \ldots, FV_{2n}\} \tag{7.12}$$

7.3.3 Clustering Interface Feature Vectors

As the final step, we will now assign the representative interfaces into their appropriate groups based on the similarities of their respective interface feature vectors.

For any two feature vectors FV_i and FV_j, we can measure their *feature vector distance* with the inverse cosine distance function $df(\bullet, \bullet)$ [ZIB01] which can be defined as:

$$df(FV_j, FV_j) = \cos^{-1} \frac{FV_i \cdot FV_j}{\parallel FV_i \parallel \cdot \parallel FV_j \parallel} \tag{7.13}$$

where $(\bullet \cdot \bullet)$ is the dot product between two vectors, and $(\parallel \bullet \parallel)$ is the norm of a vector. Although $df(\bullet, \bullet)$ is a non-metric distance (as it violates the triangular inequality property), it still can reflect the human perceptions of similarity and non-similarity [ZIB01]. We have also tested our system with the metric Euclidean distance function, but found out that the inverse cosine distance function is superior. (Comparisons are not shown in here.)

Now, we can create the clusters of interface feature vectors on the data set $\mathcal{FV}$ using distance function $df(\bullet, \bullet)$ and distance threshold df_t with the clustering function:

$$(\mathcal{C}, \mathcal{M}) \leftarrow NNCluster(\mathcal{FV}, df, df_t)$$

where $\mathcal{C} = \{C_1, \ldots, C_{|\mathcal{C}|}\}$ is the set of output clusters, and $\mathcal{M} = \{m_1, \ldots, m_{|\mathcal{C}|}\}$ is the set of output cluster medoids. We will show the effects of different df_t values in Section 7.4.

We can logically map the clusters and the medoids of interface feature vectors back into those of the original interface matrices. It should be noted that the resultant clusters include both the representative interface matrices and their transposed versions. However this is still meaningful. For example, a particular cluster may include the interface matrices IM_{pAB} and IM_{qXY} and another cluster may include the interface matrices IM_{pBA} and IM_{rEF}. It means that IM_{pAB}

is compatible with IM_{qXY}, and IM_{pBA} is compatible with IM_{rEF}. But IM_{qXY} and IM_{rEF} are not compatible. However, if a particular interface matrix and its transposed version both belong to a same cluster, only the one closer to the cluster medoid is kept, and the other is discarded.

7.4 Results and Discussions

We analyze the quality of the interface clusters we have found both by means of statistical analysis and visual verification. Furthermore, we also analyze the biological significance of the clusters.

7.4.1 Statistical Analysis

We conduct a statistical test called *silhouette analysis* [KR90] to ensure the quality of the interface clusters we have found. In this analysis, the *silhouette width* $s(i)$ of an object i is defined as:

$$s(i) = \frac{b(i) - a(i)}{\max(\, a(i), b(i)\,)} \tag{7.14}$$

where $a(i)$ is the average distance of i to all other objects in its own cluster, and $b(i)$ is the average distance of i to all objects in its nearest neighbor cluster. A silhouette width lies between -1 (the worst case) and $+1$ (the ideal case). The *average silhouette width* $\overline{s}$ of a clustering scheme is simply calculated as the average of the silhouette widths of all the members in all clusters. The larger the value of $\overline{s}$, the better the clustering scheme.

We can observe in Figures 7.7 and 7.8 that as the distance threshold df_t increases, the number of clusters decreases, so does the total number of members in all clusters. (As we prune away either an original interface or its transposed version if they fall under a same cluster, the total number of member interfaces in all clusters is not always equal to the total number of original unclustered interfaces and their transposed ones, that is, $2n = 2,890$.) Among the set of clusters found, there exist some clusters with only one member each. Obviously, these single-member

clusters does not carry much useful information. So, we emphasize on the clusters with at least two members. The number of such clusters and that of the members in them are also shown in Figures 7.7 and 7.8.

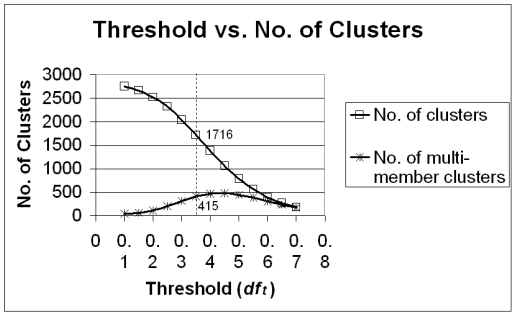

Figure 7.7: Feature vector distance threshold df_t versus the number of clusters found.

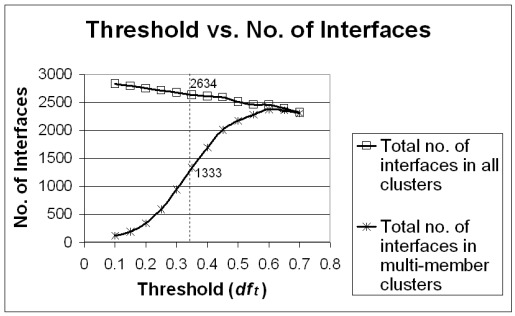

Figure 7.8: Feature vector distance threshold df_t versus the number of interfaces in clusters.

We can also observe the effect of varying distance threshold df_t values on the average silhouette width ($\overline{s}$) of the clustering scheme as in Figure 7.9. The lower df_t values correspond to the high $\overline{s}$ values, which means that some high-quality clusters have been found. However, as can be seen in Figure 7.8, with the lower df_t values, we can yield only a few interfaces belonging to the "interesting" *multi-member clusters* which include at least two members. A large number of the remaining interfaces just form the uninteresting single-member clusters.

So, we have to tradeoff the $\overline{s}$ value and the coverage of the interesting clusters. Our criterion is that at least half of the total number of interfaces must be covered by the interesting clusters with at least two members. Thus, we set $df_t = 0.35$, which covers 50.6% of interfaces in the clusters. This corresponds to the $\overline{s}$ value of 0.85 if all the clusters are taken into account, and 0.58 if only the clusters with at least two members are taken into account. According to the interpretations given in [KR90], if the $\overline{s}$ value of a particular clustering scheme is between 0.5 and 0.7, a reasonable clustering structure has been found. Since we have the $\overline{s}$ value of at least 0.58, we can statistically assure that we have discovered the interface clusters with a reasonable quality.

With $df_t = 0.35$, we have 415 multi-member clusters. Among them, the clusters

with only 2 members are the most abundant. There are 260 such clusters. There are 79 clusters with 3 members. Subsequently, clusters with larger number of members generally become less and less frequent. The frequencies of the clusters of different sizes are shown in Figure 7.10.

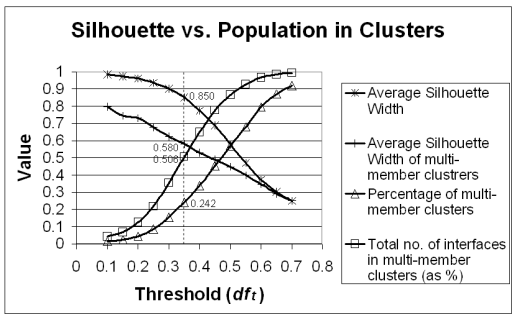

Figure 7.9: Feature vector distance threshold df_t versus the average silhouette width.

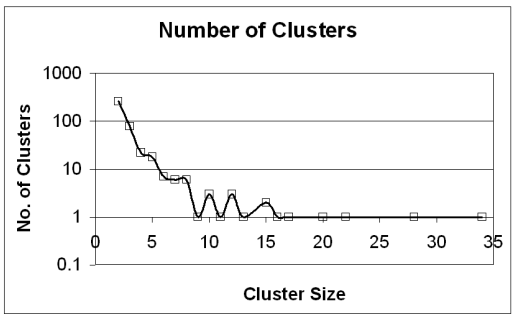

Figure 7.10: Distribution of number of clusters for various cluster sizes.

7.4.2 Visual Verification

In addition to the silhouette analysis, we inspect the quality of the interface clusters visually. It is observed that the interfaces belonging to a same cluster generally look similar. In Figure 7.11, we show a few sample interfaces in some types of clusters. The interfaces are represented as interface matrices, which are depicted as gray-scale images. The darker tones indicates the smaller residue-residue distances in an interface, and the lighter tones the larger distances.

7.4.3 Biological Significance of Clusters

In this sub-section, we will discuss the biological significance of the interface clusters we have obtained.

Structural Diversity of Interfaces' Parent Chains

When looking into the interface clusters, we can notice the similar interfaces belonging to the similar parent chains. However, such a finding can be regarded as

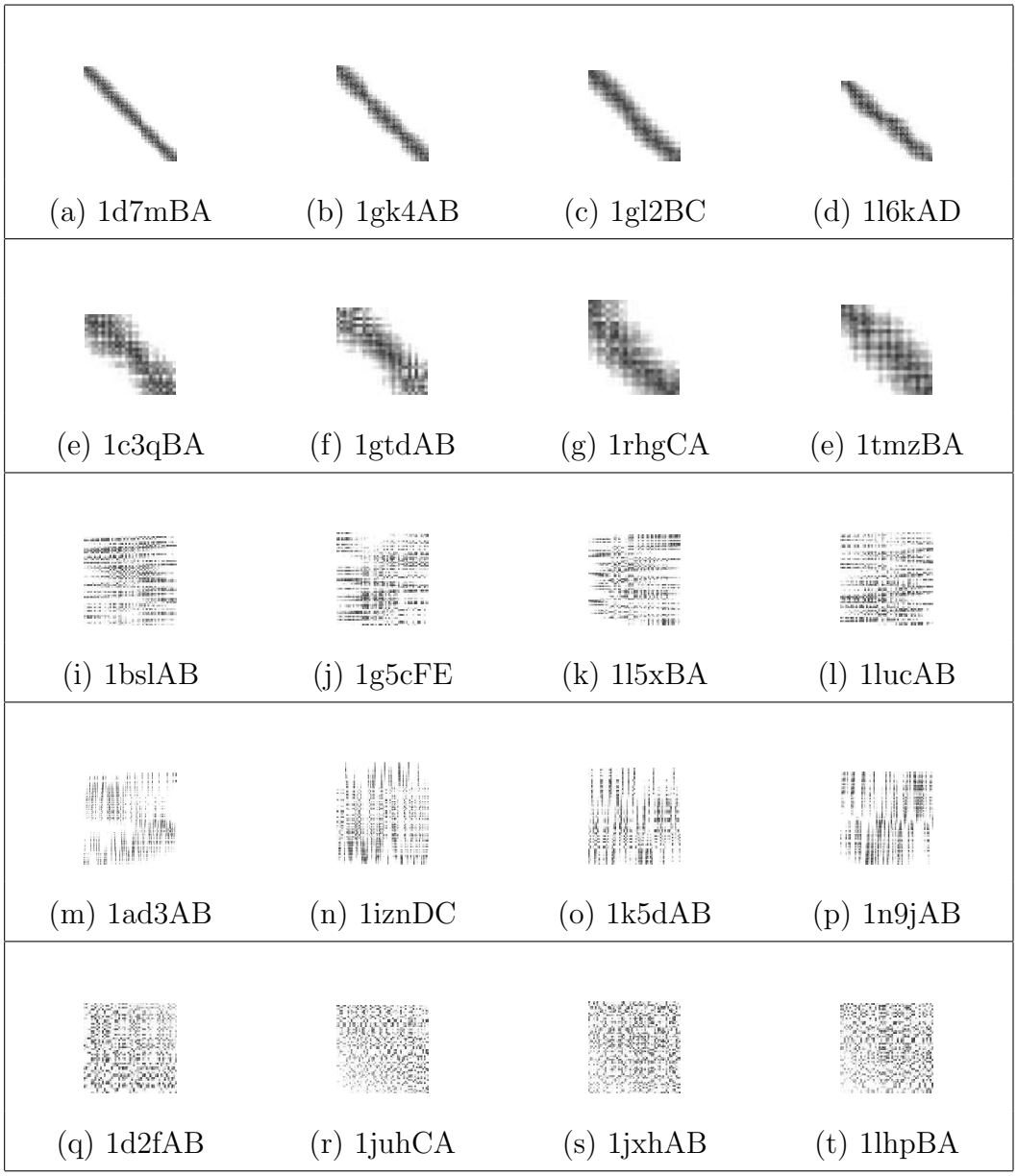

Figure 7.11: Examples of some similar interface shapes (represented as interface matrices) belonging to the clusters of their kinds respectively: (a)–(d) thin diagonals, (e)–(h) thick diagonals, (i)–(l) horizontal ripples, (m)–(p) vertical ripples, and (q)–(t) sparse patterns.

trivial. What is more exciting is the discovery of the similar interfaces whose parent chains are quite different. We have found a surprisingly large number of such interfaces.

For example, let us consider an interacting pair `1kacAB` of protein complex `1kac` (*The λ Repressor C-Terminal Domain Octamer*) and `1mbxCA` of protein complex

1mbx (*ClpSN with Transition Metal Ion Bound*) as shown in Figure 7.12. For simplicity, the interfaces are shown as space-filled structures whilst the remaining parts of the chains are shown as wire frames.

It is observed that while the interface structures of 1kacAB and 1mbxCA are quite similar, their parent chain structures are very different. 1kacA belongs to Fold b.21 according to SCOP structural annotation system. Similarly, 1kacB belongs to Fold b.1, 1mbxC to Fold d.45, and 1mbxA to Fold a.174. In other words, 1mbxCA belongs to the parent *Fold pair* b.21–b.1, and 1mbxCA belongs to the parent Fold-pair d.45–a.174.

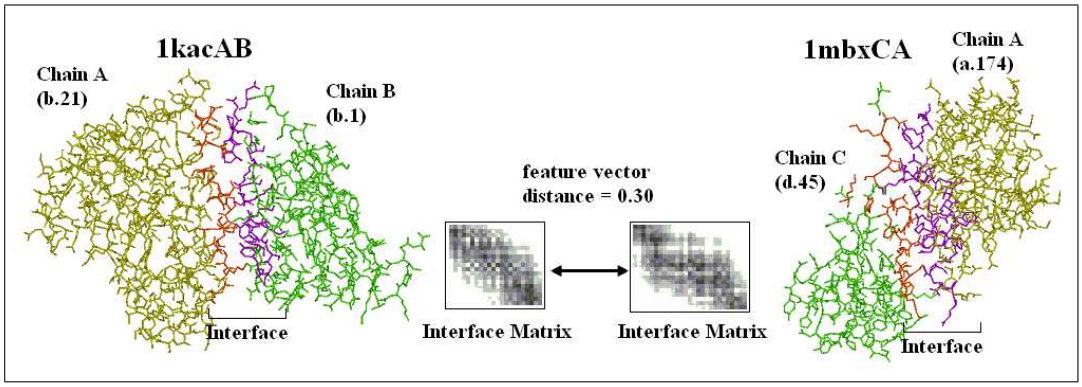

Figure 7.12: Similar interfaces in different protein complexes.

We can measure the diversity of a given interface cluster C with its Fold pair-based *entropy value* [Sha48], donated $Ent(C)$, which is defined as:

$$Ent(C) = \sum_{i=1}^{k} -p_i \times \lg p_i \tag{7.15}$$

where k is the total number of distinct parent Fold pairs that the interfaces in cluster C belongs to, and p_i is the proportion of C belonging to a particular Fold pair i.

For example, if we have a cluster C with 6 interfaces, where 3 of them belongs to the parent Fold pair a.1–a.1, 2 to b.1–b.1, and 1 to a.1–b.1 respectively, the entropy value of C is:

$$Ent(C) = (-\frac{3}{5} \times \lg \frac{3}{5}) + (-\frac{2}{5} \times \lg \frac{2}{5}) + (-\frac{1}{5} \times \lg \frac{1}{5}) = 1.435$$

In the ideal case when a cluster is totally homogeneous (i.e. all interfaces in the cluster belongs to a single Fold pair), its entropy value will be: $-\frac{n}{n} \times \lg \frac{n}{n} = 0$, where n is the number of members in the cluster. On the other hand, if a cluster is totally diverse (i.e. each member interface belongs to a distinct Fold pair from the others), its entropy value will be: $n \times (-\frac{1}{n} \times \lg \frac{1}{n}) = \lg(n)$.

The average entropy values for the different cluster sizes are given in Figure 7.13. We also show two reference curves for the ideal (zero) and the maximum entropy cases in the figure. We can observe that the entropy values for the interface clusters we have found are generally close to the maximum values. Thus, we can infer that we discover the clusters of structurally similar interfaces belonging to the parent proteins whose overall structures are very diverse.

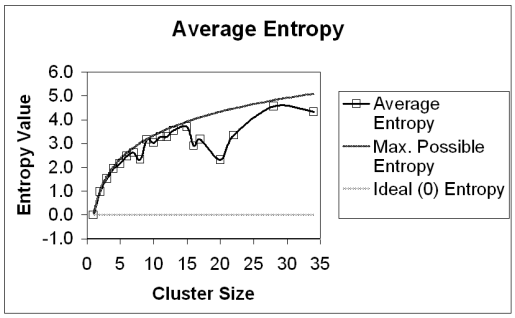

Figure 7.13: Average entropies for different cluster sizes.

Discovery of Important Biological Motifs

Overall, the average entropy of each cluster is 1.37. The result indicates that similar interfaces are mediating interactions among different structural fold types and raise the question of whether these interfaces are basic interaction framework preserved during evolution while proteins adopted diverse functionality through different structural conformations. These recurring interfaces could also arise spontaneously during evolution. Regardless of the cases, these interface clusters represent favorable binding structural scaffolds that had been reused in nature for interactions. An application is to use these interface clusters for identifying putative binding sites on proteins of known structures [PEB+04]. These interfaces

could also facilitate studies on the critical residues [BT98, HMWN00] and motifs [LFNW01, TXN97] important for the stability of protein–protein interactions.

In general, the interfaces tend to be compact (each interface fragment contains an average of 30.81 residues). This is significant biologically as it implies that large surface complementary between two structures is not an essential prerequisite for interactions. Instead, interactions can also be mediated by short recurring interfaces. Identified interface clusters could be used to detect possible interactions among proteins with known structures [AGK05, FPVC02], as a supplementary to existing protein docking approaches.

To further assess the significance of the clusters derived, we attempt to identify known linear binding motifs (expressed commonly in regular expression) from our clusters. First, for each cluster, we derive two sets of interface residue sequences that are sequential in 3D space after PCA transformation. Note that these interface residues may not be continuous or sequential in primary sequences. For example in Figure 7.2, the derived interface residue sequence for chain B is $\{s_1, s_2, s_3, s_{17}, s_{16}, s_{10}, s_{11}, s_{12}\}$ instead of $\{s_1, s_2, s_3, s_{10}, s_{11}, s_{12}, s_{16}, s_{17}\}$. Then we attempt to match a set of binding motifs extracted from biomedical literature and *ELM database* [PLG$^+$03] to these derived interface sequences. The most significant matches are listed in Table 7.1. Motifs are expressed as regular expression where "x" represent any amino acid. For matched interface sequences, the chain ID and the corresponding amino acid numberings in PDB are given. The odd-ratio is calculated as O/E where O is observed occurrence of linear motif in the cluster, and E is occurrence of linear motif expected by random in the cluster.

Among the clusters, we identified many helix-helix interactions and manage to found the common **AxxxA** [KGME02, RE00] helix-helix interaction motifs in our derived sequences. We also identified the popular **PxxP** binding motif [DFGB$^+$03] found numerously in various signaling pathways in one of our clusters. This indicates that we able to cluster interfaces that contain similar biologically significant interaction motifs.

On visual inspection, we identified many cases where our interface residue se-

quences which are not continuous and not sequential in primary sequences are matched by known linear binding motifs. This is interesting because linear sequence motifs, by definition, occur as a continuous sequence segment but we had found instances where the residues from different parts of a protein chain that had come together spatially to mimic some known linear binding motifs. For example, Figure 7.14 shown two interface residue sequences in one cluster that come together spatially to resemble **KPxx[QK]** linear motif (ELM ID: LIG_SH3_4).

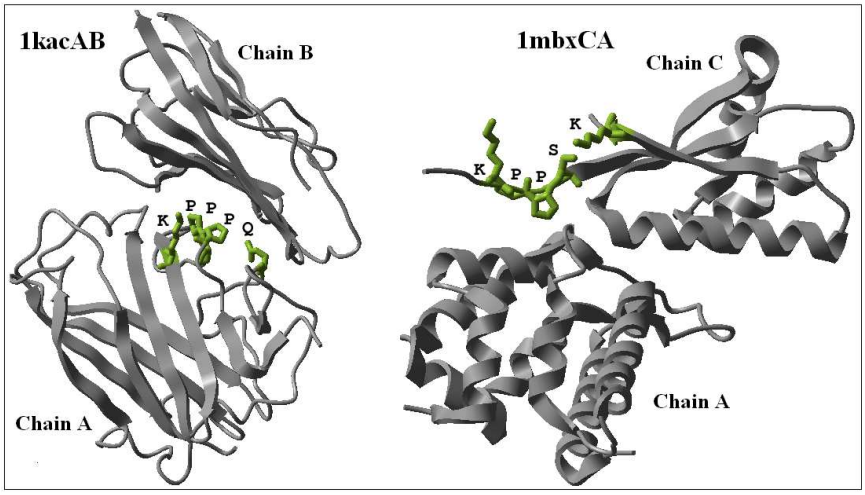

Figure 7.14: Conservation of motif **KPxx[QK]** in a particular interface cluster. (Images are rendered with Molsoft ICM-Browser [ABC+97].)

Figure 7.15 shown another example of interface residues that come down to resemble another known linear motif (**RxLx[EQ]**) [PL04]. In this example, both sets of residues seem to form a similar interface that interacts with an α-helix. Thus, in our analysis, we had shown here that foldings of protein chains can be combined to yield similar motifs, some which resemble known linear sequence motifs. This observation hinted that many reported biologically important linear motifs could occur more frequently than expected. For example, the **RxLx[EQ]** motif which attribute to the virulency of malarial parasite, *P. falciparum*, in human was found in 250 to 350 of the parasite proteins by primary sequence match [PL04]. The actual number of proteins containing the motif could be more based on what had been observed in this work. This analysis also suggests that it is possible to derive linear sequences motifs from derived interface residue sequences for further inter-

action studies. Such linear sequence motifs will be important for identifying short binding peptides for interaction studies and drug discovery.

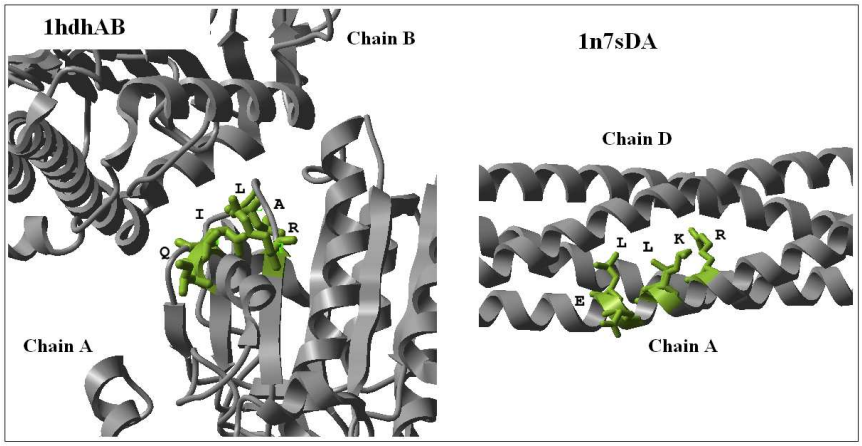

Figure 7.15: Conservation of motif **RxLx[EQ]** in a particular interface cluster. (Images are rendered with Molsoft ICM-Browser [ABC+97].)

7.4.4 Comparison with Sequence-Only Analysis

As mentioned before, taking the structural data into account in the studies of proteins can give us the information of high quality though relatively limited in quantity. We compare the quality of the interface clusters found by our scheme against that of the clusters found by a scheme which takes only the sequence information into account, and find out that our scheme is clearly better.

In this sequence-only scheme, we try to find the interface clusters based on the sequence identity distance, which is the inverse of the average of sequence identity scores of the corresponding interface fragment pairs. The sequence identity score of a pair of AA sequences is the ratio of the number of identical residues to the total number of aligned residues. We use Needleman and Wunsch global sequence alignment algorithm [NW71, SM97], with affine gap model using BLOSUM 50 matrix and open gap penalty of -10 and gap symbol penalty of -2, in order to find the aligned residues. These are the default parameters used for SSEARCH (Smith and Waterman's Search [SW81]) service in FASTA web server (`http://fasta.bioch.virginia.edu/`).

Table 7.1: Significant matches between known linear binding motifs and clusters of interface sequences.

Linear Binding Motif	Matched Interface Sequences	Odd-Ratio	Refs
KPxx[QK]	1kacA $\mathbf{K}_{429}\mathbf{P}_{418}\mathbf{P}_{417}\mathbf{P}_{416}\mathbf{Q}_{487}$ 1mbxC $\mathbf{K}_{23}\mathbf{P}_{24}\mathbf{P}_{25}\mathbf{S}_{26}\mathbf{K}_{105}$	150.76	LIG_SH3_4 [PLG$^+$03]
RxLx[EQ]	1n7sA $\mathbf{R}_{56}\mathbf{K}_{59}\mathbf{L}_{60}\mathbf{L}_{63}\mathbf{E}_{62}$ 1hdhA $\mathbf{R}_{390}\mathbf{A}_{38}\mathbf{L}_{394}\mathbf{I}_{37}\mathbf{Q}_{397}$	66.70	[PL04]
RGD	1bslA $\mathbf{R}_{115}\mathbf{G}_{50}\mathbf{D}_{18}$ 1bouA $\mathbf{R}_{127}\mathbf{G}_{126}\mathbf{D}_{19}$	64.94	LIG_RGD [PLG$^+$03]
L[IVLMF]x[IVLMF][DE]	1lm8V $\mathbf{L}_{178}\mathbf{I}_{180}\mathbf{S}_{183}\mathbf{L}_{184}\mathbf{D}_{187}$ 1b79A $\mathbf{L}_{96}\mathbf{L}_{83}\mathbf{A}_{87}\mathbf{I}_{84}\mathbf{E}_{91}$	28.14	LIG_Clathr_ClatBox_1 [PLG$^+$03]
PxxP	1nkzE $\mathbf{P}_{12}\mathbf{A}_{13}\mathbf{I}_{16}\mathbf{P}_{17}$ 1ix2A $\mathbf{P}_{52}\mathbf{K}_{38}\mathbf{R}_{86}\mathbf{P}_{94}$	27.56	[RCGRA$^+$04]
[VILMAFP]KxE	1hqgC $\mathbf{V}_{203}\mathbf{K}_{205}\mathbf{D}_{204}\mathbf{E}_{256}$ 1rypI $\mathbf{V}_{195}\mathbf{K}_{29}\mathbf{A}_{27}\mathbf{E}_{197}$	15.05	MOD_SUMO par[PLG$^+$03]
[PSAT]x[QE]E	1kacB $\mathbf{A}_{127}\mathbf{P}_{128}\mathbf{Q}_{52}\mathbf{E}_{50}$ 1mbxA $\mathbf{P}_{80}\mathbf{F}_{24}\mathbf{Q}_{79}\mathbf{E}_{23}$	19.10	LIG_TRAF2_1 [PLG$^+$03]
AxxxA	1svfC $\mathbf{A}_{179}\mathbf{V}_{175}\mathbf{H}_{171}\mathbf{V}_{168}\mathbf{A}_{167}$ 1svfC $\mathbf{A}_{164}\mathbf{T}_{163}\mathbf{L}_{161}\mathbf{S}_{160}\mathbf{A}_{157}$ 1svfC $\mathbf{A}_{157}\mathbf{Q}_{156}\mathbf{V}_{154}\mathbf{D}_{153}\mathbf{A}_{150}$ 1svfC $\mathbf{A}_{149}\mathbf{T}_{147}\mathbf{K}_{146}\mathbf{I}_{144}\mathbf{A}_{143}$ 1svfC $\mathbf{A}_{143}\mathbf{N}_{142}\mathbf{L}_{140}\mathbf{N}_{139}\mathbf{A}_{136}$ 1gl2B $\mathbf{A}_{213}\mathbf{H}_{216}\mathbf{V}_{217}\mathbf{Q}_{219}\mathbf{A}_{220}$ 1gl2B $\mathbf{A}_{220}\mathbf{N}_{221}\mathbf{Q}_{223}\mathbf{L}_{224}\mathbf{A}_{227}$ 1bgyE $\mathbf{A}_{48}\mathbf{G}_{46}\mathbf{V}_{45}\mathbf{T}_{44}\mathbf{A}_{41}$ 1gmjC $\mathbf{A}_{21}\mathbf{K}_{24}\mathbf{G}_{23}\mathbf{Q}_{27}\mathbf{A}_{28}$ 1n7sB $\mathbf{A}_{240}\mathbf{Y}_{243}\mathbf{V}_{244}\mathbf{R}_{246}\mathbf{A}_{247}$ 1n7sB $\mathbf{A}_{247}\mathbf{T}_{251}\mathbf{D}_{250}\mathbf{K}_{253}\mathbf{A}_{254}$ 1bkvB $\mathbf{A}_{47}\mathbf{L}_{46}\mathbf{G}_{45}\mathbf{R}_{44}\mathbf{A}_{43}$ 1bkvB $\mathbf{A}_{48}\mathbf{D}_{49}\mathbf{N}_{45}\mathbf{A}_{44}\mathbf{A}_{42}$ 1bkvB $\mathbf{A}_{41}\mathbf{K}_{38}\mathbf{A}_{37}\mathbf{Q}_{35}\mathbf{A}_{24}$ 1bkvB $\mathbf{A}_{37}\mathbf{Q}_{35}\mathbf{A}_{34}\mathbf{R}_{31}\mathbf{A}_{30}$ 1bkvB $\mathbf{A}_{34}\mathbf{R}_{31}\mathbf{A}_{30}\mathbf{N}_{28}\mathbf{A}_{27}$ 1bkvB $\mathbf{A}_{30}\mathbf{N}_{28}\mathbf{A}_{27}\mathbf{S}_{24}\mathbf{A}_{23}$ 1bkvB $\mathbf{A}_{23}\mathbf{A}_{20}\mathbf{D}_{21}\mathbf{N}_{17}\mathbf{A}_{16}$ 1bkvB $\mathbf{A}_{20}\mathbf{D}_{21}\mathbf{N}_{17}\mathbf{A}_{16}\mathbf{A}_{13}$ 1bkvB $\mathbf{A}_{16}\mathbf{A}_{13}\mathbf{Q}_{14}\mathbf{S}_{10}\mathbf{A}_{9}$ 1bkvB $\mathbf{A}_{13}\mathbf{Q}_{14}\mathbf{S}_{10}\mathbf{A}_{9}\mathbf{A}_{6}$ 1ek9B $\mathbf{A}_{336}\mathbf{S}_{339}\mathbf{S}_{340}\mathbf{Y}_{334}\mathbf{A}_{343}$ 1ek9B $\mathbf{A}_{343}\mathbf{A}_{347}\mathbf{Q}_{346}\mathbf{T}_{378}\mathbf{A}_{351}$	6.81	[KGME02]

As described in Section 7.3.1, in our study, we use only the representative interfaces with the chains having less than 30% sequence identity to each other. Hence, the interface fragments in these chains also do not have significant sequence similarities to each other. As a result, we cannot find any significant clusters when

we try to cluster the interfaces based on their sequence identity distance. We can only achieve the very low average silhouette width ($\overline{s}$) values as shown in Figure 7.16.

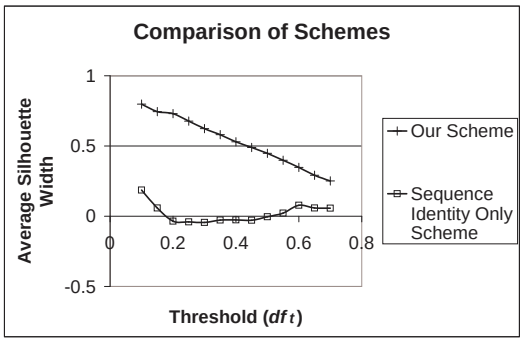

Figure 7.16: Comparison of our clustering scheme against the clustering scheme by sequence identity only.

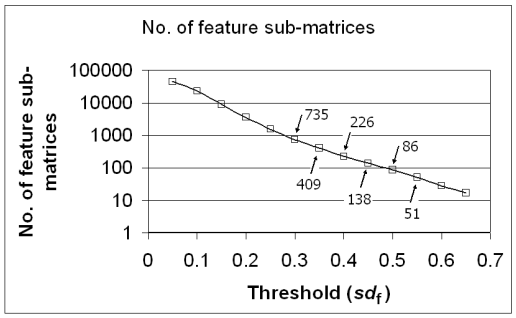

Figure 7.17: Effect of various values of feature submatrix distance threshold (sd_f).

7.4.5 Effect of Different sd_f Values

The value of the feature submatrix threshold (sd_f) determines the dimension of the feature vector that we use to represent an interface matrix, as described in Section 7.3.2. We show the different number of feature submatrices (i.e. the dimension of feature vector) for the different sd_f values in Figure 7.17.

The dimension of the interface feature vector in turns affects the quality of the interface clusters we found. We choose $sd_f = 0.35$, which results in 409 dimensions, as the optimal value because it can provide the best average silhouette width ($\overline{s}$) values.

7.4.6 PICluster vs Other Methods

Now, we will highlight the similarities and differences between PICluster and the other existing protein–protein interface clustering methods.

1. The main contribution of our work is that we quantitative analyze the resultant interface clusters, and can confirm that they are statistically significant.

According to [HKK05], such an analysis and confirmation is highly desirable for all biological data clustering systems (including interface clustering). To our knowledge, none of the existing interface clustering method report the statistical significance of its clusters.

2. In PICluster, we only use the pure geometrical properties (based on distance measures) of interfaces — as opposed to using other physco-chemical properties such as hydrophobicity, packing, hydrogen bonds, and disulfide bonds. PICluster is similar to [KTWN04, TLWN96], and different from [DS05, LCCJ99, MSPWN05, SPMNW04] in this respect.

   In our opinion, the geometrical shape is the most important factor in inferring the functions of proteins. In other words, "function follows form" [Ros96]. Although there is no doubt that these physco-chemical properties are the driving forces in determining the final 3D shapes of the interfaces (and more generally the entire structures) of proteins, we believe they may be of little use in further determining their structural similarities, and deducing their functions. (A similar observation can be made in the field of ordinary protein structure comparison. The mainstream methods such as DALI [HS93], CE [SB98], VAST [GMB96], and SSAP [TO89] focus only on the pure geometrical properties, such as distance and angles, of protein structures rather than their physico-chemical properties. Although there are some methods that incorporate physico-chemical properties into structural comparison [LMPP04, SKK98, OAA03], this approach is not widely adopted.)

3. We analyze the two interacting protein fragments on an interface simultaneously and synchronously (by using interface matrix representation), rather than analyzing them separately. For this aspect, PICluster is similar to the methods like [DS05, MSPWN05, SPMNW04], but dissimilar to [KTWN04, SPNW04, TLWN96].

4. Since we use an easy-to-handle multi-dimensional vector representation of the interfaces, we can compare a considerable number of interfaces in all-

against-all fashion within a relatively short time, as opposed to the structural alignment-based methods which may take a tremendously long time for such an all-against-all comparison. PICluster shares the same characteristics with [DS05, MW03] with respect to this feature, unlike [SPMNW04, TLWN96].

Anyhow, we cannot directly compare our proposed PICluster method against the existing interface clustering methods because their source codes or software are not public available. Although their resultant sets of clusters are published online, these cannot be analyzed statistically because the interface–interface similarity values are not reported. Moreover, in this area of protein–protein interface studies, there is no widely accepted standard benchmark (like SCOP and CATH in protein classification area) to compare the performances of the different methods objectively.

7.5 Conclusion

In this chapter we have presented a scheme for representing and clustering a relatively large number of protein–protein interfaces of the protein complexes. We have discovered quite a number of interface clusters which are biologically significant. Firstly, we have found a number of very similar interface structures belonging to the protein complexes from different structural fold types. This indicates the full or partial functional similarities among diverse protein complexes. Secondly, we have found the highly conserved motifs of well-known biological functions in some of the interface clusters. We hope our discovery can somehow contribute useful knowledge to real-life applications such as drug design.

CHAPTER 8

Conclusion and Future Work

8.1 Conclusion

Computational studies of 3D protein structures plays an important role in bioinformatics. In this thesis, we have presented the four methods to accomplish the four different, yet somewhat related, tasks in the area of protein structure studies, viz, structural alignment, database search, classification and clustering.

For protein structure alignment, we have come up with a method for detailed structural alignment based on aligning the distance profiles. Our experimental results show that, in a majority of cases, our method can offer better alternative alignments to those of the commonly used methods. In particular, we can find the tighter albeit slightly shorter alignments, which means that our method can detect the conserved cores.

For rapid searching on large structural databases, we have proposed the use of indexing and information retrieval (IR) strategies. The experimental results confirm that our approach is both efficient and effective. Our system can be ideally used as a filtering tool before a more detailed alignment process.

For protein structure classification, we have developed a nearest-neighbor classification system incorporated with active learning. We have highlighted that the

classification problem is different from the ordinary structural comparison and database searching problems, and should be treated differently. Our experimental results show that our filter-and-refine, abstract representation, and coarse scoring schemes are well-suited for our classification purpose.

For clustering of protein–protein interfaces, we have proposed an easy-to-handle feature vector representation based on the sub-structures of interfaces. We have confirmed the reliability of the resultant clusters by statistical validation and visual inspection. We have also demonstrated the usefulness of the clusters by a biological analysis in which we can rediscover some well-known biological motifs from the clusters.

8.2 Future Work

In this section, we discuss the possible improvements in the performances and usability of the methods reported in the previous chapters. We also outline some related problems that we might try to solve as our future research directions.

In order to improve the run time efficiency of the MatAlign method proposed in Chapter 4, we plan to implement it as a parallel system. Because of its simple nature, MatAlign is easy to be parallelized. Since most of its running time is incurred in all-against-all alignments of the distance profiles (rows) in distance matrices, we can assign these independent row–row alignment tasks to a number of processors, and execute them concurrently. We also plan to test MatAlign on a larger data set, and tune its various parameters (cell–cell distance thresholds, bandwidth, cutoff distance for row reduction, etc.) in order to ensure a generally good performance for any arbitrary pair of protein structures.

As for the ProtDex2 method reported in Chapter 5, we plan to work on the updating of the inverted index after the new protein structures are added. The current system does not support such an update, and requires to rebuild the index when the new structures are added in batches.

For the ProtClass method presented in Chapter 6, we have a plan to assess the

general behavior of our scheme by trying it with a greater number of training and testing proteins taken from a larger number of structural classes, and fine-tune the required parameters accordingly. We also would like to look for the better strategies for PA representation, CPset representation, and filtration so as to further improve the system's speed as well as its accuracy.

To further improve the usability of PICluster and its resultant clusters (Chapter 7), we plan to perform some more biological data analyses on the clusters in addition to the ones reported in this thesis. For example, we might study the entropies of the parent protein complexes' EC (Enzyme Commission) numbers and GO (Gene Ontology) annotations. We will also try to carry out the clustering of interfaces based on the detailed interface–interface alignment method using a modified version of MatAlign in a distributed computing environment (as in [MSPWN05]). We hope we can achieve better clustering results by doing so.

In addition to upgrading the existing methods, we have a plan to extend our research into the other related areas in structural bioinformatics. It is possible to solve the *protein threading* (sequence–structure alignment) problem by using our pairwise structural alignment algorithm as a basic component. We also plan to use some portions of both of our structural alignment and structural database search algorithms in developing a method for *homology modeling* (predicting the 3D structure of a protein from its AA sequence and the 3D structures of its sequence homologs) and *model validation* (checking the resultant model). Finally, we hope to utilize all of our expertise and knowledge in the various areas of structural bioinformatics with a view to developing a method for *ab initio structural prediction* (predicting a 3D protein structure directly from its AA sequence without an additional input), which is one of the most important problems remaining unsolved in the field of bioinformatics.

Furthermore, we ultimately plan to incorporate our methodologies in protein structure analysis into a larger bioinformatics consortium enabling a joint learning from multiple types of genomic data: sequences, structures, micro-arrays, protein–protein interaction networks, metabolic pathways, etc. From such a joint explo-

ration system, we hope to acquire a comprehensive knowledge on the functioning of life, and exploit this knowledge in intelligent drug design, bioengineering, food engineering, etc., to being about the benefits for mankind.

BIBLIOGRAPHY

[ABC+97] R. A. Abagyan, S. Batalov, T. Cardozo, M. Totrov, and Y. Zhou. Homology modeling with ICM: deformation zone mapping and improvements of models via conformational search. *Proteins: Structure, Function, and Genetics*, Suppl. 1:29–37, 1997. `http://www.molsoft.com/icm_browser.html`.

[AF96] N. N. Alexandrov and D. Fischer. Analysis of topological and nontopological structural similarities in the PDB: new examples with old structures. *Proteins: Structure, Function, and Genetics*, 25(3):354–365, 1996.

[AFT03] Z. Aung, W. Fu, and K. L. Tan. An efficient index-based protein structure database searching method. In *Proceedings of 8th International Conference on Database System for Advanced Applications (DASFAA'03)*, pages 311–318, 2003.

[AGK05] A. S. Aytuna, A. Gursoy, and O. Keskin. Prediction of protein–protein interactions by combining structure and sequence conservation in protein interfaces. *Bioinformatics*, 21(12):2850–2855, 2005.

[AGM+90] S. F. Altschul, W. Gish, W. Miller, E. W. Meyers, and D. J. Lipman. Basic local alignment search tool. *Journal of Molecular Biology*,

215(3):403–410, 1990.

[AHB87] K. Arun, T. Huang, and S. Blostein. Least-squares fitting of two 3-D point sets. *IEEE Transactions on Pattern Analysis and Machine Intelligence*, 9(5):698–700, 1987.

[AKKS99] M. Ankerst, G. Kastenmüller, H. P. Kriegel, and T. Seidl. 3D shape histograms for similarity search and classification in spatial databases. In *Proceedings of 6th International Symposium on Spatial Databases (SSD'99)*, pages 207–226, 1999.

[Aku95] T. Akutsu. Protein structure alignment using a graph matching technique. In *Proceedings of Genome Informatics Workshop (GIW'95)*, pages 1–8, 1995.

[AS03] N. Alexandrov and I. Shindyalov. PDP: protein domain parser. *Bioinformatics*, 19(3):429–30, 2003.

[AT04a] Z. Aung and K. L. Tan. Automatic protein structure classification through structural fingerprinting. In *Proceedings of 4th IEEE Symposium on Bioinformatics and Bioengineering (BIBE'04)*, pages 508–515, 2004.

[AT04b] Z. Aung and K. L. Tan. Rapid 3D protein structure database searching using information retrieval techniques. *Bioinformatics*, 20(7):1045–1052, 2004.

[AT05] Z. Aung and K. L. Tan. Automatic 3D protein structure classification without structural alignment. *Journal of Computational Biology*, 12(9):1221–1241, 2005.

[AT06] Z. Aung and K. L. Tan. MatAlign: precise protein structure comparison by matrix alignment. *Journal of Bioinformatics and Computational Biology*, In press, 2006.

[ATNT06] Z. Aung, S. H. Tan, S. K. Ng, and K. L. Tan. Efficient clustering of 3-D protein–protein interfaces from protein complex structural data. Submitted for publication, 2006.

[BAW+05] A. Bairoch, R. Apweiler, C. H. Wu, et al. The universal protein resource (UniProt). *Nucleic Acids Research*, 33:D154–159, 2005.

[BCHM96] S. E. Brenner, C. Chothia, T. J. P. Hubbard, and A. G. Murzin. Understanding protein structure: using SCOP for fold interpretation. In *Methods in Enzymology*, volume 266, pages 635–643. Academic Press, 1996.

[BDH+03] D. Bolser, P. Dafas, R. Harrington, J. Park, and M. Schroeder. Visualisation and graph-theoretic analysis of a large-scale protein structural interactome. *BMC Bioinfromatics*, 4(45), 2003.

[BFNW93] O. Bachar, D. Fischer, R. Nussinov, and H. J. Wolfson. A computer vision based technique for 3-D sequence independent structural comparison of proteins. *Protein Engineering*, 6(3):279–288, 1993.

[BKB02] P. Bradley, P. S. Kim, and B. Berger. TRILOGY: Discovery of sequence–structure patterns across diverse proteins. *Proceedings of the National Academy of Sciences of the United States of America*, 99(13):8500–8505, 2002.

[BKL00] S. E. Brenner, P. Koehl, and M. Levitt. The ASTRAL compendium for sequence and structure analysis. *Nucleic Acids Research*, 28:254–256, 2000.

[BM03] H. Bian and L. Mazlack. Fuzzy-rough nearest-neighbor classification approach. In *Proceedings of 22nd International Conference of the North American Fuzzy Information Processing Society (NAFIPS'03)*, pages 500–505, 2003.

[BOSD+97] E. Bertino, B. C. Ooi, R. Sacks-Davis, K. L. Tan, J. Zobel, B. Shidlovsky, and B. Catania. *Indexing Techniques for Advanced Database Systems*. Kluwer Academic Publishers, 1997.

[Bou05] P. E. Bourne. Reductionism and classification require detailed comparison. *Biological Data Representation and Analysis* lecture notes, San Diego Supercomputer Center, 2005. `http://www.sdsc.edu/pb/edu/pharm201/12/12.ppt`.

[Bre01] S. E. Brenner. A tour of structural genomics. *Nature Reviews Genetics*, 2(10):801–809, 2001.

[BSV04] D. L. Bostick, M. Shen, and I. I. Vaisman. A simple topological representation of protein structure: implications for new, fast, and robust structural classification. *Proteins: Structure, Function, and Bioinformatics*, 56(3):487–501, 2004.

[BT98] A. A. Bogan and K. S. Thorn. Anatomy of hot spots in protein interfaces. *Journal of Molecular Biology*, 280(1):1–9, 1998.

[BT99] C. Branden and J. Tooze. *Introduction to Protein Structure*. Garland Publishing, 2nd edition, 1999.

[BWF+00] H. M. Berman, J. Westbrook, Z. Feng, G. Gilliland, T.N. Bhat, H. Weissig, I.N. Shindyalov, and P.E. Bourne. The protein data bank. *Nucleic Acids Research*, 28:235–242, 2000.

[BYRN99] R. Baeza-Yates and B. Ribeiro-Neto. *Modern Information Retrieval*. ACM Press, 1999.

[CCI+04] A. Caprara, R. Carr, S. Istrail, G. Lancia, and B. Walenz. 1001 optimal PDB structure alignments: integer programming methods for finding the maximum contact map overlap. *Journal of Computational Biology*, 11(1):27–52, 2004.

[CCSW05] O. Camoglu, T. Can, A. K. Singh, and Y. F. Wang. Decision tree based information integration for automated protein classification. *Journal of Bioinformatics and Computational Biology*, 3(3):717–742, 2005.

[CGZ04] M. Comin, C. Guerra, and G. Zanotti. PROuST: a server-based comparison method of three-dimensional structures of proteins using indexing techniques. *Journal of Computational Biology*, 11(6):1061–1072, 2004.

[CH88] G. M. Crippen and T. F. Havel. *Distance Geometry and Molecular Conformation*. John Wiley and Sons, 1988.

[CHTY05] C. H. Chionh, Z. Huang, K. L. Tan, and Z. Yao. Towards scaleable protein structure comparison and database search. *International Journal on Artificial Intelligence Tools*, 14(5):827–848, 2005.

[CJ02] P. Chakrabarti and J. Janin. Dissecting protein–protein recognition sites. *Proteins: Structure, Function and Genetics*, 47(3):334–343, 2002.

[CKK04] I. G. Choi, J. Kwon, and S. H. Kim. Local feature frequency profile: a method to measure structural similarity in proteins. *Proceedings of the National Academy of Sciences of the United States of America*, 101(11):3797–3802, 2004.

[CKS04] O. Camoglu, T. Kahveci, and A. K. Singh. Index-based similarity search for protein structure databases. *Journal of Bioinformatics and Computational Biology*, 2(1):99–126, 2004.

[CP02] O. Carugo and S. Pongor. Protein fold similarity estimated by a probabilistic approach based on C(alpha)–C(alpha) distance comparison. *Journal of Molecular Biology*, 315(4):887–898, 2002.

[CSM04] A. Chinnasamy, W. K. Sung, and A. Mittal. Protein structure and fold prediction using tree-augmented bayesian classifier. In *Proceedings of 9th Pacific Symposium on Biocomputing (PSB'04)*, pages 387–398, 2004.

[DBG+03] P. Dafas, D. Bolser, J. Gomoluch, J. Park, and M. Schroeder. Fast and efficient computation of domain–domain interactions from known protein structures in the PDB. In *Proceedings of German Conference Bioinformatics on 2003 (GCB'03)*, pages 27–32, 2003.

[DD01] C. H. Q. Ding and I. Dubchak. Multi-class protein fold recognition using support vector machines and neural networks. *Bioinformatics*, 17:349–358, 2001.

[DFGB+03] P. Dombrosky-Ferlan, A. Grishin, R. J. Botelho, M. Sampson, L. Wang, W. A. Rudert, S. Grinstein, and S. J. Corey. Felic (CIP4b), a novel binding partner with the Src kinase Lyn and Cdc42, localizes to the phagocytic cup. *Blood*, 101(7):2804–2809, 2003.

[dHINM04] M. J. L. de Hoon, S. Imoto, J. Nolan, and S. Miyano. Open source clustering software. *Bioinformatics*, 20(9):1453–1454, 2004.

[DS05] F. P. Davis and A. Sali. PIBASE: a comprehensive database of structurally defined protein interfaces. *Bioinformatics*, 21(9):1901–1907, 2005.

[Dun03] M. H. Dunham. *Data Mining: Introductory and Advanced Topics*. Prentice Hall, 2003.

[DWNT99] D. Gilbert D, D. Westhead, N. Nagano, and J. Thornton. Motif-based searching in tops protein topology databases. *Bioinformatics*, 15(4):317–326, 1999.

[EA62] C. J. Epstein and C. B. Anfinsen. The reversible reduction of disulfide bonds in Trypsin and Ribonuclease coupled to Carboxymethyl Cellulose. *Journal of Biological Chemistry*, 237:2175–2179, 1962.

[EJT00] I. Eidhammer, I. Jonassen, and W. R. Taylor. Protein structure comparison and structure patterns. *Journal of Computational Biology*, 7(5):685–716, 2000.

[Erd05] M. A. Erdmann. Protein similarity from knot theory: geometric convolution and line weavings. *Journal of Computational Biology*, 12(6):609–637, 2005.

[FA95] D. Frishman and P. Argos. Knowledge-based secondary structure assignment. *Proteins: Structure, Function and Genetics*, 23:566–579, 1995.

[FC96] A. Falicov and F. E. Cohen. A surface of minimum area metric for the structural comparison of proteins. *Journal of Molecular Biology*, 258(5):871–892, 1996.

[FERE96] D. Fischer, A. Elofsson, D. Rice, and D. Eisenberg. Assessing the performance of fold recognition methods by means of a comprehensive benchmark. In *Proceedings of 1996 Pacific Symposium on Biocomputing (PSB'96)*, pages 300–318, 1996.

[FPVC02] P. Fariselli, F. Pazos, A. Valencia, and R. Casadio. Prediction of protein–protein interaction sites in heterocomplexes with neural networks. *European Journal of Biochemistry*, 269(5):1356–1361, 2002.

[FS96] Z. K. Feng and M. J. Sippl. Optimum superimposition of protein structures: ambiguities and implications. *Fold and Design*, 1(2):123–132, 1996.

[FTNW95] D. Fischer, C. J. Tsai, R. Nussinov, and H. J. Wolfson. A 3D sequence-independent representation of the protein data bank. *Protein Engineering*, 8:981–997, 1995.

[GARW93] H. Grindley, P. Artymiuk, D. Rice, and P. Willett. Identification of tertiary structure resemblance in proteins using a maximal common sub-graph isomorphism algorithm. *Journal of Molecular Biology*, 229:707–721, 1993.

[GFH03] S. Goldsmith-Fischman and B. Honig. Structural genomics: computational methods for structure analysis. *Protein Science*, 12:1813–1821, 2003.

[GL96] M. Gerstein and M. Levitt. Using iterative dynamic programming to obtain accurate pairwise and multiple alignments of protein structures. In *Proceedings of 4th International Conference on Intelligent Systems for Molecular Biology (ISMB'96)*, pages 59–67, 1996.

[GMB96] J. F. Gibrat, T. Madej, and H. Bryant. Surprising similarities in structure comparison. *Current Opinion in Structural Biology*, 6:377–385, 1996.

[God96] A. Godzik. The structural alignment between two proteins: is there a unique answer? *Protein Science*, 5(7):1325–1338, 1996.

[GRSE99] J. Grassmann, M. Reczko, S. Suhai, and L. Edler. Protein fold class prediction: new methods of statistical classification. In *Proceedings of 7th International Conference on Intelligent Systems for Molecular Biology (ISMB'99)*, pages 106–112, 1999.

[GSLB99] J. Gorodkin, H. H. Stærfeldt, O. Lund, and S. Brunak. MatrixPlot: visualizing sequence constraints. *Bioinformatics*, 15:769–770, 1999. `http://www.cbs.dtu.dk/services/MatrixPlot/`.

[GZ05] F. Gao and M. J. Zaki. PSIST: Indexing protein structures using suffix trees. In *Proceedings of IEEE Computational Systems Bioinformatics Conference (CSB'05)*, pages 212–222, 2005.

[HAB+97] T. J. P. Hubbard, B. Ailey, S. E. Brenner, A. G. Murzin, and C. Chothia. SCOP: a structural classification of proteins database. *Nucleic Acids Research*, 25(1):236–239, 1997.

[HBW+05] J. Huan, D. Bandyopadhyay, W. Wang, J. Snoeyink, J. Prins, and A. Tropsha. Comparing graph representations of protein structure for mining family-specific residue-based packing motifs. *Journal of Computational Biology*, 12(6):657–671, 2005.

[HK05] J. Han and M. Kamber. *Data Mining: Concepts and Techniques*. Morgan Kaufmann Publishers, 2nd edition, 2005.

[HKK05] J. Handl, J. Knowles, and D. B. Kell. Computational cluster validation in post-genomic data analysis. *Bioinformatics*, 21(15):3201–3212, 2005.

[HMWN00] Z. Hu, B. Ma, H. Wolfson, and R. Nussinov. Conservation of polar residues as hot spots at protein interfaces. *Proteins: Structure, Function and Genetics*, 39(4):331–342, 2000.

[HP00] L. Holm and J. Park. DaliLite workbench for protein structure comparison. *Bioinformatics*, 16(6):566–567, 2000.

[HPS+03] A. Harrison, F. Pearl, I. Sillitoe, T. Slidel, R. Mott, J. Thornton, and C. Orengo. Recognizing the fold of a protein structure. *Bioinformatics*, 19(14):1748–59, 2003.

[HS93] L. Holm and C. Sander. Protein structure comparison by alignment of distance matrices. *Journal of Molecular Biology*, 233:123–138, 1993.

[HS94a] L. Holm and C. Sander. The FSSP database of structurally aligned protein fold families. *Nucleic Acids Research*, 22(17):3600–3609, 1994.

[HS94b] L. Holm and C. Sander. Parser for protein folding units. *Proteins: Structure, Function and Genetics*, 19:256–268, 1994.

[HS94c] L. Holm and C. Sander. Searching protein structure databases has come of age. *Proteins: Structure, Function and Genetics*, 19:165–173, 1994.

[HS95] L. Holm and C. Sander. 3-D lookup: fast protein structure database searches at 90% reliability. In *Proceedings of 3rd International Conference on Intelligent Systems for Molecular Biology (ISMB'95)*, pages 179–187, 1995.

[HS98] L. Holm and C. Sander. Dictionary of recurrent domains in protein structures. *Proteins: Structure, Function and Genetics*, 33:88–96, 1998.

[HSZK03] J. Hou, G. E. Sims, C. Zhang, and S. H. Kim. A global representation of the protein fold space. *Proceedings of the National Academy of Sciences of the United States of America*, 100(3):2386–2390, 2003.

[HWW+04] J. Huan, W. Wang, A. Washington, J. Prins, and A. Tropsha. Accurate classification of protein structural families using coherent subgraph analysis. In *Proceedings of 9th Pacific Symposium on Biocomputing (PSB'04)*, pages 411–422, 2004.

[HZS05] Z. H. Huang, X. Zhou, and D. Song. High dimensional indexing for protein structure matching using Bowties. In *Proceedings of 3rd Asia-Pacific Bioinformatics Conference (APBC'05)*, pages 21–30, 2005.

[IYS04] Z. Isik, B. Yanikoglu, and U. Sezerman. Protein structural class determination using support vector machines. In *Proceedings of 19th International Symposium on Computer and Information Sciences (ISCIS'04)*, pages 82–89, 2004.

[JECT02] I. Jonassen, I. Eidhammer, D. Conklin, and W. R. Taylor. Structure motif discovery and mining the PDB. *Bioinformatics*, 18:362–367, 2002.

[Kab78] W. Kabsch. A discussion of the solution for the best rotation to relate two sets of vectors. *Acta Crystallographica Section A*, A34:827–828, 1978.

[Kar03] Kevin Karplus, University of California Santa Cruz. Personal communications, September 2003.

[KFDDG02] M. Kirsten Frank, F. Dyda, A. Dobrodumov, and A. M. Gronenborn. Core mutations switch monomeric protein GB1 into an intertwined tetramer. *Nature Structural Biology*, 9(11):877–885, 2002.

[KGME02] G. Kleiger, R. Grothe, P. Mallick, and D. Eisenberg. GXXXG and AXXXA: common alpha-helical interaction motifs in proteins, particularly in extremophiles. *Biochemistry*, 41(19):5990–5997, 2002.

[KH04] E. Krissinel and K. Henrick. Secondary-structure matching (SSM), a new tool for fast protein structure alignment in three dimensions. *Acta Crystallographica Section D*, D60:2256–2268, 2004.

[Kim94] J. W. Kimball. *Biology.* Wm. C. Brown Publishers, 6th edition, 1994.

[KJ94] G. J. Kleywegt and A. Jones. Superposition. *CCP4/ESF-EACBM Newsletter on Protein Crystallography*, 31:9–14, 1994.

[KJ97] G.J. Kleywegt and T. A. Jones. Detecting folding motifs and similarities in protein structures. In *Methods in Enzymology*, volume 277, pages 525–545. Academic Press, 1997.

[KKL05] R. Kolodny, P. Koehl, and M. Levitt. Comprehensive evaluation of protein structure alignment methods: scoring by geometric measures. *Journal of Molecular Biology*, 346:1173–1188, 2005.

[KL97] I. Koch and T. Lengauer. Detection of distant structural similarities in a set of proteins using a fast graph-based method. In *Proceedings of 5th International Conference on Intelligent Systems for Molecular Biology (ISMB'97)*, pages 167–187, 1997.

[Kle96] G.J. Kleywegt. Use of non-crystallographic symmetry in protein structure refinement. *Acta Crystallographica Section D*, D52:842–857, 1996.

[KN00] T. Kawabata and K. Nishikawa. Protein structure comparison using the Markov transition model of evolution. *Proteins: Structure, Function, and Genetics*, 41:108–122, 2000.

[Koe01] P. Koehl. Protein structure similarities. *Current Opinion in Structural Biology*, 11:348–353, 2001.

[KR90] L. Kaufman and P. J. Rousseeuw. *Finding Groups in Data: An Introduction to Cluster Analysis*. Wiley-Interscience, 1990.

[KS83] W. Kabsch and C. Sander. DSSP: definition of secondary structure of proteins given a set of 3D coordinates. *Biopolymers*, 22:2577–2637, 1983.

[KTWN04] O. Keskin, C. J. Tsai, H. Wolfson, and R. Nussinov. A new, structurally nonredundant, diverse data set of protein–protein interfaces and its implications. *Protein Science*, 13:1043–1055, 2004.

[LCCJ99] L. Lo Conte, C. Chothia, and J. Janin. The atomic structure of protein–protein recognition sites. *Journal of Molecular Biology*, 285(5):2177–2198, 1999.

[LFNW01] N. Leibowitz, Z. Fligelman, R. Nussinov, and H. J. Wolfson. Automated multiple structure alignment and detection of a common substructural motif. *Proteins: Structure, Function, and Genetics*, 43:235–245, 2001.

[LG98] M. Levitt and M. Gerstein. A unified statistical framework for sequence comparison and structure comparison. *Proceedings of the National Academy of Sciences of the United States of America*, 95(11):5913–5920, 1998.

[LI03] G. Lancia and S. Istrail. Protein structure comparison: algorithms and applications. In C. Guerra and S. Istrail, editors, *Mathematical Methods for Protein Structure Analysis and Design*, pages 1–33. Springer-Verlag Heidelberg, 2003.

[Lic01] O. Lichtarge. Getting past appearances: the many-fold consequences of remote homology. *Nature Structural Biology*, 8:918–920, 2001.

[LLTN04] H. Li, J. Li, S.H. Tan, and S. K. Ng. Discovery of binding motif pairs from protein complex structural data and protein interaction sequence data. In *Proceedings of 9th Pacific Symposium on Biocomputing (PSB'04)*, pages 312–323, 2004.

[LMPP04] H. Li, K. Marsolo, S. Parthasarathy, and Dmitrii Polshakov. A new approach to protein structure mining and alignment. In *Proceedings of 4th ACM SIGKDD Workshop on Data Mining in Bioinformatics (BIOKDD'04)*, 2004.

[Mar00] A. C. R. Martin. The ups and downs of protein topology: rapid comparison of protein structure. *Protein Engineering*, 13:829–837, 2000.

[MEWN03] B. Ma, T. Elkayam, H. Wolfson, and R. Nussinov. Protein–protein interactions: structurally conserved residues distinguish between binding sites and exposed protein surfaces. *Proceedings of the National Academy of Sciences of the United States of America*, 100(10):5772–5777, 2003.

[MH87] F. Murtagh and A. Heck. *Multivariate Data Analysis*. Kluwer Academic Publishers, 1987.

[MLM+05] J. Martin, G. Letellier, A. Marin, J. F. Taly, A. G. de Brevern, and J. F. Gibrat. Protein secondary structure assignment revisited: a detailed analysis of different assignment methods. *BMC Structural Biology*, 5(17), 2005.

[MSMP99] H. Müller, D. M. Squire, W. Müller, and T. Pun. Efficient access methods for content-based image retrieval with inverted files. In *Proceedings of Multimedia Storage and Archiving Systems IV (VV'02)*, 1999.

[MSPWN05] S. Mintz, A. Shulman-Peleg, H. J. Wolfson, and R. Nussinov. Generation and analysis of a protein–protein interface data set with similar chemical and spatial patterns of interactions. *Proteins: Structure, Function, and Bioinformatics*, 61:6–20, 2005.

[MW03] J. Mintseris and Z. Weng. Atomic contact vectors in protein–protein recognition. *Proteins: Structure, Function, and Genetics*, 53:629–639, 2003.

[NMK04] M. Novotny, D. Madsen, and G. J. Kleywegt. Evaluation of protein fold comparison servers. *Proteins: Structure, Function and Bioinformatics*, 54:260–270, 2004.

[NT04] S. K. Ng and S. H. Tan. Discovering protein–protein interactions. *Journal of Bioinformatics and Computational Biology*, 1(4):711–741, 2004.

[NW71] S. B. Needleman and C. D. Wunsch. A general method applicable to the search for similarities in the amino acid sequence of two proteins. *Journal of Molecular Biology*, 48:443–453, 1971.

[NW91] R. Nussinov and H. J. Wolfson. Efficient detection of three-dimensional structural motifs in biological macromolecules by computer vision techniques. *Proceedings of the National Academy of Sciences of the United States of America*, 88:10495–10499, 1991.

[OAA03] S. D. O'Hearn, A.J.Kusalik, and J. F. Angel. MolCom: a method to compare protein molecules based on 3-D structural and chemical similarity. *Protein Engineering*, 16(2):169–178, 2003.

[OHN99] T. Ohkawa, S. Hirayama, and H. Nakamura. A method of comparing protein structures based on matrix representation of secondary structure pairwise topology. In *Proceedings of 4th IEEE Symposium on Intelligence in Neural and Biological Systems (INBS'99)*, pages 10–15, 1999.

[OJT03] C. Orengo, D. Jones, and J. Thornton. *Bioinformatics: Genes, Proteins and Computers*. Oxford BIOS Scientific Press, 2003.

[OMJ+97] C. A. Orengo, A. D. Michie, S. Jones, D. T. Jones, M.B. Swindells, and J.M. Thornton. CATH: a hierarchic classification of protein domain structures. *Structure*, 5(8):1093–1108, 1997.

[Ore99] C. A. Orengo. CORA: topological fingerprints for protein structural families. *Protein Science*, 8:699–715, 1999.

[OSO02] A. R. Ortiz, C. E. M. Strauss, and O. Olmea. MAMMOTH (Matching Molecular Models Obtained from THeory): an auto-

mated method for protein model comparison. *Protein Science*, 11:2606–2621, 2002.

[PD75] E. A. Padlan and D. R. Davies. Variability of three-dimensional structure in Immunoglobulins. *Proceedings of the National Academy of Sciences of the United States of America*, 72(3):819–823, 1975.

[PEB+04] U. Pieper, N. Eswar, H. Braberg, et al. MODBASE, a database of annotated comparative protein structure models, and associated resources. *Nucleic Acids Research*, 32:D217–222, 2004.

[PL04] J. Przyborski and M. Lanzer. Parasitology. The malarial secretome. *Science*, 306(5703):1897–1898, 2004.

[PLG+03] P. Puntervoll, R. Linding, C. Gemund, et al. ELM server: A new resource for investigating short functional sites in modular eukaryotic proteins. *Nucleic Acids Research*, 31(13):3625–3630, 2003.

[PLT01] J. Park, M. Lappe, and S. A. Teichmann. Mapping protein family interactions: intramolecular and intermolecular protein family interaction repertoires in the PDBand yeast. *Journal of Molecular Biology*, 307(3):929–938, 2001.

[PR04a] S. H. Park and K. H. Ryu. Effective filtering for structural similarity search in protein 3D structure databases. In *Proceedings of 15th International Conference on Database and Expert Systems Applications (DEXA'04)*, pages 761–770, 2004.

[PR04b] S. H. Park and K. H. Ryu. Fast similarity search for protein 3D structure databases using spatial topological patterns. In *Proceedings of 15th International Conference on Database and Expert Systems Applications (DEXA'04)*, pages 771–780, 2004.

[RA76] M. G. Rossmann and P. Argos. Exploring structural homology of proteins. *Journal of Molecular Biology*, 105:75–95, 1976.

[RA00] J. Rosamond and A. Allsop. Harnessing the power of the genome in the search for new antibiotics. *Science*, 287(5460):1973–1976, 2000.

[RCGRA+04] B. Ravi Chandra, R. Gowthaman, R. Raj Akhouri, D. Gupta, and A. Sharma. Distribution of proline-rich (PxxP) motifs in distinct proteomes: functional and therapeutic implications for malaria and tuberculosis. *Protein Engineering Design and Selection*, 17(2):175–182, 2004.

[RE00] W. P. Russ and D. M. Engelman. The GxxxG motif: a framework for transmembrane helix-helix association. *Journal of Molecular Biology*, 296(3):911–919, 2000.

[RF03] P. Røgen and B. Fain. Automatic classification of protein structure by using Gauss integrals. *Proceedings of the National Academy of Sciences of the United States of America*, 100(1):119–124, 2003.

[RG88] S. Rackovsky and D. A. Goldstein. Protein comparison and classification: a differential geometric approach. *Proceedings of the National Academy of Sciences of the United States of America*, 85:777–781, 1988.

[Ros96] G. D. Rose. No assembly required. *The Sciences*, 36:26–31, 1996.

[Ros99] B. Rost. Twilight zone of protein sequence alignments. *Protein Engineering*, 12(2):85–94, 1999.

[Ros03] B. Rost. Predict structure and function: biochemistry and molecular biology of eukaryotes. *Bioinformatics 2003* lecture notes, CUBIC Columbia University, 2003. `http://cubic.bioc.columbia.edu/talks/course-2003/cu2/cu2.ppt`.

[SB90] A. Sali and T. L. Blundell. Definition of general topological equivalence in protein structures: a procedure involving comparison of

properties and relationships through simulated annealing and dynamic programming. *Journal of Molecular Biology*, 212:403–428, 1990.

[SB97] A. P. Singh and D. L. Brutlag. Hierarchical protein structure superposition using both secondary structure and atomic representations. In *Proceedings of 5th International Conference on Intelligent Systems for Molecular Biology (ISMB'97)*, pages 284–293, 1997.

[SB98] I. N. Shindyalov and P. E. Bourne. Protein structure alignment by incremental combinatorial extension (CE) of the optimal path. *Protein Engineering*, 11(9):739–747, 1998.

[SCSX04] C. R. Shyu, P. H. Chi, G. Scott, and D. Xu. ProteinDBS — a content-based retrieval system for protein structure database. *Nucleic Acids Research*, 32:w572–575, 2004.

[Sfy04] K. Sfyrakis. Geometrical transformations, 2004. `http://lcvmwww.epfl.ch/~kostas/GeometricalTransformations.htm#Anchor-New-49572`.

[SH03] E. S. C. Shih and M. J. Hwang. Protein structure comparison by probability-based matching of secondary structure elements. *Bioinformatics*, 19:735–741, 2003.

[Sha48] C. E. Shannon. A mathematical theory of communication. *Bell System Technical Journal*, 27:379–423, 1948.

[SKK98] T. Seidl, G. Kastenmüller, and H. P. Kriegel. Similarity search in 3D protein databases. In *Proceedings of German Conference on Bioinformatics*, 1998.

[SLL93] S. Subbiah, D. V. Laurents, and M. Levitt. Structural similarity of DNA-binding domains of bacteriophage repressors and the globin core. *Current Biology*, 3:141–148, 1993.

[SM97] J. C. Setubal and J. Meidanis. *Introduction to Computational Biology*. PWS Publishing, 1997.

[SM01] E. Sprinzak and H. Margalit. Correlated sequence-signatures as markers of protein–protein interaction. *Journal of Molecular Biology*, 311(4):681—692, 2001.

[SP04] M. L. Sierk and W. R. Pearson. Sensitivity and selectivity in protein structure comparison. *Protein Science*, 13:773–785, 2004.

[SPMNW04] A. Shulman-Peleg, S. Mintz, R. Nussinov, and H. J. Wolfson. Protein–protein interfaces: recognition of similar spatial and chemical organizations. In *Proceedings of 4th International Workshop Algorithms in Bioinformatics (WABI'04)*, pages 194–205, 2004.

[SPNW04] A. Shulman-Peleg, R. Nussinov, and H. J. Wolfson. Recognition of functional sites in protein structures. *Journal of Molecular Biology*, 339(3):607–633, 2004.

[SSS02] B. Schmidt, H. Schorder, and M. Schimmler. Massively parallel solutions for molecular sequence analysis. In *Proceedings of 2nd IEEE International Workshop on High Performance Computational Biology (HiCOMB'02)*, page 201, 2002.

[Sun04] D. Sunday. Distance between lines and segments with their closest point of approach, 2004. `http://softsurfer.com/Archive/algorithm_0106/algorithm_0106.htm`.

[SW81] T. F. Smith and M. S. Waterman. Comparison of biosequences. *Advances in Applied Mathematics*, 2:482–489, 1981.

[SW00] J. D. Szustakowski and Z. Weng. Protein structure alignment using a genetic algorithm. *Proteins: Structure, Function, and Genetics*, 38:428–440, 2000.

[Tay02] W. R. Taylor. Protein structure comparison using bipartite graph matching and its application to protein structure classification. *Molecular and Cellular Proteomics*, 1:334–339, 2002.

[TLWN96] C. J. Tsai, S. L. Lin, H. J. Wolfson, and R. Nussinov. A dataset of protein–protein interfaces generated with sequence-order-independent comparison technique. *Journal of Molecular Biology*, 260:604–620, 1996.

[TO89] W. R. Taylor and C. A. Orengo. Protein structure alignment. *Journal of Molecular Biology*, 208:1–22, 1989.

[TSN04] S. H. Tan, W. K. Sung, and S. K. Ng. Discovering novel interacting motif pairs from large protein–protein interaction datasets. In *Proceedings of 4th IEEE Symposium on Bioinformatics and Bioengineering (BIBE'04)*, pages 568–575, 2004.

[TT04] Z. Tan and A. K. H. Tung. Substructure clustering on sequential 3D object datasets. In *Proceedings of 20th International Conference on Data Engineering (ICDE'04)*, pages 634–645, 2004.

[TXN97] C. J. Tsai, D. Xu, and R. Nussinov. Structural motifs at protein–protein interfaces: protein cores versus two-state and three-state model complexes. *Protein Science*, 6(9):1793–1805, 1997.

[VBAS04] S. Veretnik, P. E. Bourne, N. N. Alexandrov, and I. N. Shindyalov. Toward consistent assignment of structural domains in proteins. *Journal of Molecular Biology*, 339:647–678, 2004.

[vMKS+02] C. von Mering, R. Krause, B. Snel, M. Cornell, S. G. Oliver, S. Fields, and P. Bork. Comparative assessment of large-scale data sets of protein–protein interactions. *Nature*, 417:399–403, 2002.

[WCH05] S. L. Wang, C. M. Chen, and M. J. Hwang. Classification of protein 3D folds by hidden Markov learning on sequences of structural

alphabets. In *Proceedings of 3rd Asia-Pacific Bioinformatics Conference (APBC'05)*, pages 65–72, 2005.

[WFB03] S. Wallin, J. Farwer, and U. Bestolla. Testing similarity measures with continuous and discrete protein models. *Proteins: Structure, Function, and Genetics*, 50(1):144–157, 2003.

[Wik06] Wikimedia, Foundation. Wikipedia: The Free Encyclopedia, 2006. `http://en.wikipedia.org/`.

[WKHK04] N. Weskamp, D. Kuhn, E. Hüllermeier, and G. Klebe. Efficient similarity search in protein structure databases by k-clique hashing. *Bioinformatics*, 20:1522–1526, 2004.

[Wol01] H. Wolfson. Protein structure. *Algorithms in Molecular Biology* lecture notes, Tel Aviv University, 2001. `http://www.math.tau.ac.il/~rshamir/algmb/01/scribe12/lec12.ps.gz`.

[WR97] H. J. Wolfson and I. Rigoutsos. Geometric hashing: an overview. *IEEE Computational Science and Engineering*, 4(4):10–21, 1997.

[WSB98] R. Weber, H. J. Schek, and S. Blott. A quantitative analysis and performance study for similarity-search methods in high-dimensional spaces. In *Proceedings of 24th International Conference on Very Large Data Bases (VLDB'98)*, pages 194–205, 1998.

[Wu03] Z. Wu. Protein structure determination and dynamic simulation. *ISU Summer Institute on Bio-Informatics* lecture notes, Iowa State University, 2003. `http://www.math.iastate.edu/wu/LectureNotes/SummerInstitute.ppt`.

[WZ02] H. E. Williams and J. Zobel. Indexing and retrieval for genomic databases. *IEEE Transactions on Knowledge and Data Engineering*, 14(1):63–78, 2002.

[YCCO05] J. S. Yeh, D. Y. Chen, B. Y. Chen, and M. Ouhyoung. A web-based three-dimensional protein retrieval system by matching visual similarity. *Bioinformatics*, 21(13):3056–3057, 2005.

[YG03] Y. Ye and A. Godzik. Flexible structure alignment by chaining aligned fragment pairs allowing twists. *Bioinformatics*, 19 Suppl. 1:ii246–255, 2003.

[Yon02] G. Yona. Protein classification and meta-organization. Methods for global organization of the protein universe. Tutorial in *10th International Conference on Intelligent Systems for Molecular Biology (ISMB'02)*, 2002.
`http://www.cs.cornell.edu/golan/Papers/ismb2002.ppt`.

[ZG02] B. Zhang and A. Godzik. The meaning and limitations of protein structure alignments. In *Proceedings of 1st International Symposium on 3D Data Processing Visualization and Transmission (3DPVT'02)*, pages 729–726, 2002.

[ZIB01] J. Zachary, S. S. Iyengar, and J. Barhen. Content based image retrieval and information theory: a general approach. *Journal of the American Society for Information Science and Technology*, 52(10):840–852, 2001.

[ZK03] C. Zhang and S. H. Kim. Overview of structural genomics: from structure to function. *Current Opinion In Chemical Biology*, 7:28–32, 2003.

[ZW05] J. Zhu and Z. Weng. FAST: a novel protein structure alignment algorithm. *Proteins: Structure, Function, and Bioinformatics*, 58:618–627, 2005.